Aus dem Munich Cluster for Systems Neurology (SyNergy)
am Institut für Schlaganfall- und Demenzforschung (ISD)
Klinikum der Ludwig-Maximilians-Universität München

Vorstand: Prof. Dr. med. Martin Dichgans

MASS SPECTROMETRY-BASED EXPLORATION OF NOVEL INTERACTORS IN UBIQUITIN-MEDIATED PROCESSES

Dissertation

zum Erwerb des Doktorgrades der Naturwissenschaften

an der Medizinischen Fakultät der

Ludwig-Maximilians-Universität München

vorgelegt von

Alexander Siebert

aus Michailowka

München 2023

Mit Genehmigung der Medizinischen Fakultät

der Universität München gedruckt

Betreuer:	Prof. Dr. Christian Behrends
Zweitgutachterin:	Prof. Dr. Angelika Harbauer
Dekan:	Prof. Dr. med. Thomas Gudermann
Tag der mündlichen Prüfung:	04. März 2024

Table of Contents

Table of Contents

Abbreviations

4HB	Four-helix bundle
A	Alanine
AD	Alzheimer's disease
ADP	Adenosine diphosphate
AHA1	Activator of Heat shock protein 90 ATPase 1
ALL	Acute lymphoblastic leukemia
ALS	Amyotrophic lateral sclerosis
AMPK	AMP-activated protein kinase
APC/C	Anaphase-promoting complex/Cyclosome
APEX2	Ascorbate peroxidase 2
APP	Amyloid precursor protein
ATG12	Autophagy related 12
ATG13	Autophagy related 13
ATG14L	Autophagy related 14 like
ATG16L1	Autophagy related 16 like 1
ATG8	Autophagy related 8
ATG9	Autophagy-related 9
ATP	Adenosine triphosphate
Aβ	Amyloid β
B-myb	Myb-related protein B
C9orf72	Guanine nucleotide exchange factor C9orf72
CAND1	Cullin-associated NEDD8-dissociated protein 1
CASH	Carbohydrate-interacting

Abbreviations

CCNF	Cyclin F gene
CDC37	Hsp90 co-chaperone Cdc37
CDK	Cyclin-dependent kinase
CNN2	Calponin 2
CP110	Centriolar coiled-coil protein of 110 kDa
CR	Charged linker region
CR1/2/3	Charged-linker region 1/2/3
CRL	Cullin-Ring-Ligase
CSN	COP9 Signalosome
CTD	C-terminal domain
CUL1/2/3/4/5	Cullin 1/2/3/4/5
DDB1	Damage binding protein 1
diGly	Glycine-Glycine
DNA	Deoxyribonucleic acid
DNAJC7	DnaJ homolog subfamily C member 7
DUB	Deubiquitinase
E1	Ubiquitin-activating enzyme
E2	Ubiquitin-conjugating enzyme
E2F	Transcription factor E2
E3	Ubiquitin ligase
EMT	Epithelial-mesenchymal transition
ER	Endoplasmic reticulum
ERAD	Endoplasmic-reticulum-associated protein degradation
fALS	Familial amyotrophic lateral sclerosis

Abbreviations

FAT10	Human leukocyte antigen-F adjacent transcript 10
FIP200	FAK family kinase-interacting protein of 200 kDa
FTD	Frontotemporal dementia
FUS	Fused in sarcoma
Fzr1	Fizzy-related protein homolog
GHKL	Gyrase, HSP90, histidine kinase, MutL
Glu	Glutamic acid
GRP78	78 kDa glucose-regulated protein
HECT	Homologous to the E6-AP Carboxyl Terminus
HeLa	Henrietta Lacks
HIP	Hsc70-interacting protein
His	Histidine
HSF1/2	Heat shock factor 1 / 2
HSP10	Heat Shock Protein 10
HSP40	Heat Shock Protein 40
HSP60	Heat Shock Protein 60
HSP70	Heat Shock Protein 70
HSP90AB1	Heat Shock Protein 90β
HSPB1	Heat shock protein β1
HspB8	Heat shock protein β8
Ile	Isoleucine
ISG15	Interferon-stimulated gene 15
JAMM	JAB1/MPN/Mov34 metalloenzyme
K	Lysine

Abbreviations

K8	Heavy lysine
KO	Knockout
L0	Light lysine
LAMP1/2	Lysosomal-associated membrane protein 1/2
LB	Lewy Bodies
LC3B	Autophagy-related protein LC3 B
LCL	Lymphoblastoid cell line
Leu	Leucine
LLOME	L-Leucyl-L-Leucine methyl ester
M	Methionine
M1	Methionine
MAPK	Mitogen-activated protein kinase
MAPT	Microtubule-associated protein tau
MD	Middle Domain
MEEVD	Methionine, Glutamic acid, Glutamic acid, Valine, Asparagine
MK2/3	Protein kinase 2/3
mRNA	Messenger ribonucleic acid
mTORC1	mTOR complex 1
N2a	Neuro 2a
NDP52	Nuclear domain protein 52
NEDD8	Neural precursor cell expressed developmentally down-regulated protein 8
NLS	Nuclear localizing sequences
NTD	N-terminal domain
OPTN	Optineurin

Abbreviations

PD	Parkinson's disease
PDAC	Pancreatic ductal adenocarcinoma
PE	Phosphatidylethanolamine
Phe	Phenylalanine
PI3KC3/VPS34	Phosphatidylinositol 3-kinase catalytic subunit type 3
PI3P	Phosphatidylinositol 3
POI	Protein of interest
PPIase	Peptidyl-propyl-cis trans isomerase
PTM	Posttranslational modification
RBP	RNA binding proteins
RBR	RING in between RING
RBX1/2	RING Box protein 1/2
RING	Really new interesting gene
RNA	Ribonucleic acid
ROS	Reactive oxygen species
RRM2	Ribonucleotide reductase M2
sAPPβ	Secreted amyloid precursor protein β
SCF	Skp1-Cullin-F-box
Ser	Serine
SH-SY5Y	Subclone of the parental SK-N-SH human neuroblastoma cell line
sHSPs	Small heat shock proteins
SKP1	S-phase-kinase-associated protein-1
SOD1	Superoxide dismutase 1
SQSTM1	Sequestosome-1

Abbreviations

SR	Substrate receptor
STIP1	Stress-induced-phosphoprotein 1
SUMO	Small ubiquitin-like modifier
TAX1BP1	Tax1-binding protein 1
TDP43	TAR DNA-binding protein 43/TARDBP
TFEB	Transcription factor EB
Thr	Threonine
TPR	Tetratricopeptide repeat
TriC	T-complex protein Ring Complex
TRIM	Tripartite motif-containing protein
TRIM16	Tripartite motif-containing protein 16
TUBE	Tandem ubiquitin-binding entities
Ub	Ubiquitin
UBA1	Ubiquitin-like modifier-activating enzyme 1
UBA6	Ubiquitin-like modifier-activating enzyme 6
UBAN	Ubiquitin binding in ABIN and NEMO domains
UBC domain	Ubiquitin-conjugating domain
UBD	Ubiquitin binding domain
UBE2M	Ubiquitin-conjugating enzyme E2 M
Ube2N	Ubiquitin-conjugating enzyme E2 N
UBE2QL1	Ubiquitin Conjugating Enzyme E2 Q Family Like 1
UBL	Ubiquitin-like proteins
ULK1/2	Unc-51 Like Autophagy Activating Kinase 1
UPS	Ubiquitin-proteasome-system

Abbreviations

USP	Ubiquitin specific protease
Val	Valine
VCP	Valosin containing protein
VSP15	Vacuolar protein sorting 15
WD40	Tryptophan-aspartic acid dipeptide 40
WH-A	Winged-helix A
WH-B	Winged-helix B
WIPI	WD repeat domain phosphoinositide-interacting protein
ZFYVE1 /DFCP1	Zinc finger FYVE domain-containing protein 1

Publications in this Thesis

I. **ALS-linked loss of Cyclin-F function affects HSP90.**

Siebert A., Gattringer V., Weishaupt J.H., Behrends C.

Life Science Alliance 2022. Vol. 5 (12), e202101359, DOI: 10.26508/lsa.202101359

II. **Ubiquitin profiling of lysophagy identifies actin stabilizer CNN2 as a target of VCP/p97 and uncovers a link to HSPB1**

Kravić B., Bionda T., **Siebert A.**, Gahlot P., Levantovsky S., Behrends C., Meyer H.

Molecular Cell 2022. Vol. 82 (14), 2633-2649.e7, DOI: 10.1016/j.molcel.2022.06.012

Zusammenfassung

Die Proteinhomöostase ist eine entscheidende Komponente der zellulären Integrität, die durch interne und umweltbedingte Stressfaktoren aus dem Gleichgewicht geraten kann. Um dem entgegenzuwirken, haben Zellen mehrere Systeme für die Faltung, Regulation und den Abbau von Proteinen entwickelt. Proteine müssen zunächst de novo synthetisiert werden und in ihre native Form gebracht werden, damit sie die gewünschte Funktion erfüllen können. Die Faltung von Proteinen ist ein komplexer Prozess, der die Hilfe von molekularen Chaperonen wie HSP90 (Hitzeschockprotein HSP 90-beta) erfordert, die neu synthetisierten oder fehlgefalteten Proteinen dabei helfen ihre native Form einzunehmen und sie vor Aggregation bewahren. Krankheitsmutationen oder zelluläre Stressfaktoren können dazu führen, dass Proteine geschädigt werden oder verklumpen und somit abgebaut werden müssen. Die zwei wichtigsten Abbauwege in der Zelle, sind das Ubiquitin-Proteasom-System (UPS) und die Autophagie. Das UPS ist dafür verantwortlich, einzelne Proteine dem proteasomalen Abbau zuzuführen. Hierfür werden einzelne Lysine des Substrats mit Ubiquitin modifiziert. Dies erfordert ein komplexes Konjugationssystem, das aus einem E1-Ubiquitin-aktivierenden, einem E2-Ubiquitin-konjugierenden Enzym und einer E3-Ubiquitin-Ligase besteht. E3-Ligasen können hierbei allein oder als Teil größerer Komplexe wie z.B. dem modularen Cullin-Ring-Ligase (CRL) Komplex arbeiten. Eine spezielle CRL ist der $SCF^{Cyclin\text{-}F}$-Komplex, der aus Cullin1, RBX1, SKP1 und dem F-Box-Protein Cyclin F besteht, letzteres bestimmt die Substratspezifität. Anders als es sein Name vermuten lässt, bindet Cyclin F nicht an eine Cyclin-abhängige Kinasen. Stattdessen ubiquitiniert es eine Vielzahl von zellzyklusspezifischen Zielproteinen und Proteine, die an der Beseitigung von DNS-Schäden beteiligt sind. Mittlerweile wurden zahlreiche Zielproteine für Cyclin F beschrieben, wovon die meisten jedoch in sich teilenden Zelltypen untersucht wurden, wohingegen es nur wenig Informationen über die Funktion von Cyclin F in neuronalen oder Neuron-ähnlichen Zelllinien gibt, die nach der Differenzierung keine Mitose mehr durchlaufen. Außerdem wurden in den letzten Jahren Cyclin-F-Mutationen mit der Entstehung von Amyotropher Lateralsklerose (ALS) in Verbindung gebracht.

Autophagie, der zweite wichtige Abbaumechanismus in der Zelle, umfasst zwei Wirkmechanismen: die selektive und die nicht-selektive Autophagie. Bei der Autophagie wird Cargo von einer wachsenden Doppelmembran, dem Phagophor umgeben und erweitert bis sich ein Vesikel gebildet hat. Diese Struktur, Autophagosom genannt, fusioniert mit dem Lysosom und führt zum Abbau und Recycling des Cargos. Während die nicht-selektive Autophagie bei Nährstoffmangel wichtig ist, ist die selektive Autophagie ein spezialisierter Prozess, der Strukturen wie Proteinaggregate und beschädigte Organellen, unter anderem Lysosomen, abbaut.

Zusammenfassung

Lysosomen sind Zentren der zellulären Homöostase und am Umsatz zellulärer Komponenten beteiligt, weshalb sie in ihrem Luminalraum verschiedene Arten von Degradationsproteinen wie Hydrolasen und Nukleasen beinhalten. Eine Beschädigung dieser Organellen führt dazu, dass luminale Proteine in die Umgebung entweichen, wo sie der Zelle schaden können. Um dies zu verhindern, haben Zellen mehrere Anpassungsstrategien entwickelt, die darauf abzielen, Lysosomen zu reparieren. Bleiben diese Versuche erfolglos, wird deren Abbau eingeleitet. Der selektive Abbau von Lysosomen, auch Lysophagie genannt, wird durch die Bindung von Galektinen an β-Galaktoside initiiert und führt zu einer umfassenden Ubiquitinierung von lysosomalen Proteinen durch Ubiquitin E3-Ligasen. Diese Ubiquitinierung führt zur Rekrutierung der Autophagie-Rezeptoren p62/ SQSTM1 (Sequestosom 1) und TAX1BP1 (Tax1-bindendes Protein 1), die das beschädigte Lysosom an das LC3-besetzte Phagophor binden und weitere Komponenten der Autophagie-Maschinerie rekrutieren. Ein weiterer wichtiger Faktor für die Lysophagie ist die Ubiquitin-gesteuerte AAA-ATPase VCP, die ubiquitinierte Komponenten aus dem beschädigten Lysosom extrahiert, um den Lysophagieprozess zu unterstützen.

Das Ziel meiner Arbeit war es, mit Hilfe massenspektrometrischer Methoden neue Interaktionspartner für zwei wichtige Ubiquitin-vermittelte Prozesse zu identifizieren und zu validieren, sowie die Rolle von Cyclin F in ALS-Modellen zu untersuchen. Im ersten Teil meiner Arbeit wollte ich neue Zielproteine von Cyclin F in sich nicht teilenden Zellen finden. Zu diesem Zweck habe ich mit Hilfe der CRISPR-CAS9-Technologie CCNF Knockout (KO)-Linien in der murinen Neuroblastomlinie N2a und der humanen Neuroblastomlinie SH-SY5Y erzeugt. Diese KO-Zellen habe ich zusammen mit lymphoblastoiden Zelllinien aus ALS-Patienten mit zwei unbekannten CCNF-Mutationen verwendet, um umfangreiche massenspektrometrische Analysen durchzuführen. Die Daten, die dabei ermittelt wurden, umfassen die APEX2-induzierte Nahbereichsmarkierung (close proximity proteomics), sowie Immunpräzipitationen die zur Untersuchung möglicher Interaktionspartner verwendet werden. Darüber hinaus wurde eine massenspektrometrische Analyse zur Evaluierung des Ubiquitoms, die sogenannte diGly-Ubiquitomics, eingesetzt. Dadurch war es möglich, einen Einblick in das Cyclin-F-abhängige Ubiquitom zu erhalten. Insgesamt konnte ich eine umfangreiche Datenbank für potenzielle Interaktoren und Substrate von Cyclin F erstellen. Außerdem konnte ich die Bindung von Cyclin F an das Chaperon HSP90AB1 sowie an zwei seiner Ko-Chaperone, STIP1 (stress-induced-phosphoprotein) und DNAJC7 (DnaJ homolog subfamily C member 7) bestätigen. Zusätzlich habe ich die Fähigkeit von Cyclin F zur Ubiquitinierung von HSP90AB1 mit Immunpräzipitationsansätzen, unter denaturierenden Bedingungen sowie mit spezialisierten Tandem-Ubiquitin-Bindungseinheiten (TUBE) untersucht. TUBE bindet

promiskuitiv an verschiedene Ubiquitin Spezies und kann somit genutzt werden, um den Ubiquitin Status eines Proteins zu ermitteln. Mit Hilfe dieser Ansätze konnte ich zeigen, dass HSP90AB1 durch Cyclin F ubiquitiniert wird. Des Weiteren konnte ich auch den Einfluss dieser Modifikationen auf die Bindung von HSP90 mit seinen Ko-Chaperonen nachweisen. Schließlich habe ich auch Veränderungen bei der Interaktion zwischen HSP90AB1 und einigen seiner Maturierungsklienten in Abhängigkeit von Cyclin F beobachtet.

Im zweiten Teil meiner Arbeit habe ich zusammen mit unseren Kooperationspartnern die Funktion der Ubiquitinierung nach Schädigung der lysosomalen Membran mit L-Leucyl-L-Leucin-Methylester (LLOME) und die Rolle von Ubiquitin beim Abbau von Lysosomen untersucht.

Die Veränderung des Ubiquitoms zu verschiedenen Messzeitpunkten nach lysosomalen Schäden ermöglichte uns einen differenzierten Blick auf Lysophagy und deckte neue Faktoren auf, die an diesen Abbauweg beteiligt sind. Zu den stark modifizierten Proteinen, die hier identifiziert wurden, gehören das Aktin-stabilisierende Protein Calponin 2 (CNN2) und die Proteine des Arp2/3-Komplexes. Für beide wurde nachgewiesen, dass sie zu geschädigten Lysosomen translozieren. Hier erleichtern sie die Bildung von Phagophoren durch die Modulation der Aktinfilamentdynamik. Darüber hinaus wird CNN2 ubiquitiniert, um die rechtzeitige Entfernung aus dem Lysosom zu gewährleisten, und ist für die Rekrutierung und Lipidierung von LC3b notwendig, die es direkt mit dem Lysophagieprozess in Verbindung bringt. Um die Dynamiken des Proteins CNN2 genauer zu untersuchen, habe ich mit Hilfe der Askorbat-Peroxidase APEX2, welche an CNN2 fusioniert wurde, in LLOMe- und kontrollbehandelten Zellen close proximity proteomics durchgeführt und quantitativ verglichen. Dies ermöglichte die Identifizierung von HSPB1 als direktem Interaktor von CNN2. HSPB1 wurde bereits mit Autophagie und dem Aktinfilament-System in Verbindung gebracht und war daher ein vielversprechender Kandidat für weitere Untersuchungen. Interessanterweise zeigte die Depletion von HSPB1 ähnliche Auswirkungen wie die Depletion von CNN2, indem sie die LC3b-Rekrutierung negativ beeinflusste. Die Ähnlichkeit des Phänotyps, der bei inaktivem VCP im Vergleich zum Verlust von HSPB1 oder CNN2 beobachtet wurde, deutete auf einen Zusammenhang zwischen diesen Proteinen hin. Weitere Experimente zeigten, dass VCP CNN2 aus lysosomalen Membranen extrahiert und das ubiquitinierte Aktin-stabilisierende Protein anschließend abgebaut wird. Die Aktin-unabhängige Rekrutierung von CNN2 zum Lysosom warf jedoch die Frage auf, welche Proteine mit CNN2 assoziiert waren, bevor es durch VCP entfernt wurde. Zu diesem Zweck wiederholte ich die Untersuchung der geschädigten Lysosomen durch close proximity proteomics mit CNN2-APEX2. Um die Entfernung von CNN2 zu unterbrechen, wurden die Zellen mit NMS-873, einem VCP-Inhibitor, behandelt. Die Proteine, die in dieser Situation signifikant erhöht waren,

Zusammenfassung

waren p62 und VCP, die beide mit beschädigten Lysosomen kolokalisieren. Die Depletion von p62 führt auch zu einer Verringerung der CNN2-Rekrutierung. Schließlich konnten wir auch zeigen, dass sowohl HSPB1 als auch VCP für die Entfernung von ubiquitiniertem CNN2 aus beschädigten Lysosomen entscheidend sind, um Lysophagie zu ermöglichen.

Zusammenfassend konnte ich einen tieferen Einblick in Ubiquitin-vermittelte Prozesse wie die Lysophagie und das UPS-System geben. Durch den unbefangenen Einsatz massenspektrometrischer Methoden habe ich neue potenzielle Interaktoren von Cyclin F und CNN2 aufgedeckt, die zu einem besseren Verständnis der jeweiligen Prozesse führen. Darüber hinaus unterstreichen diese Ergebnisse die Bedeutung von Hitzeschockproteinen für die Proteinhomöostase in beiden wichtigen Abbauprozessen.

Summary

Protein homeostasis is a crucial component of cellular integrity that internal and environmental stressors can disturb. Cells have adapted several systems for protein folding, regulation, and degradation to counteract this. Initially, proteins have to be synthesized de novo and adopt their native form before fulfilling their desired function. The folding of proteins is a complex process that requires the participation of molecular chaperones such as HSP90 (heat shock protein 90), which assist newly synthesized or misfolded proteins in reaching their native state and preventing them from aggregation. Cellular stressors or disease mutations can lead to damaged proteins or aggregation, both of which require adequate degradation. Two of the major degradation pathways in the cell are the ubiquitin-proteasome-system (UPS) and autophagy. The UPS is responsible for targeting single proteins for proteasomal degradation by modifying substrate lysines with ubiquitin. This requires a sophisticated conjugation system consisting of an E1-ubiquitin-activating, an E2-ubiquitin-conjugating enzyme, and an E3-ubiquitin ligase. E3-ligases can work alone or as part of larger complexes such as the modular Cullin-Ring-Ligase (CRL) complex. One particular CRL is the SCF $^{\text{cyclin F}}$ complex consisting of Cullin1, RBX1, SKP1, and the F-Box protein cyclin F which determines substrate specificity. Contrary to the function implied by its name, cyclin F does not bind cyclin-dependent kinases. Instead, it ubiquitinates a variety of cell cycle-specific proteins as well as proteins involved in the DNA damage response. By now several targets of cyclin F were described, however, most of them were examined in cell systems that regularly undergo mitosis and little is known about cyclin F's function in neuronal or neuron-like cell types. Moreover, in recent years cyclin F mutations were implicated in the development of ALS.

Autophagy, the second important degradative pathway, includes two modes of action: selective and bulk autophagy. During autophagy cargo is engulfed by a growing double membrane, the so-called phagophore, which is elongated to form a vesicle. This structure is the autophagosome that subsequently fuses with a lysosome resulting in the degradation and recycling of cargo components. While bulk autophagy is important during nutrient starvation, selective autophagy is a specialized process in which autophagy receptors recognize structures such as aggregates and damaged organelles, including lysosomes.

Lysosomes are hubs for cellular homeostasis and are involved in the turnover of cellular components and therefore harbor various types of degradative proteins such as hydrolases and nucleases in their luminal space. Damage to these organelles results in the leakage of luminal proteins into the surrounding, where they can harm the cell. To prevent this, cells have adapted several response pathways aiming to fix lysosomes. However, if these attempts remain unsuccessful, degradation is

Summary

triggered. Lysophagy is initiated by the binding of galectins to β-galactosides and the extensive ubiquitination of lysosomal proteins by recruited E3-ligases. This ubiquitination leads to the recruitment of the autophagy receptors p62/SQSTM1 (sequestosome 1) and TAX1BP1 (Tax1-binding protein 1), that link the damaged lysosome to the LC3-decorated phagophore and recruit further components of the autophagy machinery. Another substantial factor for lysophagy is the ubiquitin-directed AAA-ATPase VCP that extracts ubiquitinated factors from the lysosome and the forming phagophore to assist in the lysophagic process.

My thesis aimed to identify and validate interaction partners in two important ubiquitin-mediated processes using mass spectrometry as well as assess cyclin F's influence in models of ALS. In the first part of my thesis, I aimed to find new targets of cyclin F in non-dividing cells. To this end, I generated CCNF knockouts (KO) in the murine Neuro 2a (N2a) and the human SH-SY5Y neuroblastoma cell line using CRISPR-Cas9 which results in the loss of cyclin F. Together with ALS-patient derived lymphoblastoid cell lines of two unreported CCNF mutations, I utilized these KO-cells to perform extensive mass spectrometry. The data I obtained included close proximity and immunoprecipitation approaches that were used to assess direct binding. Furthermore, diGly-ubiquitomics was utilized to get a glimpse into the cyclin F-dependent ubiquitome. With these experiments, I was able to provide a rich database for potential interactors and substrates of cyclin F. Based on the analysis I identified HSP90 (heat shock protein HSP 90-beta) as a prominent elevated factor and was able to confirm its binding to cyclin F. Additionally, I could provide evidence for the binding of cyclin F to HSP90's co-chaperones, STIP1 (stress-induced-phosphoprotein) and DNAJC7 (DnaJ homolog subfamily C member 7). Next, I assessed cyclin F's ability to ubiquitinate HSP90AB1 with immunoprecipitation approaches under denaturing conditions as well as with specialized tandem ubiquitin-binding entities that promiscuously bind ubiquitin. Apart from showing cyclin F-dependent HSP90AB1 ubiquitination, I could provide evidence that these modifications influence HSP90 co-chaperone binding. Further, I observed alterations in the binding of HSP90 to its maturation clients upon cyclin F knockout.

Together with our collaborators, the second part of my thesis examined the role of ubiquitination upon lysosomal membrane damage using L-Leucyl-L-Leucine methyl ester (LLOME) and the role of ubiquitin in lysosomal degradation.

Changes in the ubiquitome due to lysosomal damage at different time points allowed a differentiated look at lysophagy thereby highlighting new factors involved in this degradative pathway. Among the strongly modified proteins, the actin stabilizing protein calponin 2 (CNN2) and the Arp2/3 complex

proteins were identified and shown to translocate to damaged lysosomes. Here, they facilitate phagophore formation by modulating actin filament dynamics. Further, CNN2 is ubiquitinated for timely removal from the lysosome and is necessary for the recruitment and lipidation of LC3b to associate it directly with the lysophagic process. To assess the dynamics of CNN2 in more detail I performed close-proximity proteomics with the help of the ascorbate peroxidase APEX2 fused to CNN2 in LLOMe versus control-treated cells, followed by a quantitative analysis. This enabled the identification of HSPB1 as a direct interactor of CNN2. HSPB1 is associated with autophagy and the actin filament system and was therefore a promising candidate for additional examination. Interestingly, HSPB1 depletion showed similar effects to CNN2 depletion by negatively affecting LC3b recruitment. The resemblance of the phenotype seen with inactive VCP compared to HSPB1 or CNN2 loss hinted towards a connection between these proteins. Additional experiments revealed the extraction of CNN2 from lysosomal membranes by VCP and the subsequent degradation of the ubiquitinated actin-stabilizing protein. The actin-independent recruitment of CNN2 to the lysosome, however, posed the question of which proteins were associated with CNN2 before removal by VCP. To this end, I repeated the examination of damaged lysosomes by close proximity proteomics with CNN2-APEX2. To pause the removal of CNN2, the cells were treated with NMS-873, a VCP inhibitor. The proteins that were significantly increased in this setting were p62 and VCP, both of which colocalize on damaged lysosomes. Interestingly, p62 depletion also leads to the reduction of CNN2 recruitment. Finally, we could also demonstrate that HSPB1, as well as VCP, are crucial for the removal of ubiquitinated CNN2 from damaged lysosomes to facilitate lysophagy.

In summary, I was able to provide a deeper insight into ubiquitin-mediated processes such as lysophagy and the UPS system. By using mass spectrometry, I unveiled potential new interactors of cyclin F and CNN2 leading to a better understanding of the respective function. Also, these results iterate on the importance of heat shock proteins in protein homeostasis in both major degradative pathways.

1 Introduction

1.1 Protein regulation pathways in eukaryotic cells

Proteins are involved in virtually all aspects of life, therefore tight-knit surveillance is vital for cellular integrity and functionality. Hence, protein activity, localization, and many other aspects are regulated by complex, intertwined processes that together constitute protein homeostasis. Important aspects are the abundance of proteins as well as their integrity, each of which is highly regulated and balanced by de-novo synthesis, proper folding, and degradation [1, 2].

The life cycle of a protein starts with its de-novo synthesis. Before it can fulfill its cellular function, however, it has to adopt its native state. For this to happen cells utilize cellular chaperones that can facilitate the folding process and prevent misfolding as well as aggregation [3]. However, cellular stressors such as reactive oxygen species (ROS) or disease mutations can lead to aggregated or damaged proteins which have to be cleared to avoid toxic effects or disturbance of overall cellular pathways [4, 5].

To achieve this, eukaryotic cells mainly employ two major degradation routes, the ubiquitin-proteasome system (UPS) and the autophagosomal-lysosomal pathway. Both pathways are essential for protein degradation and maintaining protein homeostasis, yet they differ fundamentally in their mode of action. Misfolded, damaged, and highly regulated proteins are degraded by the UPS whereas the autophagosomal-lysosomal pathway is important for the clearance of bigger structures, such as aggregates or organelles, as well as bulk degradation during starvation [6, 7]. The UPS is dependent on the attachment of ubiquitin (Ub) to proteins in a highly regulated process that results in proteasomal degradation or exhibits regulatory functions [6].

The autophagosomal-lysosomal pathway can be subdivided into a minimum of three more specific pathways – macroautophagy, chaperone-mediated autophagy, and microautophagy. All of these processes lead to the clearance of proteins, aggregates, or organelles via lysosomes [7]. Macroautophagy (hereafter referred to as autophagy) can be divided into bulk and selective autophagy. The latter is often involved in the degradation of defined structures such as aggregates, lysosomes, or mitochondria. Each process has its specific term, indicating the respective process (e.g., aggrephagy, lysophagy, mitophagy) [8].

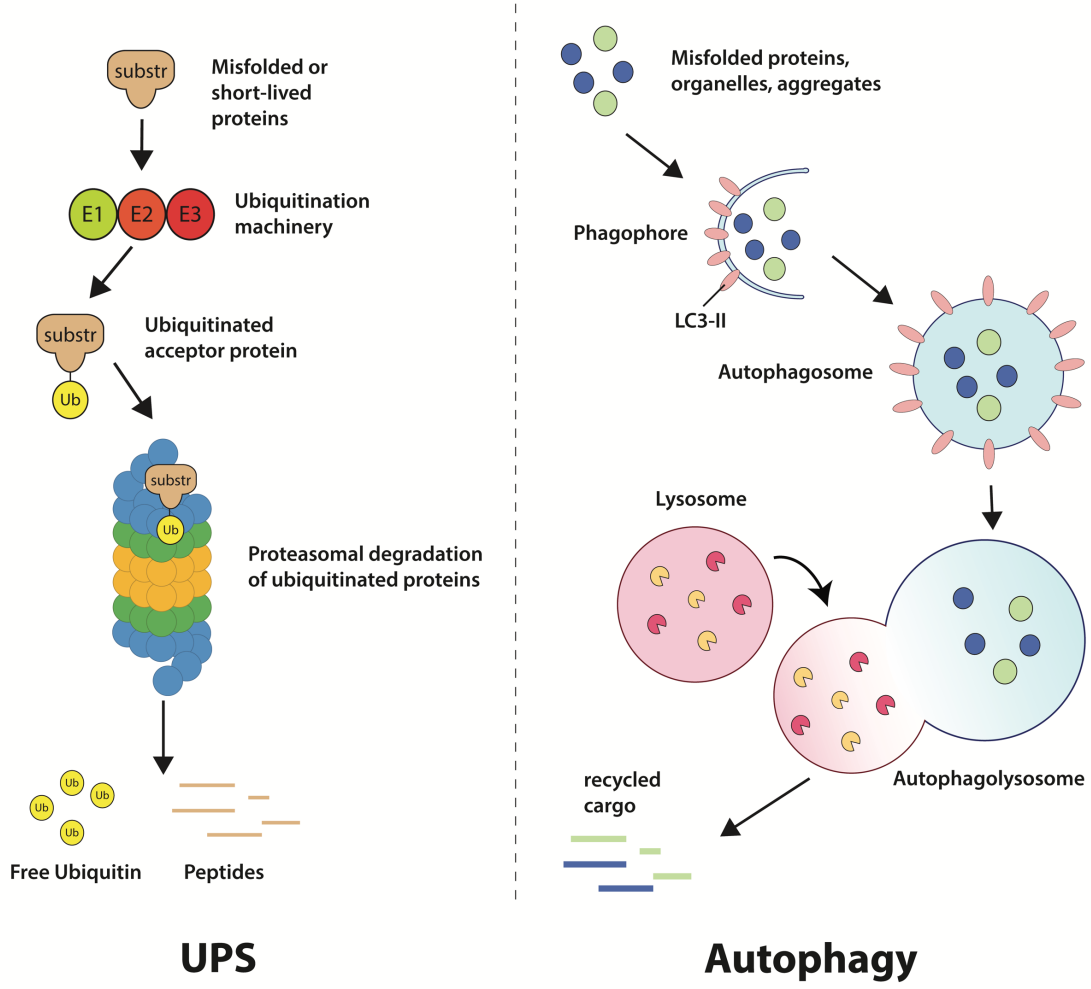

Figure 1: The main degradation pathways of the cell.
UPS (left) describes the E1-E2-E3-dependent attachment of ubiquitin to proteins and their subsequent degradation by the proteasome. In Autophagy (right), however, diverse cargo is engulfed by the phagophore, which is then elongated and closed to form the autophagosome. This structure fuses with the lysosome to allow the cargo to be degraded and released into the cytosol for recycling. substr, substrate; E1, E1-activating enzyme; E2, E2-conjugating enzyme; E3, E3-ligase; Ub, Ubiquitin; UPS, ubiquitin-proteasome-system. Adapted from Ghosh et al. [9].

1.1.1 Chaperone function

Small proteins can fold into their native state within seconds, without the need for additional factors. This suggests that the whole three-dimensional structure is encoded within the amino acid sequence of the protein [10]. Nevertheless, cells developed a system to assist in protein folding. The reason for this lies in the dynamics of bigger proteins or multi-protein complexes which take considerably longer to reach their native state *in vitro* than small proteins [11]. In addition, there are intrinsically disordered proteins that account for 20-30% of total proteins in mammalian cells, as well as mutations that can

result in conformational changes affecting the function and stability of proteins, which adds another layer of complexity [12, 13]. Beyond that, the cytosol is crowded with other macromolecules which interfere with this process simply by steric exclusion [4]. On the way to correct folding, proteins orient their hydrophobic residues inwards, thereby guiding the process towards native intermediate states that help facilitate the folding process. To achieve this, they have to traverse several energetic barriers, which can result in non-native intermediates or expose hydrophobic residues that in turn can slow down folding or lead to aggregation [3, 14].

Cells, therefore, utilize a system of molecular chaperones specially reserved for the de-novo folding of nascent polypeptides or refolding [11]. The importance of chaperones is particularly evident under conditions of cellular stress, such as heat shock, oxidative stress, or other cellular stressors, which can cause protein aggregation and an imbalance in homeostasis [15].

There are several classes of structurally distinct molecular chaperones that govern protein folding. Two well-studied heat shock proteins (HSPs) are HSP70 and HSP90. HSPs are grouped according to their molecular weight, which is indicated by the number in their name. The major chaperone systems require adenosine triphosphate (ATP) for proper function [16].

HSP70, for instance, can switch between a low- and high-affinity state for unfolded or partially folded proteins, depending on its ATP status. This process is assisted by heat shock protein 40 (HSP40, also known as DnaJ), which delivers these proteins to HSP70 and subsequently initiates the hydrolysis of ATP to adenosine diphosphate (ADP) by HSP70, leading to a closed conformation and the stable binding of the substrate [17, 18]. The C-terminal substrate binding domain of HSP70 preferentially interacts with client proteins via short hydrophobic stretches consisting of 5-7 amino acids, which are flanked by positively charged amino acids [19]. Stretches like these are present in proteins that require folding, and their exposure is associated with increased aggregation [20]. The exchange of ADP to ATP by nucleotide exchange factors is the last step of one folding cycle resulting in the release of the protein. This triggers one of three events – the client proteins either bury their hydrophobic patches in a spontaneous reaction, resume binding to HSP70 which may further facilitate the folding process, or are transferred to another chaperone system, such as chaperonin or HSP90 [3, 21, 22].

1.1.1.1 The HSP90 complex

Apart from HSP70, the maturation of proteins can be accomplished with the help of HSP90. This complex is a homodimer that together with several co-chaperones assists in folding, multiprotein complex assembly, and ligand binding to soluble receptors. The dimer is made up of two HSP90AB1

protomers, which are constitutively expressed. Additionally, a structurally similar, inducible form named HSP90AA1 exists, which was also observed to bind HSP90AB1 and form a heterodimer [23]. Both forms share a common domain structure composed of an N-terminal domain (NTD) connected to the C-terminal domain (CTD) by an unstructured charged-linker region (CR) and the middle domain (MD) [24]. The NTD harbors a nucleotide binding fold, which shares a high similarity with the GHKL (Gyrase, HSP90, histidine kinase, MutL) superfamily. This family discerns itself by not only binding ATP but also hydrolyzing it [25]. This can also be observed for HSP90 albeit the ATPase activity is very low and requires interaction with the MD [26, 27]. Beyond that, the N-terminus seems to be important for the binding of co-chaperones [28]. The linker region, following the NTD, is highly charged and is thought to allow for more dynamic and flexible interactions, enabling HSP90 to cope with a higher diversity of targets as well as the crowded environment of the cell. The impact of the CR on activity is yet to be determined since contradicting reports exist [29-32]. The subsequent MD serves the binding of client proteins and co-chaperones, as well as ATPase activation. The latter is accomplished by the interaction with the γ-phosphate of ATP [28, 33, 34].

The previously mentioned dimerization is mediated via the CTD, as is the binding of clients. Furthermore, the CTD also enables the binding of tetratricopeptide repeat (TPR) domains, present in co-chaperones, through its MEEVD (Met-Glu-Glu-Val-Asp) motif [23, 35-37].

1.1.1.2 HSP90 cycle

The activity of HSP90 is highly dependent on the rate of ATP binding and hydrolysis since this initiates substantial structural rearrangements and subsequent folding [27]. Notably, both rates are very low, with a dissociation constant of around 400 μM and a hydrolysis rate of 0.1 ATP/min in humans [38-40]. The unfolded protein is transported to HSP90 with the help of an HSP40/HSP70 complex stabilized by Hsc70-interacting protein (HIP) [28, 41]. In concert with other co-chaperones, stress induces phosphoprotein 1 (STIP1)/HOP mediates the transfer of client proteins to HSP90 by engaging with both chaperones at the same time [42, 43]. Additionally, STIP1 aids the transfer by preventing the dimerization of the NTD in a non-competitive manner [44]. Subsequent release of HSP70 is dependent on the removal of the inhibitory phosphorylation of STIP1 and further requires the action of Activator of 90 kDa heat shock protein ATPase homolog 1 (AHA1) or a combined effort from a peptidyl-propyl-cis trans isomerase (PPIase) and p23 [36, 45].

Upon client protein transfer and association with ATP, the HSP90-complex goes into an intermediate state where the lid region of the NTD, a loop with several conserved amino acids, closes over the

ATP. This initiates the dimerization of the NTD resulting in a closed HSP90 complex, ultimately leading to a twisted dimer where the distance between the NTD and MD is minimized so they can work together as a functional ATPase [36]. AHA1, contrary to STIP1, can enhance the hydrolysis of ATP and therefore accelerates the first closed state of the complex [36, 46]. In its second closed state, however, the HSP90 co-chaperone p23 stabilizes the complex by competing for HSP90 binding with AHA1. The following hydrolysis triggers the separation of the dimerized NTDs as well as the release of ADP and inorganic phosphate. This restores the initial state of the complex and liberates the substrate [36].

Overall, the HSP90 chaperone cycle is dependent on several layers of regulation, including transcriptional, post-translational, and co-chaperone-mediated regulation. Hence, also the rate of ATP hydrolyzation is subject to post-translational modification (PTM) [47]. The phosphorylation of HSP90 usually results in a decreased hydrolyzation rate. The serine (Ser)/threonine (Thr) phosphatase 5 uses this fact to assist in the maturation of kinases by dephosphorylating HSP90 and Hsp90 co-chaperone Cdc37 (CDC37), another co-chaperone which prevents the dimerization of the NTD and thereby the advancement of the cycle [48, 49]. Several other co-chaperones that harbor a PPIase, such as Peptidyl-prolyl cis-trans isomerase FKBP4 and FKBP5 or the peptidyl-prolyl cis-trans isomerase D, bind HSP90 via their TPR-domain and take part in client protein maturation [36]. Most of them are only part of specific maturation processes. While CDC37, for instance, is almost exclusively associated with protein kinases, FKB51 can help the maturation of kinases, transcription factors as well as the minichromosome maintenance protein complex [50, 51]. Apart from being fine-tuned by PTMs and co-chaperones regarding activity and client specificity, HSP90 abundance can also be regulated by proteasomal degradation, induced by E3 ubiquitin-protein ligase CHIP dependent ubiquitination [47, 52-54].

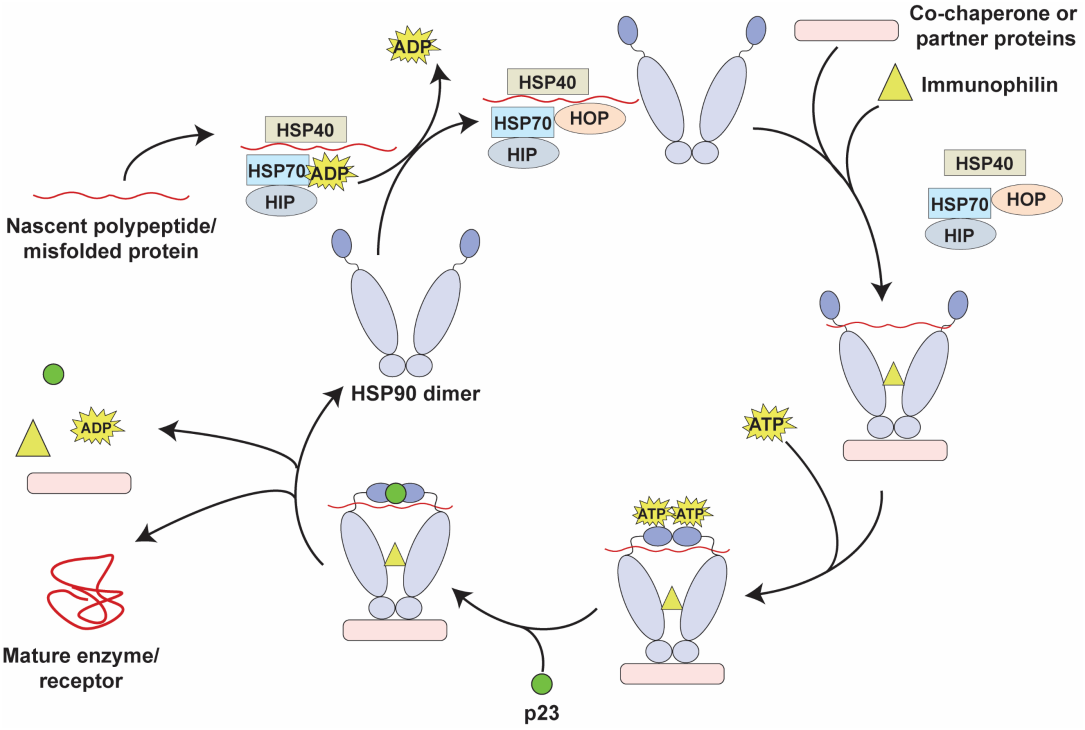

Figure 2: The HSP90 cycle.
In the HSP90 cycle, a nascent polypeptide is transported to an HSP90 dimer by the HSP70/HSP40 complex. The HSP90 dimer assists in the folding of the protein by transitioning from an open, substrate unbound form, to a closed state, that is dependent on the binding and hydrolysis of ATP. This requires the concerted action of several co-chaperones (HIP, HOP, p23; Immunophilin). After the cycle is finished the mature protein is released. ADP, adenosine diphosphate; ATP, adenosine triphosphate. Adapted from Hoter et al. [28].

1.1.1.3 HSP27/HSPB1

Heat shock protein beta-1 (HSPB1), also known as HSP27, is one of eleven crystallin-related human small heat shock proteins (sHSP), a subgroup of chaperones [55]. Its N-terminus contains a hydrophobic motif (WDPF), a highly conserved alpha-crystallin domain, which is typical for sHSPs, as well as the C-terminus [56]. Together with the alpha-crystallin domain, responsible for sHSP dimerization, the WDPF domain leads to the formation of homo-oligomeric complexes, as well as hetero-oligomeric complexes with other alpha-crystallins [56-62]. The extent of oligomerization is dependent on the phosphorylation status of the N-terminal serine residues (Ser15, Ser78, Ser82), whereby Ser78 and Ser82 are more often phosphorylated [63, 64]. Modification of these sites results in the disassembly of oligomers to tetramers or even dimers [65]. However, the question of which species is the most active in terms of chaperone activity has not been solved and might be dependent on the particular cellular context as well as the number of phosphorylation events [58, 63, 66, 67]. The extent of kinases involved in the regulation of HSPB1 is remarkable. They include p38 mitogen-

activated protein kinase (MAPK), protein kinase C, protein kinase 2/3 (MK2/MK3), the ribosomal S6 kinase (p70RSK), protein kinase G as well as protein kinase B, D, and G [59, 63, 68]. The kinases differ in their specificity towards particular serine residues, e.g. MAPK can only phosphorylate Ser15, whereas MK2 and MK3 can modify all three [69].

Contrary to its bigger counterparts (e.g. HSP70/HSP90), HSPB1 does not require ATP for its function [70]. sHSPs, although not able to refold proteins without the help of factors like HSP70, are crucial components of the proteostasis system, because they are capable of preventing the aggregation of misfolded or damaged proteins [70]. If refolding fails, HSPB1 can also enhance proteasomal degradation [71]. Initially, HSPB1 was considered to be only present upon induction via heat shock, but recent studies revealed, that exposure to several stressors can drive expression. Experiments with the murine homologue heat shock protein 25 show that the expression is also dependent on cell type and differentiation status [56, 72]. Several factors responsible for initiating transcription were found, among them were activating transcription factor 3 and 5, heat shock factor (HSF) 1, and HSF2. Which of these factors participates in activation depends on the type of stressor and the cellular context [73-76].

Apart from preventing aggregation, HSPB1 is important in many cellular processes. It exhibits anti-apoptotic functions by inhibiting the activation of procaspase-3 and counteracting tumor necrosis factor α induced apoptosis. It also plays a role in the remodeling of the cytoskeleton, and, when mutated, was shown to cause problems during axonal transport [77-81]. The importance of proper HSPB1 function can also be appreciated in several disease settings. Mutations in the HSPB1 gene result in inherited neuropathies, most prominently in Charcot-Marie-Tooth Disease 2 [77]. Further, overexpression has been associated with cancer by e.g., elevating epithelial-mesenchymal transition (EMT) or modulating the Salvador-Warts-Hippo pathway, which in turn leads to higher invasiveness or overall tumorigenesis [82, 83].

1.1.1.4 Chaperones in disease

The ample processes molecular chaperones are part of require strict regulation which in aging and diseases are subject to errors [84, 85]. As discussed later in **Protein folding affected by ALS mutations**, chaperone dysfunction contributes to disease progression in amyotrophic lateral sclerosis (ALS), which is also true for other neurodegenerative diseases such as Alzheimer's (AD) and Parkinson's (PD) disease [84].

AD is known to be one most common causes of dementia and can be characterized by two major characteristics: extracellular amyloid plaques and intracellular neurofibrillary tangles [86]. The former mainly consists of amyloid β (Aβ) peptides, which result from the amyloidogenic processing of the amyloid precursor protein (APP) by γ-secretase. APP is a transmembrane protein that is consecutively cleaved by two proteases to produce sAPPβ (secreted amyloid precursor protein β) and Aβ, with variable lengths ranging from 37 to 43 amino acids [87, 88]. Longer species such as $A\beta_{42}$ and $A\beta_{43}$ are prone to aggregation and represent the major constituents of amyloid plaques [89]. Neurofibrillary tangles, on the other hand, consist of abnormally phosphorylated tau, a protein that under normal conditions is involved in the assembly and stability of microtubules [90, 91]. Hyperphosphorylation leads to misfolded phospho-tau that aggregates within the cytoplasm, contributing to neuronal death [90, 92]. As discussed, chaperones often play a beneficial role in neurodegenerative diseases. HSP70, for example, can degrade tau and Aβ-oligomers via the UPS and was further shown to bind APP and interfere with the secretory route of APP, thereby reducing the formation of Aβ [93]. How HSPs interfere with Aβ-aggregation is not fully determined yet, nonetheless, there are two proposed mechanisms, either favoring an ATP-independent sequestration of misfolded amyloid or an ATP-dependent conformational change of Aβ, resulting in reduced aggregation [94]. While HSP70 is considered protective in AD, HSP90's role is not as clear since it was implicated in exacerbating the hyperphosphorylation of tau [95]. As discussed earlier, HSP90 is involved in the maturation of several kinases [96, 97]. Therefore, inhibiting HSP90 in AD mouse models or mouse models of other tau-related diseases, so-called tauopathies, results in a reduction of Cdk5 tau kinase activity and a concomitant decrease in phospho-tau [95].

Other proteinopathies also display characteristic misfolded proteins that are associated with disease progression. PD, for instance, is defined by a loss of dopaminergic neurons in the substantia nigra [98]. Although no definite cause was found yet, many patients show an accumulation of α-synuclein, which is the main component of Lewy bodies (LB). LBs are intracellular filamentous inclusions, that were linked with neuronal cell death in PD [95, 99]. Hence, reducing α-synuclein aggregation would be beneficial for patients. Overexpression of HSP70 in human neuroglioma cells resulted in a 50% reduction of α-synuclein [100]. Additional research has shown that HSP70 can block α-synuclein oligomerization by an ATP-independent mechanism [101]. On the other hand, HSP90 was found to co-localize with α-synuclein in LB. In PD brains elevated HSP90 levels also correlated with increased insoluble α-synuclein [102]. In line with these observations, the inhibition of HSP90 prevented α-synuclein oligomer formation and reduced toxicity [103].

Apart from neurodegenerative disorders, HSPs can have a strong impact on various other diseases, including inflammation, viral infections as well as cancer. In cancer, HSPs play a part in tumorigenesis since higher translation rates and an abnormal metabolism are common characteristics for most types of cancer. Both factors increase the need for a well-functioning protein quality machinery, that can be described as non-oncogene addition [104]. Therefore, despite not being oncogenes themselves, some HSPs are known to be associated with overall reduced survival of patients. HSP90AA1 and HSP90AB1, for instance, were associated with a significantly lower life expectancy in patients with breast, cervical, and lung carcinoma and were found to be elevated in 17 of 21 tumors analyzed in this study. However, this does not hold true for all cancer types, since in renal clear cell carcinoma and ovarian cancer the opposite effect could be observed. Here, increased HSP90 levels were linked to improved overall survival. Similar inconsistencies can be seen with HSP70 since its overexpression does not always coincide with reduced overall survival. Its influence heavily depends on the type of cancer as well as the HSP70 family member involved. One representative is the ER-localized 78 kDa glucose-regulated protein (GRP78), which was found to be overexpressed in 18 out of 21 major human cancers. In three of those, namely bladder, glioblastoma, and liver cancer, the overexpression was associated with poor overall survival in addition to showing a shorter disease-free survival in bladder cancer and squamous cell lung carcinoma. Contrary to GRP78, HSP1A showed elevated levels, that were beneficial in renal clear cell carcinoma. In summary, cancers usually overexpress at least one HSP70 family member, which in eight cancer types was also indicative of lower overall survival. The inverse effect was observed upon HSP70 knockdown. In several types of cancer, a reduction in cancer cell growth, migration, and tissue invasion was observed [104].

1.1.2 Ubiquitin Proteasome System

1.1.2.1 Ubiquitination cascade

Ubiquitination is an intricate ATP-dependent, cellular mechanism that requires three different types of enzymes, first a Ub-activating enzyme (E1), second a Ub-conjugating enzyme (E2) and third, and a Ub ligase (E3). After the initial, ATP-dependent activation of Ub by the E1 enzyme a thioester is formed on the E1, which is then transferred to an E2. From there the Ub is attached to the corresponding substrate, either indirectly by E3- really interesting new gene (RING) ligases in conjunction with an E2 enzyme or directly as is the case for Homologous to the E6-AP Carboxyl Terminus (HECT)- and RING in between RING (RBR)-E3s. The differences in Ub chain architecture are dependent on the specific E2 or E3 enzymes involved in the transfer [105, 106].

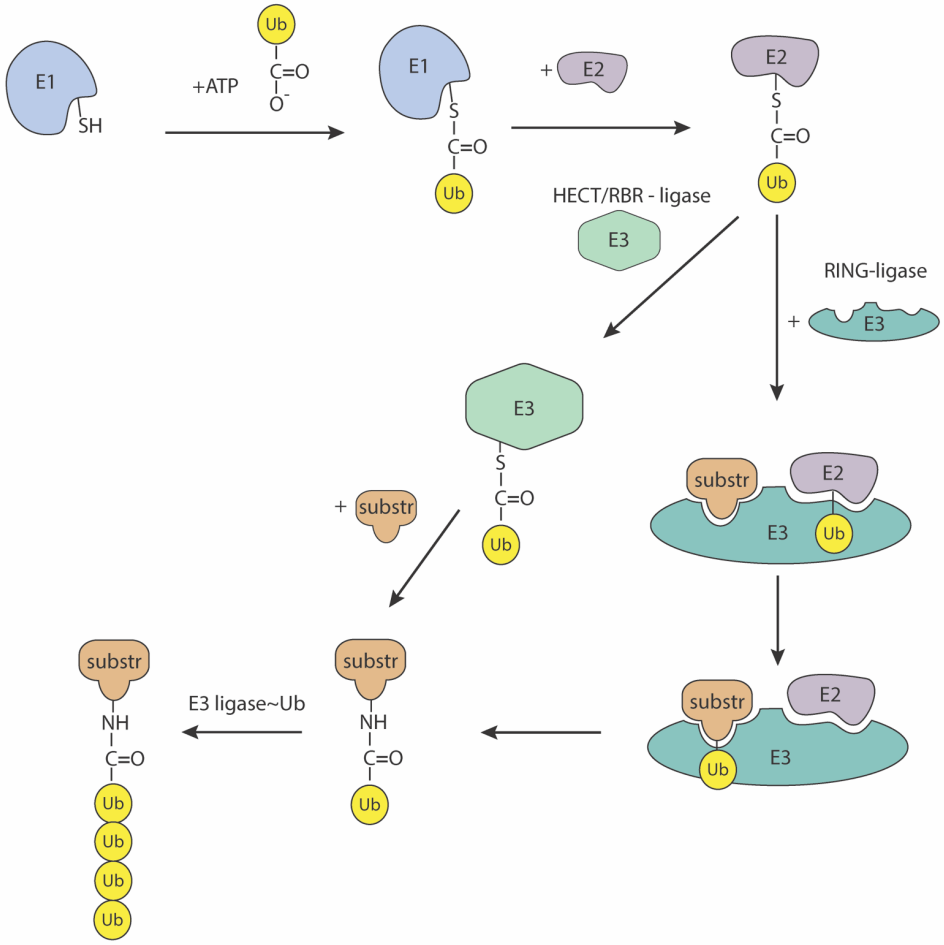

Figure 3: The role of different E3-ligases in ubiquitination.
Protein ubiquitination requires the activation (E1-activating enzyme) of ubiquitin, its subsequent conjugation (E2-conjugating enzyme), and its transfer to the substrate with the help of an E3-ligase. Depending on the ligase, ubiquitin is either transferred to an acceptor directly via the E3-ligase (HECT/RBR) or by the E2-enzyme with the assistance of a RING-ligase. This process can be repeated to yield a polyubiquitin chain. E1, E1-activating enzyme; E2, E2-conjugating enzyme; E3, E3-ligase; Ub, Ubiquitin; Acptr, acceptor. Adapted from Woelk et al. [107].

Once Ub is attached to a substrate there are several ways forward. Ub can exhibit regulatory functions, it can be removed or signal the degradation of targeted proteins by the proteasome. The removal of Ub is performed by proteases called deubiquitinases (DUBs), which are either cysteine proteases or metalloproteases that can cleave the isopeptide bond in a hydrolysis reaction. There are six superfamilies of DUBs, each of which can harbor specific domains responsible for isopeptide cleavage [108]. Degradation, on the other hand, relies on the 26S proteasome, a structure that is comprised of the 20S core subunit and the 19S regulatory cap [109]. The 20S core particle is composed of two different types of subunits the alpha subunit, relevant for structure, and the beta

subunit with predominantly catalytic features [109-111]. Shuttling factors, such as homolog of Rad23A/B, ubiquilins, and Protein DDI1 homolog 1/2 can bind ubiquitinated proteins and transport them to the proteasome. Subsequently, Ub is recognized by receptors and removed by DUBs [112, 113]. Next, the protein is unfolded, which requires ATP hydrolysis by the 19S ATPase subunit, and translocated into the catalytic chamber of the core subunit. There it is degraded into short peptides through a threonine-dependent nucleophilic attack and the remaining short peptides are subsequently released into the cytoplasm [110, 111].

1.1.2.2 Ubiquitin

Ubiquitin is a very stable, 76 amino acid long protein [105]. It is highly conserved from yeast to human with only three conservative changes to its sequence [2]. It adopts a β-grasp fold with a flexible C-terminal tail which is used to attach the initial Ub to proteins [114]. Though its overall conformation is quite rigid, the β1/β2 loop shows enough flexibility for Ub-binding proteins to bind [115]. Moreover, Ub possesses a hydrophobic surface that is essential for its recognition by proteins with ubiquitin binding domains (UBDs). This surface can be subdivided into hydrophobic patches centered around Isoleucine 44 (Ile44), Isoleucine 36 (Ile36), and Phenylalanine 4 (Phe4) [116-119]. The patch around Ile44 (Leucine (Leu)8, His68, Val70, Ile44) can be bound by most UBDs, proteasomes and is essential for cell division [116]. The second patch around Phe4 (glutamic acid (Glu) 2, phenylalanine (Phe) 4, Threonine (Thr) 14) can interact with ubiquitin binding in ABIN and NEMO domains (UBAN domains) and ubiquitin specific protease domains (USP domains) of certain DUBs [120, 121]. Further, through structural differences, this patch helps DUBs distinguish Ub from other ubiquitin like proteins (UBLs) such as Neural precursor cell expressed developmentally down-regulated protein 8 (NEDD8) [122]. The last hydrophobic patch is located around Ile36 (including Leu8, Ile36, Leu71, and Leu73) and mediates the interactions between Ub molecules in chains [2]. It can interact with HECT-E3s, DUBs, and UBDs [120, 123, 124]. Apart from the hydrophobic structures, Ub harbors a TEK-Box (Lys6, Lys11, Thr12, Thr14, Glu34), a motif that is required for mitotic degradation [125].

The main features of Ub, however, are its seven lysine (K) residues (K6, K11, K27, K29, K33, K48, K63) and the N-terminal methionine that are distributed on all sides of the protein [2].

1.1.2.3 Ubiquitin chain architecture

Proteins can be either mono-, multi-monoubiquitinated or polyubiquitinated. Each of these modifications can serve a different purpose in the cell. Monoubiquitination, for instance, was linked to protein sorting, trafficking, and other regulatory functions [126-128]. Polyubiquitination can also occur on each of the lysines and the N-terminal methionine (M1) of Ub, yielding either isopeptide- or M1-linked chains, respectively [119, 129]. Linkages assembled on Ub-lysines can have a variety of forms, namely homotypic, mixed, and branched, resulting in a complex Ub code. This code is further expanded by additional modifications such as acetylation, phosphorylation, and neddylation of Ub and its chains as well as the attachment of small ubiquitin like modifiers (SUMOylation) (Figure 4). Even combinations of SUMOylation and ubiquitination on the same chain can be found, adding another layer of complexity (Figure 4). Hence, it is not surprising that, despite some well-studied linkage types (K48 and K63), other linkages still need extensive exploration [119, 130].

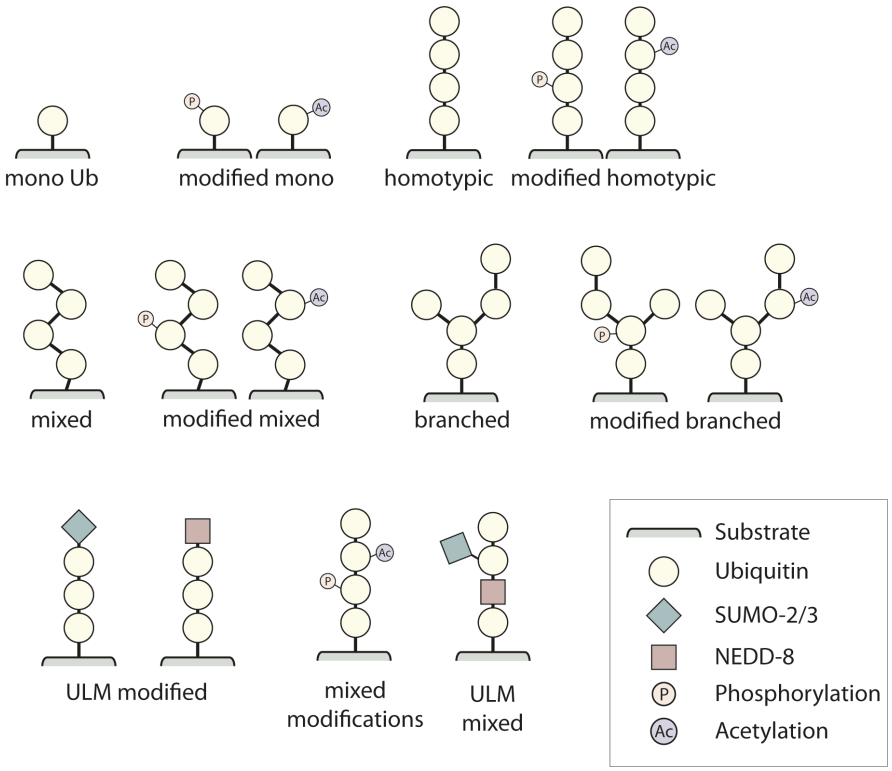

Figure 4: Ubiquitin code.
The number of processes regulated by ubiquitin gives rise to a complex code comprised of different linkage types, post-translational modifications as well as other UBLs (NEDD8/SUMO). Depending on which ubiquitin linkage type (K6, K11, K48, K63, etc.) is used to elongate the Ub chain, homotypic, mixed, or branched ubiquitin chains can occur. By further adding UBLs or other PTMs even more diverse signals can be created. UBL, ubiquitin-like proteins; P, phosphorylation; Ac, acetylation; Ub, ubiquitin; K, lysine; PTM, post-translational modification. Adapted from Swatek et al. [119].

K48-linked ubiquitination is the most dominant one in cells (50% of overall ubiquitination) and known to target proteins for 26S-proteasomal degradation [119]. It was considered to be the only

proteasomal degradation signal, however, recently other Ub species, such as K11 polyubiquitin chains were also shown to induce proteasomal clearance [125, 131]. Another very abundant type of ubiquitination is K63. It participates in various regulatory functions, with roles in trafficking, endocytosis, innate immunity, and also nuclear factor kappa B signaling [119]. Some of these roles are shared with other more atypical types of Ub chains. K33-chains for example are supposedly involved in post-Golgi trafficking, while K11 has been linked to endoplasmic-reticulum-associated protein degradation (ERAD) and membrane trafficking [132-134]. Other atypical linkages were associated with deoxyribonucleic acid (DNA) damage response after UV stress (K6 and K33) or implicated in autophagy initiation and mitochondrial homeostasis (K6) [135, 136]. Since the corresponding UBDs, DUBs, or E3s for many of these linkage types are still unknown more research has to be conducted to further dissect Ub's functions in the cell.

1.1.2.4 Ubiquitin E1 activating enzyme

The ubiquitination process starts with the binding of ATP to the respective E1, followed by the transient binding of Ub or other UBLs, such as NEDD8 or human leukocyte antigen-F adjacent transcript 10 (FAT10) [137-139]. The glycine carboxy group of Ub attacks the α-phosphate of ATP leading to the formation of an acyl-phosphate anhydride bound between Ub and AMP. This species is non-covalently bound to the E1 enzyme, which allows the thiol of the active site cysteine to start a nucleophilic attack toward the activated Ub glycine. This leads to the formation of an energy-rich E1~Ub thioester (Figure 3). To enable proper downstream transfer of Ub, the cycle is repeated with an additional Ub that associates with the E1 enzyme without being covalently attached. Following activation, the E2 enzyme is bound non-covalently to allow the transfer of Ub to the E2-conjugation enzyme in a trans-thiolation reaction allowing the E1 enzyme to start a new cycle [137, 140]. Until recently the only known E1 enzyme was Ubiquitin like modifier activating enzyme 1 (UBA1), with its two isoforms UBA1a and the shorter UBA1b, which is missing the nuclear localizing sequence, important for translocation during the cell cycle [141]. Ubiquitin like modifier activating enzyme 6 (UBA6), a second ubiquitin E1 was found more recently but is thought to only be relevant in a subset of proteins. Since there are only two E1-enzymes in the cell, both of them are essential and deletions of either UBA1 or UBA6 are lethal [140-143].

1.1.2.5 E2 conjugating enzymes

Following Ub activation and the formation of a thioester on the E1 enzyme, Ub is transferred to an E2 enzyme. This transfer is accomplished by structural rearrangements of the E1 enzyme dependent on Ub binding [144-146]. After exposing a negatively charged groove, the E2 enzyme can bind to the E1 enzyme, leading to a trans-thiolation reaction that yields an E2~Ub conjugate. It is noteworthy, that E2 enzymes bind poorly to unbound Ub or unloaded E1s compared to loaded enzymes [146, 147].

Overall, there are 38 human E2 enzymes. Four E2 enzymes work with other UBLs, five lack a catalytically active cysteine and one is only capable of Ub conjugation to cysteine but not lysine (Ubiquitin-conjugating enzyme E2 L3) [148-150]. The majority (28 E2 enzymes) however, are involved in Ub transfer in one of the following ways [133]. E2 enzymes can load HECT or RBR E3s with Ub in a trans-thiolation reaction [151]. This enables the formation of Ub chains following the specificity of the respective E3 (Figure 3) [133, 152, 153]. Alternatively, E2 enzymes can also directly function as chain-elongating enzymes, thereby defining the linkage type. This can either be achieved by using intrinsic properties, such as acidic residues, in the case of ubiquitin-conjugating enzyme E2 S or by employing auxiliary proteins, as shown for ubiquitin-conjugating enzyme E2 N. This protein uses an E2-like subunit called ubiquitin-conjugating enzyme variant 1/ variant 2 to assemble K63 chains by positioning the Ub in the right orientation. There are several more examples of Ub chain building E2s that can assemble K48, K11, or K63 chains [151].

Additionally, E2s can bind to a class of proteins called RING E3s, which help E2 enzymes to target lysins for Ub transfer in an aminolysis reaction (Figure 3) [151, 154, 155]. Notably, E2s which are important for the elongation of Ub chains, require a priming event, the initial conjugation of an Ub moiety to the substrate, to fulfill their function. Priming and chain elongation require two different types of E2 enzymes. The attachment of the first Ub, as well as monoubiquitination, usually requires the joint activity of an E2 and an E3 enzyme [156-158].

Which of these possibilities is employed depends on the domain structure of the respective E2. There are four different classes, which all share a 150 amino acid spanning ubiquitin conjugating (UBC) domain and in most cases, an active site cysteine but vary in size and the number of extra domains [159].

Due to their flexible C-terminus, E2~Ub conjugates can adopt various conformation states [160]. Open conformations are beneficial for the trans-thiolation of HECT (e.g., NEDD4L) or RBR E3s

[123, 151, 161]. In fact, HECT E3s trap Ub in an open state to allow for specific Ub transfer towards cysteine and hinder the transfer of Ub to a lysine [151, 162].

Contrasting this, E2~Ub conjugates that bind RING E3s stabilize the closed state conformation of Ub, as seen in several crystal structures [155, 163, 164]. E2/E3 complexes have a low binding affinity towards each other unless Ub is conjugated to an E2. In this state, E2~Ub/E3 complexes are more reactive towards lysine, resulting in enhanced aminolysis of substrate proteins [149, 151, 165].

1.1.2.6 E3 Ubiquitin- ligases

There are 600 – 1000 different human E3s either targeting Ub or UBLs to proteins which can be differentiated according to their domain topology as well as their mode of action [165, 166]. While HECT and RBR ligases directly transfer Ub to the acceptor proteins, RING E3s are more or less working as co-factors by binding the substrate and the E2~Ub conjugate to allow for Ub transfer between E2~Ub and the acceptor protein [167].

1.1.2.6.1 HECT E3-ligases

The HECT E3-ligase subfamily shares a conserved cysteine, located in the 350 amino acid long HECT domain, that is essential for the formation of the thioester [168]. In experiments using fragments of HECT E3s, the HECT-only fragment was able to mediate E2 binding and ubiquitination, whereas ΔHECT fragments were not. However, ΔHECT mutants could still bind downstream substrates [169-172].

How exactly linkage specificity is determined is not completely understood yet, but according to domain swapping experiments, the last 50 residues at the C-terminus are sufficient to change the specificity of a HECT E3 from K63 to K48, indicating that the HECT domain is fundamental in determining chain architecture [152]. HECT-containing proteins can build a variety of chain types as demonstrated by the E3 ubiquitin-protein ligase Itchy homolog, which can produce K27, K29, and K33 linked chains in vivo, while others such as E6-AP can only produce K48 chains [133, 152, 173-176].

1.1.2.6.2 RBR ligases

RBR ligases are comprised of a RING1 domain that is linked to a RING2 domain via an "in-between-RING" (IBR)-domain and two linkers. Together they coordinate two zinc ions that are important for domain structure. RBR E3s employ a mechanism similar to HECT E3s to modify downstream

targets with Ub. To this end the RING1 domain, which has a strong resemblance to the canonical RING domain of RING E3s, associates with an E2~Ub conjugate and stabilizes it in an open conformation [153, 177, 178]. This process facilitates the trans-thiolation reaction towards the cysteine residue within the RING2 domain, resulting in a RING2~Ub. Subsequently, the Ub can be attached to a substrate. While it is commonly accepted that RBR ligases determine the linkage type they confer, the underlying mechanism remains unclear [133, 149]. The linear Ub chain assembly complex, for instance, is the only RBR ligase that produces M1-linked chains exclusively [179]. Other RBRs, such as Parkin are more promiscuous regarding their chain specificity [180, 181].

1.1.2.6.3 RING-type E3 ligases

Another group of E3s is defined by the presence of a RING domain or an analog RING-type domain. The majority of E3s in the cell are RING E3s, with roughly 616 potential family members expressed in human cells [165]. The canonical domain consists mainly of cysteines, interspersed with histidine (His). It harbors a fairly conserved spacing, that can vary between residue three-four and six-seven, as seen in the consensus sequence: Cys-X2-Cys-X(9-39)-Cys-X(1-3)-His-X(2-3)-Cys-X2-Cys-X(4-48)-Cys-X2-Cys (X is any amino acid) [182]. Some proteins do have slight variations in this sequence, one of them being E3 ubiquitin protein ligase RBX1 (RBX1). In these proteins, some of the critical residues seen in this consensus sequence are changed to aspartyl, with so-far unknown effects on their function [165, 183]. Independent of these variations, the RING domain coordinates two zinc-ions, which are crucial for the cross-brace structure that the domain adopts, giving rise to a groove that can be bound by E2s [172, 184].

Other domains, so-called RING-type domains, take on structurally similar shapes. Among these are the B-box, which can be found in the TRIM subfamily, as well as the U-box. Both can mediate ubiquitination, however, U-box proteins, in contrast to B-box proteins, can recruit E2s. Furthermore, U-box proteins do not coordinate zinc, instead, they possess conserved charged and polar residues that built a network of hydrogen bonds to recapitulate the structural features of the RING domain [185-187].

RING E3s can have their substrate and E2~Ub binding site both within the RING domain, separated in different domains of the ligase, or if they are part of a dimeric or multimeric complex separated into different proteins. The distinct mechanism of how E3s mediate ubiquitination is still not elucidated completely. There was no direct catalytic activity and no thioester intermediates observed in E3s, independent of the configuration of the RING domain [165, 188, 189]. It is still

debated as to whether RING E3s are merely scaffolds allowing for the proximity of E2~Ub moiety and the substrate or whether significant structural rearrangements are taking place [165]. Some experiments substantiated that proximity is not sufficient to allow transfer and that E2~Ub flexibility played an important role in activity [190]. However, other studies showed that binding of E2~Ub to RING E3s reduces the E2's flexibility which results in a closed conformation [155, 163, 164, 191].

For bigger complexes such as Cullin-RING-ligase (CRL) complexes, a distance of 50-60 Å between the substrate and the E2~Ub thioester was observed. Considering that the accessibility of a particular lysine is considered an important factor for ubiquitination, this would exclude a productive reaction, unless major conformational changes occur [165, 192]. The type of ubiquitination is determined by the E2 enzyme for most of the E3 RING ligases although some RING-ligases harbor UBDs, which may orient Ub for a specific lysine attack which would influence chain specificity [133]. As is known for several types of E3s, the initial ubiquitination of any lysine is the rate-limiting factor since the subsequent elongation of the Ub chain is significantly faster [193, 194]. The two types of ubiquitination can be achieved by separate or the same E3 [165]. For example, UbcX promotes mono and oligo-ubiquitination on substrates of the anaphase-promoting complex/Cyclosome (APC/C), while Ubc4 assembles long chains subsequently [195]. Furthermore, E3-RING-ligases are capable of auto-ubiquitination [172].

1.1.2.6.3.1 Cullin-RING-ligases

RING domains can be found in single-subunit proteins or as part of multi-subunit complexes, which also include CRLs. Their modular build and interchangeable subunits enable Cullin-RING ligases to regulate a multitude of proteins by ubiquitination, rendering them crucial for almost all aspects of cellular functions. In humans, six canonical Cullins are serving as scaffolds (CUL1, CUL2, CUL3, CUL4A, CUL4B, and CUL5) for the other complex components [196]. Additional complex constituents are a RING ligase, either RBX1 (CUL1-4) or RBX2 (CUL5), and a substrate receptor (SR), that is either directly associated with the respective Cullin or binds via an adaptor protein. CUL1/ 2/ 4 and 5 use adaptor proteins to bind SRs, whereas CUL3 uses a single complexed substrate binding protein [196, 197]. CUL1 interacts with the S-phase-kinase-associated protein-1(SKP1) to build a functional complex with F-box proteins, whereas CUL4 is linked with DNA damage-binding protein 1 (DDB1) to form DDB1- and CUL4-associated factor 1 (DCAF)-DDB1 complexes for

substrate engagement [183, 198-201]. CUL2-RBX1 and CUL5-RBX2 share the multiprotein adaptor EloBC consisting of Elongin B and C, which in turn can bind to BC-box proteins [196, 202-204].

On the other hand, CUL3-RBX1 is in a complex with BTB-3-Box domain containing protein dimers, that combine both features of SKP1 and its F-box binding partners in one protein [205-209]. The canonical CLRs bound to their respective SR are structurally homologous which is also reflected in the binding of the SRs to Cullins via a helix-turn-helix motif in e.g., F-Box or BC-box [183, 204, 209, 210]. Further, most of the SRs have other substrate recruiting domains close to this motif (e.g., WD40, SH2, or Kelch). To standardize the labeling of specific complexes, the name of the CRL is combined with the SR in superscript ($CRLx^{SR}$, whereby x is the number of the Cullin). When a specific substrate-adaptor excludes other Cullins, e.g., $SCF^{F\text{-}box}$ (SKP1-CUL1-F-box), the number of the CRL is not mentioned.

Cullins have a size of roughly 100 kDa and contain multiple protein binding domains at their N- and C-terminus, which are crucial for the assembly and activation of the complex [196].

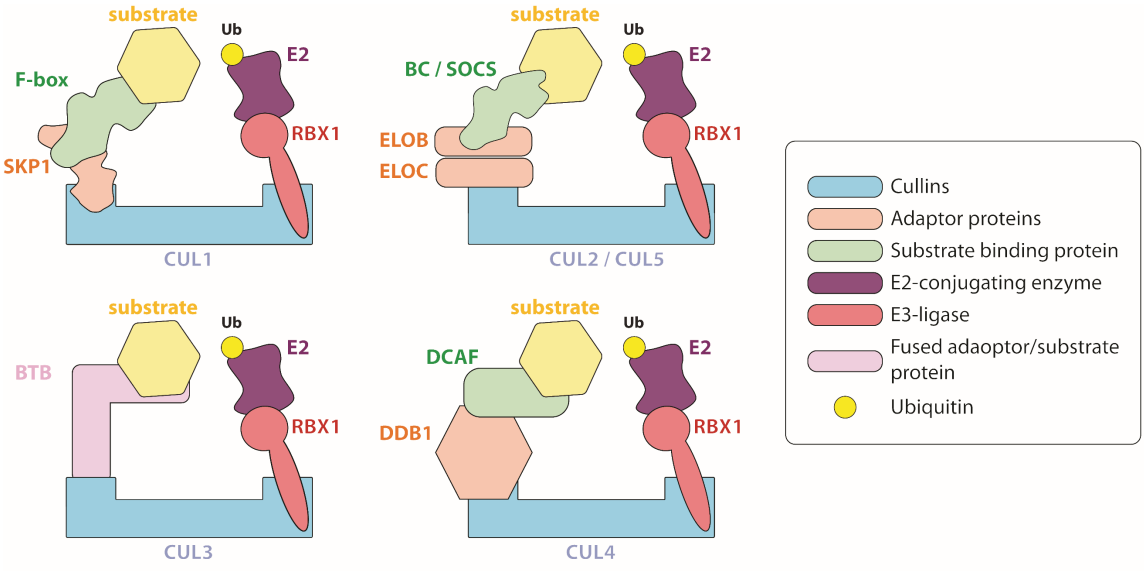

Figure 5: The different types of Cullin-Ring-Ligases.
CRLs are multi-subunit proteins with different configurations. The basic components include a scaffold protein (Cullin), an adaptor protein (SKP1, DDB1, ELOB/C), a substrate binding protein (F-box, BC/SOCS, DCAF), an E3-ligase (RBX1) and an E2-enzyme~Ub conjugate. Complexes built on Cullin 3's have a substrate-binding protein that is fused with an adaptor protein (BTB). Ub, Ubiquitin. Adapted from Wang et al. [211].

All known CRL complexes, need to be NEDDylated before they are capable of substrate ubiquitination. NEDDylation, similar to ubiquitination, requires its own E1-E2-E3 cascade, consisting of the NEDD8 activating enzyme (NAE), a NEDD8-specific E2 and an E3 complex

including DCN (defective in Cullin NEDDylation) or DCN-like proteins as well as other factors [212].

The Ubiquitin-conjugating enzyme E2 M (UBE2M) is responsible for the NEDDylation of RBX1-CUL complexes, whereas Ubiquitin-conjugating enzyme E2 F can NEDDylate RBX2-CUL5 as well as RBX1-binding complexes [213-216]. The final step of NEDD8 transfer to the respective Cullin involves the action of RBX1, which activates the UBE2M~NEDD8 intermediate in a canonical RING-E2~Ub fashion. Then, in a concerted action, DNC1, RBX1, and E2~NEDD8 transfer NEDD8 to the respective lysine situated in the winged-helix B (WH-B) domain of CUL1 or Cullins in general [196, 213-216]. The WH-B domain can be found at the C-terminus of Cullins. They also harbor a four-helix bundle (4HB), a WH-A domain, and a beta-sheet structure, that interacts with an N-terminal segment of RBX1. Furthermore, 4HB connects the N- and C-terminus leading to an organized C-terminal domain that can position the RING-domain of RBX1 into a groove [183, 196]. Since CRLs are highly abundant and regulate a plethora of processes, their composition and activity have to be tightly regulated. Therefore, CRLs can be bound by the deneddylating multiprotein COP9 signalosome (CSN) or the SR exchanging protein Cullin-associated NEDD-8 dissociated (CAND)1 [217].

CAND1 engages the whole N-terminal domain of Cullins, which consists of three tandem Cullin repeat domains (CR1, CR2, CR3) as well as the 4HB domain discussed earlier [183, 196]. Notably, the interaction with substrate receptors only requires the CR1 domain [183, 196, 218].

The presence of a substrate bound to the SR, paired with the NEDDylation status of the CRL, determines whether CSN or CAND1 are co-recruited to the complex [196].

CSN consists of eight core subunits (CSN1-8) of which CSN5 contains a JAMM (JAB1/MPN/Mov34 metalloenzyme) metalloprotease active site [219, 220]. In case CSN can access the SR, it can deneddylate and thereby deactivate CRL complexes utilizing structural rearrangements to access the WH-B domain and cleave the isopeptide bond [217, 221-224]. Association of the CSN to the CRL requires the SR to be free from ubiquitination targets since the substrates would sterically hinder CSN1 from binding to the substrate receptor [217, 225]. Another layer of CRL regulation is added by CAND1, which usually binds non-NEDDylated, SR-free Cullin-RBX complexes in vitro and cells. The interaction is enabled by CAND1's C-terminus, which binds the NTD of CUL1, and its N-terminus which engages RBX1's RING and CUL1's WH-B domain. The binding of the WH-B domain obscures the conserved lysine, thereby inhibiting NEDDylation. Interestingly, CAND1's CTD also blocks the CR1 domain, further preventing the binding of other SR modules. These

structural features allow CAND1 to perform the exchange of substrate receptors in forming or steady state CRL complexes [196, 218].

Once a fully assembled NEDDylated CRL complex binds to an E2~Ub and a substrate is present, Ub transfer can occur. As discussed earlier, E3 RING ligases, bind E2~Ub conjugates and usher them into a closed conformation for Ub transfer to a RING-bound substrate. For CRLs a similar transfer mechanism is proposed, however, how the distance between the substrate and the E2~Ub was bridged was unclear until recently. Experiments showed, that massive rearrangements of the CRL complex allow the intermediate RING-E2~Ub to orient their conjugated Ub towards the SR bound substrate, which is possible because of a specific positioning of NEDD8 in an intermediate state called "loop-out" conformation [226, 227].

1.1.2.6.3.2 SCF complex components and function

The CRL complex relevant for this work is the SCF complex, consisting of an RBX1 that is attached to the C-terminus of the scaffold protein CUL1, while the adaptor protein SKP1 binds to its N-terminus [183, 198, 228]. In turn, SKP1 can bind different F-box proteins that subsequently recruit specific ubiquitination targets [229, 230]. The binding interface between SKP1 and the F-box was determined in a crystal structure utilizing Skp1 and Skp2/FBXL1. These proteins displayed a binding surface, consisting of a triple-helix motif present in F-box domains bound to a shallow pocket in SKP1. This results in a heterodimer which continues into a hydrophobic stretch, that is formed by highly conserved F-box residues and Skp1 [183]. Additional electrostatic properties orient the F-box protein properly and thereby create a tight complex. Minor changes in the interaction surface e.g., mutations, do not abrogate the binding of yeast Skp1-Skp2. However, they result in disturbed ubiquitination possibly due to altered, less beneficial positioning of the substrate [228, 231]. The type of substrate that is recruited by the SCF complex is determined by the additional domains of the F-box protein [232, 233]. Through the binding of a particular F-box a variety of cellular functions can be regulated, ranging from cell cycle regulation and DNA damage to apoptosis [136, 234, 235].

1.1.2.6.3.2.1 F-box proteins

The F-box domain is a roughly 50 amino acid long stretch, that mediates the binding to the substrate adaptor SKP1 [230]. Additionally, F-box proteins (FBPs) are responsible for recruiting the desired ubiquitination targets to the SCF complex. In almost all FBPs, this is mediated by three different types of substrate binding domains, directly located C-terminal of the F-box domain. These domains subdivide F-box proteins into three protein families, including a total of 69 FBPs. One subfamily, which includes ten proteins, is called FBW/FBXW. It harbors an additional beta-transducin or WD40 repeat that adopts a β-propeller structure that can recognize phosphodegrons, allowing substrate recognition and their subsequent ubiquitination [236, 237].

The second subgroup includes 22 proteins and is defined by Leucine-rich repeats (FBL/FBXL). This α-β-repeat structure assumes an arc shape that also establishes substrate binding. Contrary to FBWs, phosphorylation of binding partners is neither mandatory for FBL protein binding nor the only post-translational modification that is present. FBPs were observed to interact with acetylated, hydroxylated, and glycosylated proteins [106, 238]. FBXL proteins are implicated in multiple signaling pathways, but mostly in the regulation of the cell cycle and the DNA damage response. SKP2 (also FBXL1) bound to the SCF complex, for example, targets various cyclin-dependent kinase (CDK) inhibitors (p21, p27, p57) as well as cell cycle regulators, namely c-myc or cyclin E for ubiquitination and subsequent degradation [239, 240]. Additionally, the SCF^{SKP2} complex influences other crucial pathways (AKT, mTOR, FOXO) by e.g., degrading key components such as FOXO1 [241, 242].

The last family contains 37 proteins and was initially considered to have no additional domains, which is why it was termed F-box only (FBXO/ FBX) [243]. Later analysis revealed that this family is more diverse regarding additional domains. Most FBXO proteins possess at least one of various protein-protein interaction domains. These include sugar hydrolases, so-called carbohydrate-interacting (CASH) domains, cyclin boxes, Kelch repeats as well as several others [197].

This family of F-box-containing substrate receptors also covers a myriad of functions [230]. FBX/FBXO proteins play a role in neuronal differentiation, apoptosis, the cell cycle as well as the immune system, and many other processes [244].

1.1.3 Cyclin F

Cyclin F (also called FBXO1) is a member of the FBXO family and is therefore also part of the SCF E3 ubiquitin ligase complex. CCNF, the gene encoding for cyclin F, was originally found in proximity to the locus transcribing PKD1, a gene that is important in autosomal dominant polycystic kidney disease. However, it was quickly determined to have no relation to the disease and identified as a cyclin of unknown function [245]. At around the same time Richman and Elledge isolated cyclin F from cdc4 mutant yeast as a suppressor of G1/S deficiency and thereby established a first link to cell cycle regulation [246]. They also described the fluctuation of cyclin F protein levels throughout the cell cycle. During the S-phase cyclin F starts to accumulate, reaching its peak expression in G_2 which subsequently decreases in mitosis. Cyclin F is mostly localized to the nucleus, but can also be found in the perinuclear area and to a lesser extent in the cytosol, associated with the centrosome or working, for example, as a shuttle for cyclin B to the nucleus [246-248].

Cyclins usually bind to CDKs which in turn become activated and act as serine/threonine kinases to advance the cell cycle [198, 231, 232, 249, 250]. However, even though cyclin F has a cyclin-box, it does not bind any CDKs [198, 247, 251]. Instead, it was described to harbor an F-box domain, which can interact with SKP1, linking it to the SCF complex outlined above. This F-box domain is located at the N-terminus, close to one of two nuclear localizing sequences (NLS) [198, 246]. The second NLS is located near a PEST region at the C-terminus [248]. PEST regions are amino acid stretches comprised of proline, glutamic acid, serine, and threonine and are oftentimes associated with reduced protein stability (Figure 6) [246]. In several cases, cyclin F was shown to associate with its substrates via a hydrophobic patch located in the cyclin domain. This domain interacts with an RxL motif present in substrates, similar to canonical cyclins, and mutations (e.g., M309A) in this motif lead to a loss of binding [247, 252]. Cyclin F is essential in mice and cyclin F deficient murine embryonic fibroblasts show severe cell cycle defects, further highlighting its importance [253].

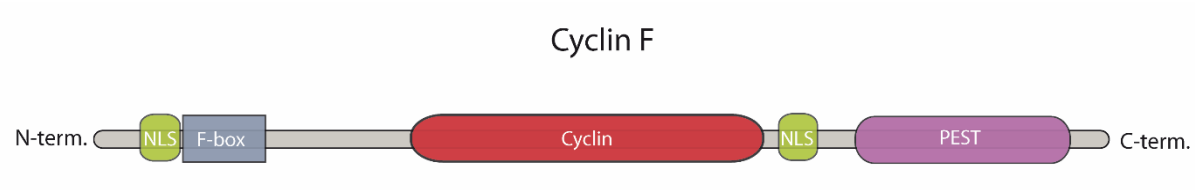

Figure 6: Cyclin F domain structure.
Cyclin F consists of two nuclear localizing sequences (NLS) responsible for the protein's nuclear localization, an F-box domain required for Cullin-Ring-Ligase (CRL) complex formation, a cyclin domain responsible for substrate binding as well as a PEST domain, which is involved in protein stability.

1.1.3.1 Functions of cyclin F and the $SCF^{cyclin\ F}$ complex

Similar to other F-box proteins, cyclin F engages in multiple cellular processes, some of which are independent of the SCF complex. One of the first publications assigning it a specific function described a direct interaction between cyclin F and cyclin B, whereby cyclin F acts as a nuclear shuttle for cyclin B [248]. Another standalone function involves the binding of Myb-related protein B (B-myb), a key player in transcriptional repression/activation of genes, regulating cell cycle progression through the G_2-phase. In case of DNA damage, cyclin F inhibits cyclin A-driven phosphorylation and activation of B-myb by competitive binding [254]. Although cyclin F is not a typical cyclin it was extensively linked to cell cycle regulation by degrading the transcriptional activators transcription factor E2 (E2F)1, E2F2, E2F3a, and E2F7, thereby orchestrating crucial aspects of cell replication, ranging from initiation to completion of the cell cycle [244, 255-257].

Furthermore, as part of the SCF-complex, cyclin F was shown to ubiquitinate CP110 (centriolar coiled-coil protein of 110 kDa) during G_2-phase. This protein is vital for centriole formation and duplication, which is why, to prevent centrosomal and mitotic abnormalities, its protein levels need to be tightly regulated [247]. Cyclin F's involvement in the preservation of nuclear integrity under normal and stress conditions is also emphasized by the regulation of DNA damage response factors such as Exonuclease 1 or RRM2 (ribonucleotide reductase M2). Further, cyclin F was shown to be responsible for mitotic spindle formation by targeting several proteins including Nucleolar and spindle-associated protein 1 [136, 244, 247, 249, 255, 258-261].

Another target called Fzr1 (Fizzy-related protein homolog) is of particular interest because its protein levels are linked with those of the $SCF^{cyclin\ F}$ complex. Fzr1 is part of the APC/C complex, where it, similarly to cyclin F, functions as a substrate receptor. APC/C^{Fzr1} degrades cyclin F during G1-phase and keeps protein levels low until late G1-phase, where cyclin F starts to accumulate, inverting the situation by degrading Fzr1 [262]. There are also other proteins involved in the degradation of cyclin F during mitosis and G1. The $SCF^{\beta\text{-}TRCP}$ complex, for instance, targets cyclin F for removal upon phosphorylation by casein kinase II [263]. Many of cyclin F's functions involve the cell cycle or genome stability, which is why in recent years cyclin F has been implicated to be crucial in multiple diseases. Several publications found that alterations in cyclin F protein levels are involved in tumorigenesis and cancer progression [264, 265]. Furthermore, mutations in CCNF were found in the context of the neurodegenerative disease ALS [266-268].

1.1.4 Autophagy

Non-selective (bulk) and selective autophagy share many components. Nevertheless, the triggers initiating selective autophagy as well as the receptors and proteins that are involved are different from those in bulk autophagy. While selective autophagy, such as lysophagy is induced upon organelle damage or similar processes, bulk autophagy can be regulated by mechanistic Target of Rapamycin (mTOR)/5' AMP-activated protein kinase (AMPK) signaling. In general, mTOR complex 1 (mTORC1) inhibits autophagy induction, however, upon activation of AMPK signaling, mTORC1 dissociates from Unc-51 Like Autophagy Activating Kinase 1 (ULK1) and allows for its phosphorylation by AMPK [269]. ULK1 is part of a complex consisting of Autophagy-related protein 101 (ATG101), Autophagy-related protein 13 (ATG13), and FAK family kinase-interacting protein of 200 kDa (FIP200) and potentially Unc-51 Like Autophagy Activating Kinase 2 (ULK2). However, the contribution of ULK2, beyond providing signaling redundancy, is not clear. Through a series of ULK1-dependent phosphorylation events the complex is activated, allowing it to trigger the production of phosphatidylinositol-3-phosphate (PI3P) via the VPS34/Phosphatidylinositol 3-kinase catalytic subunit type 3 (PI3KC3) complex. Also, it initiates the relocation of autophagy-related protein 9 (ATG9)-containing vesicles required for the generation of the autophagosomal membrane [269-277]. The VPS34 complex consists of the catalytic subunit VPS34 as well as the proteins vacuolar protein sorting 15 (VPS15), Autophagy-related protein 14 L (ATG14L), and Beclin-1. This complex produces a local pool of PI3P which initiates the formation of the phagophore via Zinc finger FYVE domain-containing protein 1 (ZFYVE1/DFCP1) and WD repeat domain phosphoinositide-interacting protein (WIPI) proteins [278-281]. The phagophore is the precursor of the final autophagosome, which is created by the elongation and closure of the circular structure, containing the engulfed cargo. One member of this family, WIPI2B is important for the recruitment of the Microtubule-associated protein 1A/1B-light chain 3 (LC3) conjugation machinery. It binds Autophagy related 16 like 1 (ATG16L1), a protein that together with Autophagy-related 12 (ATG12) and Autophagy-related protein 5 (ATG5) forms a complex that enhances the ATG3-mediated conjugation of Autophagy-related protein 8 (ATG8) family members, including LC3, to phosphatidylethanolamine (PE) present in the membrane [282]. Once ATG8 members are conjugated to the membrane, other LC3-interacting region binding components involved in autophagy and cargo recruitment can bind [283]. Furthermore, ATG8 family members are needed for the elongation and closure of the phagophore membrane, which is called the autophagosome [284, 285]. Lastly, this double-membraned structure fuses with lysosomes, which contain acidic hydrolases that degrade the engulfed cargo, making its building blocks available for the cell [286].

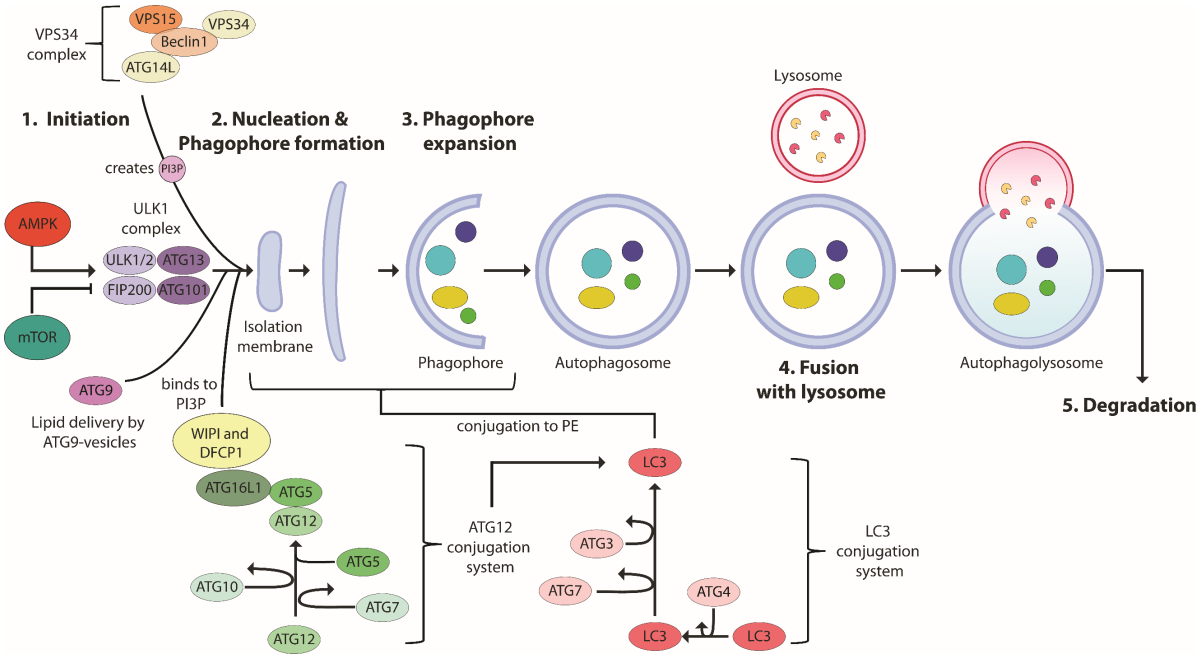

Figure 7: The autophagy machinery.
Autophagy can be initiated by several triggers such as AMPK. This leads to downstream phosphorylation events activating the ULK1 complex. ULK1 once activated, leads to the recruitment of ATG9-vesicles and the generation of PI3P by the VPS34 complex, which in turn can be bound by WIPI and DFCP1. Additionally, WIPI proteins assist in building the ATG12 conjugation system thereby enhancing the conjugation of LC3 (an ATG8 family member) to PE in the membrane. The phagophore engulfs the cargo, which requires autophagy receptors such as p62. During this process, the phagophore is elongated and closed. The resulting structure is called the autophagosome. Finally, the autophagosome fuses with a lysosome to form the autophagolysosome responsible for the degradation of the engulfed cargo. PE, phosphatidylethanolamine. Adapted from Hansen et al. [287].

1.1.4.1 Lysophagy

Lysosomes are a hub for cellular homeostasis. Not only are they crucial compartments for cargo degradation of endosomes, phagosomes, and autophagosomes, but also for metabolic signaling, membrane repair, and migration [288]. Their low pH and the multitude of hydrolytic enzymes allow lysosomes to degrade and release many cellular and extracellular components that can be recycled. Damage of this compartment, if left unresolved, results in the leakage of hydrolases, nucleases, and other degradative factors which can have a detrimental effect on cellular homeostasis, including random degradation of cellular components, the production of ROS, necrosis, and apoptosis [289].

Lysosomal damage can occur by physical disruption of the vacuole membrane caused by certain types of diseases. In the case of uric acid nephropathy, for instance, uric acid crystals form and rupture the membrane. Damage to the membrane can also be observed after the pathogen escape from the phagolysosome [290, 291]. Given the importance of lysosomal integrity, occurring damage has to be

resolved quickly. To this end, the endo-lysosomal damage response gets triggered. There are three branches, which are deployed depending on the severity of the occurring damage [292]. The first one utilizes the endosomal sorting complexes required for transport machinery to seal smaller holes after lysosomal membrane permeabilization. Afterward, lysosomes are restored to full functionality [293-295]. The second branch is linked to mTOR signaling localized at the lysosome. Upon lysosomal damage, mTOR dissociates from lysosomes and becomes deactivated, which leads to the dephosphorylation of transcription factor EB (TFEB) and its activation. This allows TFEB to translocate into the nucleus, where it induces the so-called coordinated lysosomal expression and regulation gene network which is involved in the de novo biogenesis of lysosomes and lysosomal components [292, 296-298]. However, if none of these approaches are successful lysosomes are targeted for degradation by lysophagy.

One crucial trigger for lysophagy is the exposure of glycans such as β-galactosides, which usually reside at the inner lysosomal membrane, to the cytosol [299]. In this context, galectin-1, -3, -8, and -9 are of particular interest, since they can bind to β-galactosides and trigger downstream ubiquitination events [299, 300]. Interestingly, not all galectins overlap in their function, suggesting more nuanced adaptations toward the type of inflicted damage. While galectin-8, for instance, activates antibacterial autophagy and is crucial for inhibiting the growth of *Salmonella typhimurium*, galectin-1 does not recognize damaged endosomes or vesicles containing *Salmonella* [299]. Despite these differences, galectins activate lysophagy by recruiting E3s to ubiquitinate damaged lysosomes. Tripartite motif-containing protein 16 (TRIM16), for instance, has been attributed to the ubiquitination of galectin-3 marked lysosome components, upon chemical or pathogen-induced damage [301]. TRIM16 was also shown to serve as a platform for the recruitment of core autophagy components. Of these, ULK1 and ATG16L (Autophagy) are modified with K63-linked Ub chains which are known to stabilize autophagy regulators [301, 302]. Selective autophagy, similar to LC3 in bulk autophagy, requires the recruitment of cargo receptors to enable proteins/organelle degradation. In the case of lysophagy, Tax1-binding protein 1 (TAX1BP1), Sequestosome-1 (SQSTM1/p62), Nuclear domain 10 protein 52 (NDP52), and Optineurin (OPTN) were reported to be recruited upon different cues [298, 299, 303, 304]. OPTN, for instance, was found to be involved in the clearance of lysosomes after α-synuclein induced damage, whereas NDP52 was shown to directly interact with galectin-8 upon pathogen-associated damage to endomembranes [299, 303]. Apart from galectin-associated E3s, there are F-box proteins such as FBXO2, FBXO6, and FBXO27, bound to the SCF complex, that can recognize glycans and assist in their ubiquitination. FBXO2 and FBXO6 only ubiquitinate Lysosomal-associated membrane protein (LAMP) 1 while the ubiquitination of LAMP2

requires FBXO27 [304]. The list of identified E3s that are involved in lysophagy is not exhaustive and other UPS components are yet to be deciphered. Nevertheless, Ubiquitin Conjugating Enzyme E2 Q Family Like 1 (UBE2QL1), was confirmed to be essential in K48 ubiquitination of damaged lysosomes. This further facilitates the recruitment of p62, LC3 positive membranes as well as valosin-containing protein (VCP) [298]. The triple A-ATPase VCP can bind to K48-ubiquitin chains and extract them from membranes, supposedly shuttling them for proteasomal degradation to prevent the stalling of lysosomal engulfment [298, 305]. UBE2QL1-mediated modification also occurs at the lumen of ruptured lysosomes, which also includes glycan-associated galectins [298]. Once the lysosome is fully engulfed into the autophagosome, fusion with an intact lysosome takes place leading to the degradation of the ruptured structure.

1.1.5 ALS – FTD

Amyotrophic lateral sclerosis (ALS) and frontotemporal dementia (FTD) are two fatal neurodegenerative diseases, which appear as distinct maladies. However, they form a disease continuum, sharing some of its pathomechanisms as well as clinical and genetic features [306]. Although overall progress was made by identifying common genes and mechanisms, this disease spectrum remains uncurable [307].

1.1.5.1 Frontotemporal dementia

FTD is part of the frontotemporal lobe degeneration (FTLD) disease spectrum, the second most common type of dementia in patients under 65 [308-311]. Arnold Pick described the first patients in this disease spectrum in 1892, which led to the denomination Pick's Disease (PiD) [312, 313]. This particular subtype shows histological inclusions which were first described by Alois Alzheimer [314]. Nowadays PiD is classified as a subgroup of FTD, and evaluations show that Pick bodies, which mainly consist of MAPT (microtubule associated protein tau), are present in around 10-30% of sporadic FTD cases [311, 313]. Clinically, FTD can be subdivided into a behavioral variant, associated with cognitive and behavioral changes, semantic dementia, and progressive non-fluent aphasia, in accordance with the patient's symptoms. All of these clinical manifestations are rooted in the atrophy of the frontal and temporal lobes, with distinguishable patterns that can be attributed to each subtype [315-317]. With progressive neurodegeneration, patients show a convergence resulting in severe cognitive deficits. At this stage, people struggle with everyday tasks. Approximately eight years post symptom onset, patients die from secondary infections or pneumonia [318].

1.1.5.2 Amyotrophic lateral sclerosis

ALS was first described by Jean-Martin Charcot, as a motor neuron disease (MND), naming the disease according to the symptoms he observed [319]. We now know that ALS is defined as a progressive paralysis caused by the loss of upper motor neurons in the motor cortex and lower motor neurons in the brainstem and spinal cord. Clinically, ALS presents itself with hyperreflexia, spasticity, atrophy, and progressive muscle weakness. These initial symptoms may occur in one limb or show themselves during swallowing. In later stages, the phenotype is exacerbated and bodily functions such as speaking or chewing are impaired. Ultimately this progression results in respiratory failure and death [320]. ALS is the most common motor neuron disease, with 2.1 new cases per 100.000 inhabitants a year and roughly 6.000 newly affected people in the US [321, 322]. Familial ALS (fALS) accounts for 10% of cases, implying that most cases are sporadic (sALS). Interestingly, there is an overlap of symptoms between ALS and FTD patients. In about 40-50% of the cases, ALS patients exhibit some form of FTD symptoms [323, 324].

1.1.5.3 Genetic variations and pathology in ALS/FTD

ALS and FTD are part of one disease spectrum ranging from ALS-only symptoms, over mixed pathologies, to FTD-only symptoms. So far, more than 50 genes were found to be attributed to different manifestations of the ALS/ FTD disease continuum, covering a range of important cellular functions [325-329]. While mutations in SOD1 (superoxide dismutase 1), FUS (fused in sarcoma), or TDP43 (TAR DNA-binding protein 43/TARDBP), for example, are often found in ALS; MAPT, PGRN (progranulin) and VCP (valosin-containing protein) mutations are common in FTD [330-335]. SOD1 mutations are the cause of 12-20% of hereditary ALS cases, which are genetically passed on in a dominant fashion [326, 329, 336]. The superoxide dismutase [Cu-Zn] is involved in the clearance of reactive oxygen species in the cytosol and mitochondria. Therefore, mutations can cause oxidative stress thereby deregulating cellular processes, such as protein degradation [328, 337, 338]. TDP43 and FUS, on the other hand, are both involved in RNA (ribonucleic acid) linked functions, such as splicing or mRNA trafficking [339-342]. Both proteins have a nuclear localization and were shown to shuttle between the cytosol and the nucleus [339, 343, 344]. Mutations in TARDBP, the gene encoding TDP43, are linked to 5% of familial and 1% of sporadic ALS cases, respectively [329]. Similar values (4% in fALS, 1% in sALS) can be found for FUS, which, however, are more often concurrent with juvenile onset of ALS [329]. A common feature of mutations in both genes is

cytoplasmic localization, which on one hand leads to the loss of nuclear functions and on the other to toxic aggregations of TDP43 and FUS in the cytosol [345-349]. In ALS, increased expression as well as loss of TDP43, can play a causal role, whereby additional factors such as post-translational modifications contribute to the disease [350, 351]. Lately, a liquid-liquid phase separation has been proposed as an alternative pathomechanism for FUS-related neurodegeneration [352]. While mutations in FUS and TDP43 can be found primarily in ALS, these pathological, cytosolic inclusions are also occurring in FTD patients. TDP43 inclusions are present in 97% of ALS cases and also 45% of FTD cases show these aggregates. Intriguingly, FUS inclusions are even more common in FTD (9%) than in ALS (< 1%).

Although many aggregation phenotypes are shared within the spectrum, there are exceptions. Tau, for instance, is a protein encoded by the MAPT gene, which is found in 45% of FTD inclusions but is not commonly found in ALS. [330, 331]. As a microtubule associated protein, it is vital for microtubule assembly and stabilization [331, 353]. Tau is also found to be aggregated in the brain of Alzheimer patients and is the decerning factor for other tauopathies [354, 355].

VCP mutations, in contrast to MAPT, were not only reported for FTD but also in ALS [334, 335]. The corresponding protein is the transitional endoplasmic reticulum ATPase, which belongs to the AAA-ATPase family taking part in cell division, DNA repair, lysosomal homeostasis as well as Ub-dependent protein degradation [356, 357]. Other genes associated with both ALS and FTD are SQSTM1 and TBK1, both of which are also implicated in autophagy, despite having other functions [358-361].

Figure 8: Mutations in the ALS/FTD spectrum.
Selection of mutated genes associated with ALS-only (e.g., SOD1), FTD-only (e.g., PGRN), and mixed disease phenotypes (e.g., C9orf72) on the ALS/FTD spectrum. ALS, amyotrophic lateral sclerosis; FTD, frontotemporal dementia. Adapted from Ling et al. [330].

However, the most prolific inducer of ALS/FTD is an expansion of a hexanucleotide repeat present in the guanine nucleotide exchange factor C9orf72 (C9orf72) that is the genetic cause for approximately 11% and 13% in all ALS and FTD cases, respectively [361-364].

A GGGGCC (G4C2) repeat stretch present in the untranslated region of the gene encoding for C9orf72 is usually present 20-30 times in healthy individuals [365]. Hundreds of these repeats can be found in ALS patients, although some studies suggest, that as little as 24 repeats can be enough to drive pathogenesis [362-364, 366]. Therefore, repeat length is not always a good predictor for the observed clinical phenotype [367, 368]. Resulting from these changes in the C9orf72 gene, three non-exclusive disease-driving mechanisms are proposed. First, alternative splicing may lead to haploinsufficiency, which would be associated with a loss of function mechanism. In support of this, decreased levels of C9ORF72 were readily reported in patient brain tissues. Second, a gain of function could be disease-relevant, for example, through the sequestration of RNA binding proteins (RBPs) by long repeat RNAs and the subsequent formation of stable RNA foci. Thereby RBPs can no longer execute their normal functions. Third, the production of dipeptide repeat proteins via Repeat Associated Non-AUG translation can lead to their aggregation and toxicity in cells [369].

1.1.5.3.1 Overview of deregulated pathways and involved genes & neuro-inflammation

The molecular mechanisms causing ALS are not fully understood, however, several factors contributing to the disease, such as oxidative stress, RNA toxicity as well as neuro-inflammation have been identified. Among them are also a disturbance in protein homeostasis manifesting itself in protein aggregation, altered chaperone function, and defects in autophagy. Protein homeostasis encompasses everything from protein translation up to degradation and is crucial to maintain cellular health. Upon stress, several coping mechanisms are initiated, including the unfolded protein response, ERAD, and heat shock response. Interestingly, almost every process in this intricate system seems to be affected in ALS in some way [370].

1.1.5.4 Protein folding affected by ALS mutations

In ALS, the chaperone system is disturbed, and crucial HSPs are mutated or sequestered. Several studies using human cell lines established a link between important chaperones and aggregation-prone ALS-linked proteins. Similar to TDP43, chaperones can also be found in ALS inclusions [370, 371]. In fALS-mimicking SOD1G93A mice, Hsc70 and Hsp90 were found in the insoluble fraction [372, 373]. Mouse cells harboring the same mutation or the SOD1G85R mutation also exhibited increased binding to molecular chaperones [374, 375]. Both of these results point to the sequestration of chaperones and subsequent dysfunction of the system, which can also be seen in the SOD1G93A mouse model. Here, a decrease in alpha(B)-crystallin and other chaperones are associated with faster

disease progression [376]. Interestingly, a transgenic TDP43 Q331K mouse model shows a similar decrease in Hsp70 and Hsp40, coinciding with a decrease in heat shock factor 1 (HSF1) protein levels, a protein that is usually involved in the heat shock response. This finding suggests an additional layer of dysregulation [377]. However, in contrast to a decrease in Hsp70/Hsp40, the changes in HSF1 levels could not be recapitulated in ALS patient brains [377]. Furthermore, knockdown of Hsp70 and Hsp90 in neuroblastoma cell lines increased cytoplasmic TDP43 species, prone to aggregation, whereas activation of Hsp70 decreased TDP43 aggregation [378, 379].

Intriguingly, a study in fruit flies indicates that this is also true for FUS aggregates. Overexpression of Hsc70 decreased FUS in the insoluble fraction [380]. The upregulation of chaperones may therefore be a protective mechanism to reduce toxicity in ALS, as implied by an increase in heat shock protein family B (small) member 1 (HspB1) and member 8 (HspB8) chaperones compared to healthy controls. [381]. Nevertheless, chaperones may not only play a beneficial role in ALS. Truncations in DnaJ homolog subfamily C member 7, the gene encoding for Hsp40, were also reported in ALS [382].

1.1.5.5 Cyclin F in ALS

The number of reported disturbances of protein homeostasis in ALS suggests the involvement of a malfunctioning UPS in disease progression. In line with these observations, overexpression of the CCNF mutant S621G in SH-SY5Y and Neuro-2A cells was reported to cause elevated K48 ubiquitination levels and a downstream disturbance of autophagosome-lysosome fusion [383]. This mutation, among others, was further analyzed in HEK cells and patient-induced pluripotent stem cells where it was shown to cause an activation of apoptosis pathways, potentially via increased cleavage of caspase 3 [384]. By overexpressing the S621G mutant of CCNF, this could be confirmed in zebrafish [385]. Additionally, these zebrafish showed aberrant neuronal branching and reduced motor function [385]. Other mutations in CCNF are less well characterized and distributed throughout the gene, with no obvious clustering at functionally described sites, such as the cyclin- or PEST-domain [267, 268, 386-388]. Nevertheless, for several of those mutations, an increased ubiquitination phenotype was described which postulates a gain of function [383, 386]. Among those hyper-ubiquitinated proteins was TDP43, one of the major inclusions in ALS-aggregates [386]. Additionally, the binding of cyclin F toward VCP is enhanced in N-terminal CCNF ALS-mutants and drives increased VCP activity in some of those mutants, which in turn promotes cytoplasmic aggregation of TDP43 [389].

1.1.6 Methods

1.1.6.1 diGly profiling

Because of their volatile nature and constant rearrangements, post-translational modifications are hard to pinpoint. Therefore, many different techniques have been developed, some of which also help to determine if and where proteins are ubiquitinated. Taking advantage of the isopeptide bond between the C-terminal glycine of Ub and the ε-amino group of substrate lysines allows the identification of ubiquitinated proteins and their specific sites. By trypsinizing the Arg-Gly-Gly sequence, a remnant glycine-glycine (diGly) motif remains on the substrate, which can then be bound by an α-diGly antibody to purify diGly modified peptides [390-393]. Using mass spectrometry to identify these modified peptides enables the investigation of potential ubiquitination sites. This approach is often paired with stable isotope labeling by amino acids in cell culture (SILAC) [394, 395]. Light (K0) and heavy (K8) lysine are utilized to label cells in cell culture and compare the relative ubiquitination levels of specific sites in two conditions [396]. However, the diGly motif is not unique to trypsinized Ub bonds, since it also occurs in two other ubiquitin-like modifiers after trypsin cleavage, namely NEDD8 and Interferon-stimulated gene 15 (ISG15). In one study, ISG15 accounts for only 17 diGly sites and is therefore negligible compared to the overall 720.000 diGly modified peptides. NEDD8 accounts for up to 25% of diGly sites after combined treatment with Bortezomib (proteasome inhibitor) and USP2cc (recombinant DUB) [393].

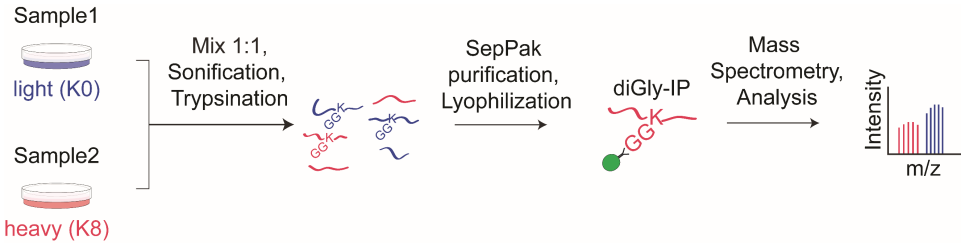

Figure 9: Remnant glycine-glycine (diGly) analysis of ubiquitinated proteins by mass spectrometry. To assess differences in ubiquitination between the two conditions, samples are labeled with heavy or light amino acids (in this case lysine) and mixed in a 1:1 ratio. Then they are further processed under denaturing conditions to prepare them for immunoprecipitation with an anti-diGly antibody. After purification, the proteins are analyzed via mass spectrometry. GG, glycine-glycine; K, lysine; K0, light lysine; K8, heavy lysine; m/z, mass/charge. Adapted from Fulzele et al. [397].

1.1.6.2 Proximity proteomic profiling

The identification of stable protein-protein interactions benefited from readily available tools in the form of affinity tags immunoprecipitations, that, coupled with mass spectrometry or immunoblotting,

could provide a better insight into many pathways. However, more transient interactions are harder to capture. Therefore, two methods for mapping the vicinity of proteins were developed over the past years. The first one, referred to as BioID, utilizes the promiscuous *Escherichia coli* biotin ligase BirA fused to a protein that is subject to investigation. By providing biotin to the reaction, all lysines within approximately a 10 nm radius are biotinylated and can be subsequently purified for mass spectrometry analysis [398, 399]. However, labeling takes several hours, which tilts the analysis towards more static proximity partners. The second approach deploys an ascorbate peroxidase known as APEX or APEX2 (2^{nd} generation) that is fused to a protein of interest (POI) and introduced in cell culture. These cells are provided with biotin-phenol for 30 minutes and subsequently treated with H_20_2 for only one minute, thereby creating a very short-lived biotin phenoxyl radical that tags electron-dense side chains within a 20 nm radius [400, 401]. The short hydrogen peroxide pulse creates a snapshot of the short-term environment of the POI, supplementing missing information gathered from other approaches.

1.2 Aim of the study

Degradation pathways such as the UPS system and autophagy are crucial for cellular integrity. The UPS system is involved in the degradation of short-lived or damaged proteins and also regulates several biological processes, including mitosis. Autophagy, on the other hand, is responsible for the removal of larger structures such as protein aggregates and organelles. It is also known to be responsible for nutrient availability during starvation.

Although much is known about both degradation processes, many details remain to be elucidated. My Ph.D. will focus on finding new substrates for cyclin F and new proteins associated with lysophagy after lysosomal damage. cyclin F is the substrate recognition module of the $SCF^{cyclin\ F}$ RING ubiquitin ligase complex, a complex involved amongst other things in genomic stability and mitosis. As cyclin F has been implicated in the motor neuron disease amyotrophic lateral sclerosis (ALS), the main part of my Ph.D. thesis aims to identify novel substrates of cyclin F in neuron-like cells using affinity-based immunoprecipitation approaches in wild-type and ALS-associated mutants of the protein. In addition, together with our collaborators from the group of Hemmo Meyer, I intend to use APEX-2-based proximity proteomics to investigate potential new interactors of Calponin 2, a protein that regulates actin filaments to drive lysophagy after substantial lysosomal damage.

2 Publications

2.1 Publication I

ALS-linked loss of Cyclin-F function affects HSP90

Published as:

Siebert A, Gattringer V, Weishaupt JH, Behrends C. ALS-linked loss of Cyclin-F function affects HSP90. Life Sci Alliance. 2022 Sep 16;5(12):e202101359. doi: 10.26508/lsa.202101359. PMID: 36114006; PMCID: PMC9481933.

Contribution:

As the first author of this publication, I played a substantial role in the conceptual design of the study. I performed all experiments, their formal analysis, and visualization, with minimal experimental contributions from Vanessa Gattringer during the revision process. I wrote the original draft of the publication and, together with Christian Behrends, reviewed and edited this study.

Research Article

TRANSPARENT PROCESS OPEN ACCESS Life Science Alliance

ALS-linked loss of Cyclin-F function affects HSP90

Alexander Siebert[1], Vanessa Gattringer[1], Jochen H Weishaupt[2], Christian Behrends[1]

The founding member of the F-box protein family, Cyclin-F, serves as a substrate adaptor for the E3 ligase Skp1-Cul1-F-box (SCF)$^{Cyclin-F}$ which is responsible for ubiquitination of proteins involved in cell cycle progression, DNA damage and mitotic fidelity. Missense mutations in *CCNF* encoding for Cyclin-F are associated with amyotrophic lateral sclerosis (ALS). However, it remains elusive whether *CCNF* mutations affect the substrate adaptor function of Cyclin-F and whether altered SCF$^{Cyclin-F}$–mediated ubiquitination contributes to pathogenesis in *CCNF* mutation carriers. To address these questions, we set out to identify new SCF$^{Cyclin-F}$ targets in neuronal and ALS patient–derived cells. Mass spectrometry–based ubiquitinome profiling of *CCNF* knockout and mutant cell lines as well as Cyclin-F proximity and interaction proteomics converged on the HSP90 chaperone machinery as new substrate candidate. Biochemical analyses provided evidence for a Cyclin-F–dependent association and ubiquitination of HSP90AB1 and implied a regulatory role that could affect the binding of a number of HSP90 clients and co-factors. Together, our results point to a possible Cyclin-F loss-of-function–mediated chaperone dysregulation that might be relevant for ALS.

DOI 10.26508/lsa.202101359 | Received 30 December 2021 | Revised 2 September 2022 | Accepted 5 September 2022 | Published online 16 September 2022

Introduction

Conjugation of ubiquitin (Ub) to proteins (i.e., ubiquitination) controls many cellular processes by directing its targets to proteasomal degradation or altering the functional properties of its targets in a regulatory manner. These different outcomes are the results of an intricate interplay between different types of Ub modifications and their recognition by distinct Ub-binding proteins. The complexity arises from the fact that proteins can be modified either by single Ub molecules on one or multiple lysines and/or by homotypic or branched Ub chains in which Ub moieties are linked via one or several of their seven lysine residues (K6, K11, K27, K29, K33, K48, and K63) and/or the N-terminal methionine (M1) (1). Ubiquitination involves an enzymatic cascade consisting of three orchestrated steps (2). First, an E1-activating enzyme uses ATP to form a Ub thioester on its active cysteine. Subsequently, this Ub is transferred to an E2 conjugating enzyme yielding an E2~Ub thioester (E2~Ub). Last, an E3 ligase recognizes the substrate and brings it into proximity of the E2~Ub. Depending on the class of E3 ligase, the final step involves either the formation of an E3~Ub thioester before the Ub transfer onto substrates or the direct transfer of Ub from the E2 to the substrate (2, 3). The latter mechanism is used by the family of really interesting new gene (RING) E3 ligases of which Cullin-RING ligases (CRLs) represent the largest subgroup. CRLs are modularly built complexes consisting of one of the seven scaffolding Cullins (e.g., CUL1), the RING-finger protein RBX1 which recruits the E2~Ub and a member of one of the several substrate adaptor families such as the F-box proteins (4).

The founding member of this latter family, FBX1 (also known as FBXO1 or Cyclin-F), uses its F-box to bind to CUL1 via the adaptor SKP1, whereas the cyclin domain of Cyclin-F interacts with ubiquitination targets (5, 6). This is different from other cyclins which use their cyclin domain to bind to cyclin-dependent kinases as part of their signaling function during the cell cycle (5, 7, 8, 9, 10). Nevertheless, the Skp1-Cul1-F-box (SCF)$^{Cyclin-F}$ ligase complex controls cell cycle progression by binding to the substrate adaptor fizzy-related protein homolog (FZR1) and by ubiquitinating the transcription factor E2F7 (11, 12). Moreover, Cyclin-F binds the centriole regulator CP110 and the ribonucleotide reductase RRM2 in a cell cycle-dependent manner and mediates their ubiquitination which targets both proteins for proteasomal degradation and is required for maintenance of mitotic fidelity and genome integrity (13, 14). Besides, SCF$^{Cyclin-F}$ contributes to the regulation of other diverse cellular processes such as DNA damage response and mitotic spindle formation by ubiquitinating Exonuclease 1 and Nucleolar and spindle-associated protein 1 (15, 16).

Cyclin-F has been implicated in several diseases. For example, alterations in Cyclin-F protein levels are linked to tumorigenesis and cancer progression (17, 18). Furthermore, mutations in *CCNF*, the Cyclin-F gene, are associated with amyotrophic lateral sclerosis (ALS) (19, 20, 21). ALS is a rapidly progressing neurodegenerative disorder that clinically presents itself through progressive paralysis caused by upper and lower motor neurons loss, which ultimately leads to respiratory failure and thereby death (22). The molecular mechanisms causing ALS are not fully understood; however, several processes contribute to the disease such as increased oxidative stress, dysbalanced cytoskeleton dynamics, disrupted RNA homeostasis and

[1]Munich Cluster for Systems Neurology (SyNergy), Medical Faculty, Ludwig-Maximilians-University München, Munich, Germany [2]Division of Neurodegenerative Disorders, Department of Neurology, Medical Faculty Mannheim, Mannheim Center for Translational Neurosciences, Heidelberg University, Mannheim, Germany

Correspondence: christian.behrends@mail03.med.uni-muenchen.de

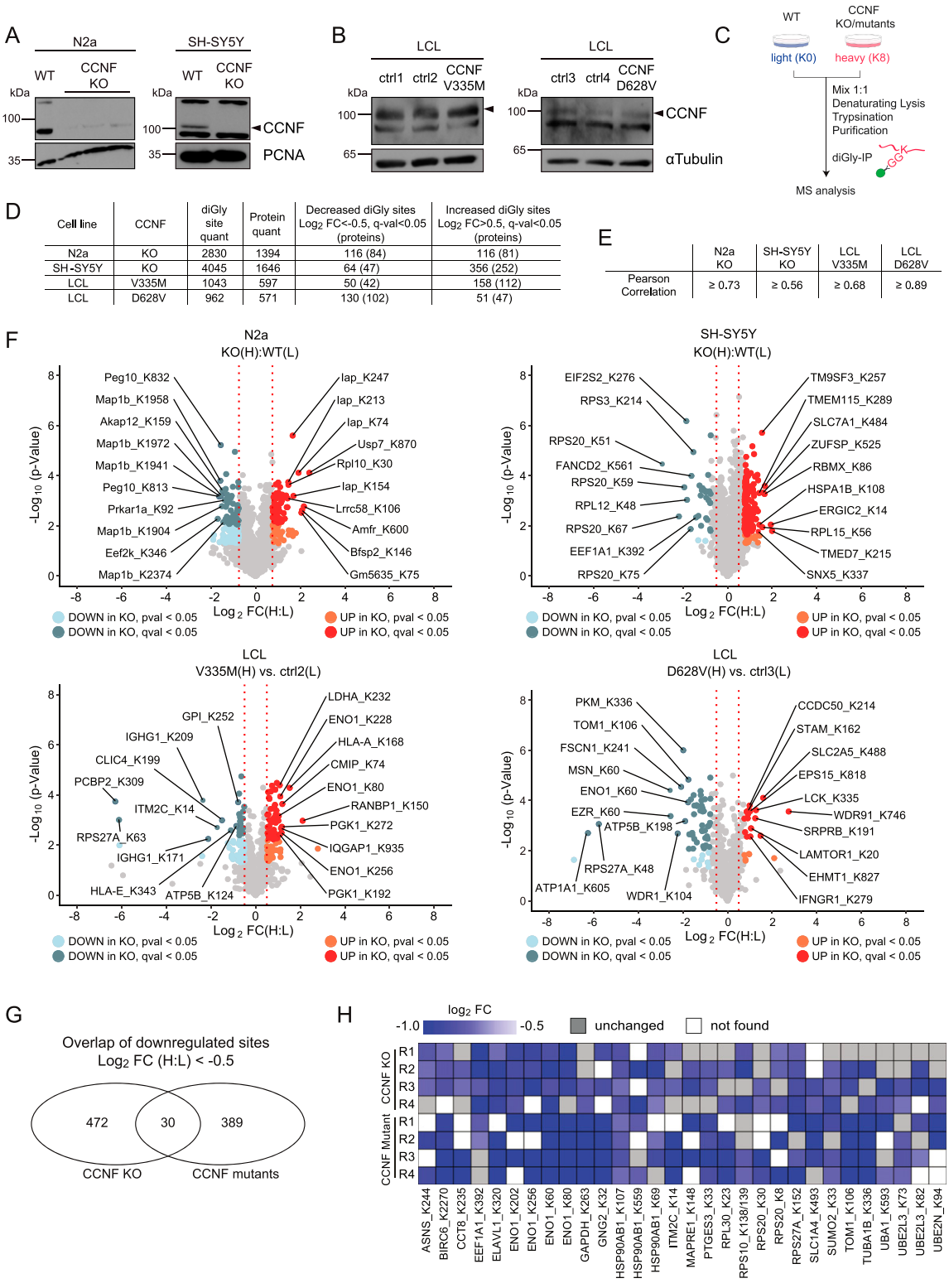

Figure 1. Ubiquitinome analysis of *CCNF* knockout and mutant cells.
(A, B) Immunoblot analysis of N2a and SH-SY5Y CCNF wild-type (WT) and knockout (KO) cells (A) as well as of lymphoblastoid cells (LCLs) from healthy individuals (ctrl1-4) and amyotrophic lateral sclerosis patients carrying the CCNF mutations V335M and D628V (B). **(C)** Schematic overview of diGly proteomic experiments. Differential SILAC-labeled CCNF WT (N2a, SH-SY5Y) or ctrl (LCLs) and CCNF KO (N2a, SH-SY5Y) or mutant cells (LCLs) were mixed at a 1:1 ratio followed by denaturing lysis, sequential diGly immunoprecipitation, tryptic digestion, desalting, and mass spectrometry analysis. **(D)** Summary of diGly-modified lysines (sites) and proteins from biological replicate experiments (n = 4). Threshold for regulated sites was $\log_2$ fold change (FC) (H:L) > 0.5 or <−0.5 with a q-value < 0.05 (*t* test). **(E)** Pearson correlation of H:L ratios for

disturbance in protein homeostasis. The latter is manifested by protein aggregation, altered chaperone function and unfolded protein response as well as defects in autophagy and the ubiquitin-proteasome system (UPS) (23). Consistently, overexpression of Cyclin-F carrying the ALS linked S621G mutation was reported to increase ubiquitination in general and in particular ubiquitination of the known $SCF^{Cyclin\text{-}F}$ target RRM2 and of the neuropathological ALS marker RNA-binding protein TDP43 in combination with UPS and autophagy impairments (24, 25). In addition, this mutation caused apoptosis activation in different cell models including patient-derived iPSCs and in zebrafish overexpressing Cyclin-F S621G. Intriguingly, these animals showed aberrant neuronal branching and reduced motor function (26, 27). Whereas other ALS mutations in *CCNF* are less well characterized and distributed throughout the *CCNF* gene with no obvious clustering at encoded domains such as the cyclin or PEST domain (20, 21, 24, 28, 29), Cyclin-F S621G served as a paradigm to postulate a gain of toxic function mechanism. Notably, some ALS *CCNF* mutations might perturb cellular proteostasis independent of the SCF substrate adaptor function of Cyclin-F (30). Hence, it remains elusive to what extent altered substrate ubiquitination by $SCF^{Cyclin\text{-}F}$ contributes to phenotypic manifestations related to ALS pathogenesis. For the most part, this is due to a lack of knowledge on $SCF^{Cyclin\text{-}F}$ targets in neuronal and patient-derived cells.

In this work, we combined quantitative mass spectrometry-based ubiquitin remnant profiling in N2a and SH-SY5Y CCNF knockout cells as well as patient-derived lymphoblastoid cell lines with proximity and interaction proteomics to uncover Cyclin-F ubiquitination targets. Using this approach, we identified the chaperone HSP90AB1 as a new Cyclin-F binding protein which is constitutively ubiquitinated in a Cyclin-F wild-type dependent manner. Importantly, Cyclin-F–mediated ubiquitination of HSP90AB1 regulates the binding of a number of HSP90 clients and co-factors. Overall, our findings indicate that $SCF^{Cyclin\text{-}F}$ is required for fine tuning of parts of the cellular chaperone machinery and highlight a role for a loss-of-function mechanism in CCNF ALS.

Results

Ubiquitinome analysis of Cyclin-F–deficient cells

To advance our understanding of Cyclin-F malfunctioning in ALS, we set out to identify potential new $SCF^{Cyclin\text{-}F}$ substrates in two complementary cellular systems. First, we used CRISPR/Cas9 technology to delete CCNF in two neuron-like cell types, namely murine N2a and human SH-SY5Y (Fig 1A). Second, we used two different ALS patient–derived lymphoblastoid cell lines (LCLs) which expressed Cyclin-F carrying the mutations V335M and D628V. Whereas V335M is located in the cyclin domain responsible for binding $SCF^{Cyclin\text{-}F}$ substrates, D628V is part of the PEST domain which is thought to control the stability of Cyclin-F (31). Notably, both CCNF mutant LCLs did not show overt differences in Cyclin-F protein levels compared with their two respective gender- and age-matched control LCLs (ctrl1-4) carrying wild-type CCNF (Fig 1B). Next, we performed quantitative diGly proteomics to uncover ubiquitination sites which show decreased abundance in this panel of CCNF KO and mutant cell lines and hence represent potential ubiquitination targets of $SCF^{Cyclin\text{-}F}$. For this purpose, we combined stable isotope labeling by amino acids in cell culture (SILAC) with immunoaffinity-based enrichment of diGly remnant-containing peptides after tryptic digestion of ubiquitinated proteins. Briefly, CCNF WT and KO N2a and SH-SY5Y cells as well as CCNF WT and mutant LCLs were differentially SILAC labeled, lysed under denaturing conditions and combined in a 1:1 ratio per cell line. After protein extraction and proteolytic digestion, tryptic peptides were subjected to sequential anti-diGly immunoprecipitation (IPs) and analyzed by mass spectrometry (MS) (Fig 1C). In quadruplicate experiments, we quantified a total of 2,830 and 4,045 non-redundant diGly sites in 1,394 and 1,646 proteins in N2a and SH-SY5Y, respectively (Figs 1D and S1A). In LCLs, diGly experiments were performed using four biological replicates for each of the two controls. Therefore, the values reported are the sum of both controls compared with each mutant. The amount of total diGly sites and corresponding proteins was lower in LCLs compared to the KO cell lines with 1,043 and 962 unique diGly sites in 597 and 571 proteins in LCLs expressing CCNF V335M and D628V, respectively (Figs 1D and S2A). Using statistical analysis (*t* test with a q-value of <0.05), we identified between 50 and 130 diGly sites (42–102 proteins) with $\log_2$ fold change (FC) < −0.5 in SH-SY5Y, N2a, and LCL cells (Fig 1D and Table S1). Pearson's correlation coefficients between 0.56 and 0.89 indicated high reproducibility between biological replicate samples (Fig 1E). Consistent with Cyclin-F's role in nuclear processes (7, 11, 32, 33), a number of diGly sites that decreased in abundance upon CCNF KO or mutation were found in proteins associated with RNA- or DNA-binding and other nuclear functions (Peg10 in N2a; RPS20, RPL12, and FANCD2 in SH-SY5Y; PCBP2 in CCNF V335M LCLs) (Fig 1F). Other strongly decreased ubiquitination sites were associated with the cytoskeleton which is known to be altered in ALS. For example, five different diGly sites in MAP1B, an α-tubulin binding protein, were found to be down-regulated with a $\log_2$ FC < −1.5 in N2a cells, whereas several actin-binding proteins such as MSN, FSCN1, and WDR1 showed decreased ubiquitination in CCNF D628V LCL cells (Fig 1F). Notably, Ub diGly sites representing K63- and K48-linked chains were decreased in both LCLs (RPS27A_K63 in V335M; RPS27A_K48 in D628V) which is different from reports describing elevated Ub K48 levels in cells expressing the ALS-linked Cyclin-F mutation S621G (34). Taking into account that the four cell

four respective eight biological replicates in N2a, SH-SY5Y, and LCLs described in Fig 1D. **(F)** Volcano plots depicting relative changes in diGly site abundance for N2a and SH-SY5Y CCNF WT versus KO as well as for representative ctrl versus CCNF mutant LCLs. Significantly decreased or increased diGly sites in CCNF KO and mutant cells were labeled in indicated bright or dark colors representing *P*-value < 0.05 or q-value < 0.05 (*t* test). Top 10 increased and decreased diGly sites with the highest fold change are highlighted. Known CCNF interactors are labeled with black circles. **(G)** Overlap of decreased diGly sites in CCNF KO (N2a and SH-SY5Y) and CCNF mutant conditions (LCLs) with $\log_2$ FC < −0.5 in two of four biological replicates. **(H)** Heat map of commonly decreased diGly sites in CCNF KO and mutant cells. Blue scale indicates $\log_2$ FC compared with the respective control. Grey boxes mark biological replicates of unchanged diGly sites. White boxes mark biological replicates where the diGly site was not found.

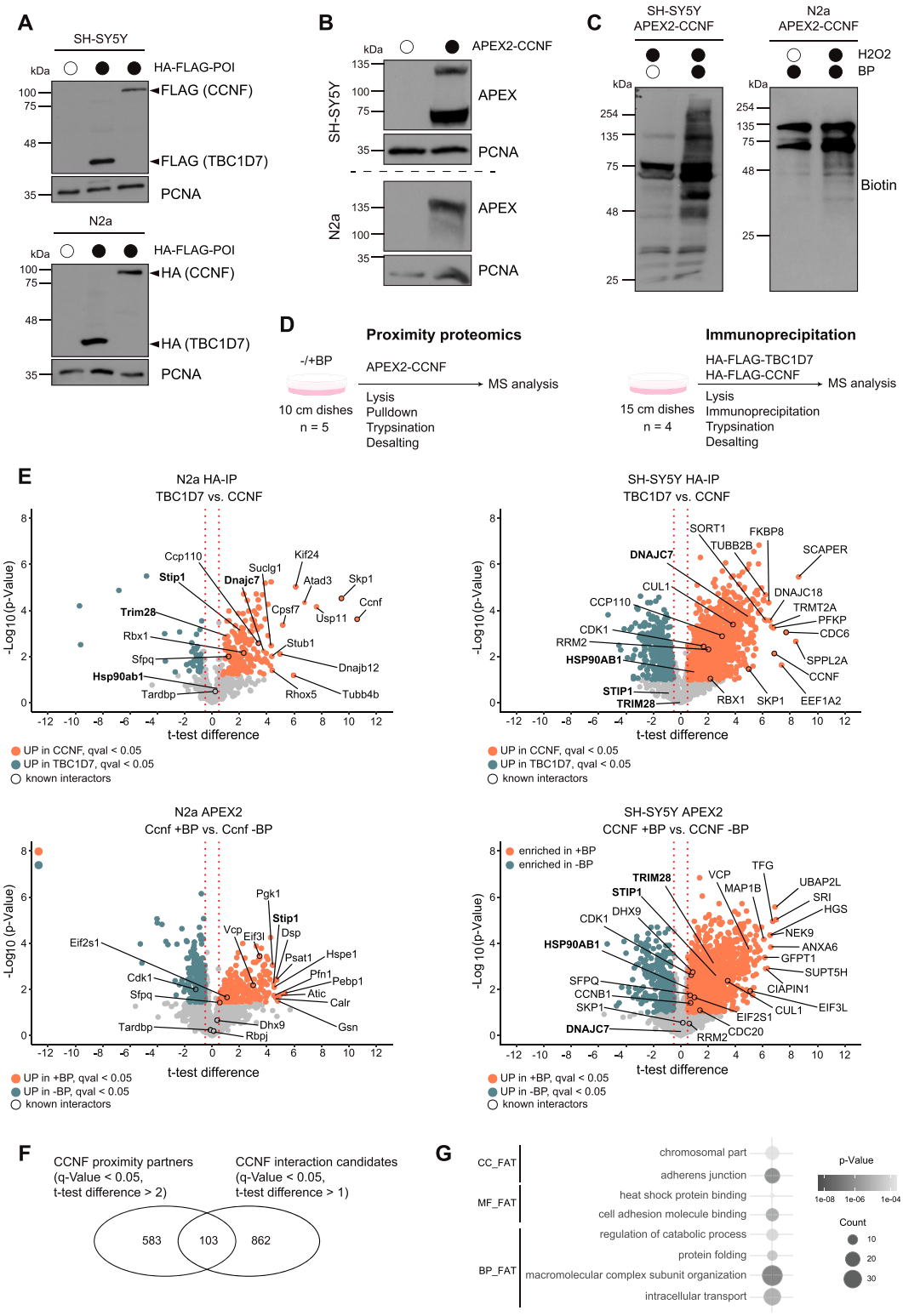

Figure 2. Cyclin-F proximity and interaction proteomics.
(A, B) Lysates from empty and HA-FLAG-CCNF or -TBC1D7 (A) and APEX2-CCNF (B) overexpressing SH-SY5Y and N2a cells were analyzed by SDS–PAGE and immunoblotting. **(C)** Biotinlyation in SH-SY5Y and N2a cells overexpressing APEX2-CCNF was induced by 30 min biotin-phenol (BP) and 1 min H_2O_2 treatment followed by lysis and immunoblot analysis. **(D)** Schematic overview of proximity and interaction proteomics workflow. **(E)** Volcano plots showing changes in abundance of candidate interacting proteins of HA-FLAG-TBC1D7 (control) and HA-FLAG-CCNF in N2a and SH-SY5Y (upper panel) and of proximity partners of APEX2-CCNF in the absence (control) and presence of BP in N2a and SH-SY5Y (lower panel). Proteins enriched in HA-FLAG-CCNF immune complexes or in proximity to APEX2-CCNF are shown in orange

lines are from very different origins and genetic backgrounds, we applied less stringent filtering using $\log_2$ fold change ($\log_2$ FC < −0.5 in at least two biological replicates per each condition) without statistical testing to identify commonly decreased diGly sites in CCNF KO and mutant cells. Using this approach, we found 30 potential ubiquitination sites shared between both CCNF deficiency conditions (Fig 1G). Importantly, protein expression profiling revealed that the vast majority of these potential Cyclin-F ubiquitination targets remained unchanged at the total protein level (Fig S1B and C and Table S2). The corresponding proteins participate in various cellular processes such as RNA (RPL30, RPS10, RPS20, and ELAVL1) and microtubule (MAPRE1) binding as well as ubiquitination (UBA1, UBE2N, and RPS27) (Fig 1H). Of particular interest were diGly sites found in chaperones (HSP90AB1 and CCT8) because disturbance of protein homeostasis is thought to commonly contribute to ALS pathogenesis (23).

Identification of proximity and interaction partners of Cyclin-F

Complementary to the ubiquitinome profiling approach, we performed proximity biotinylation and IP coupled to MS analysis to identify potential $SCF^{Cyclin\text{-}F}$ targets. For this purpose, we generated N2a and SH-SY5Y cell lines, stably expressing Cyclin-F either tagged with a HA-FLAG-tag or fused to a myc tagged version of the engineered ascorbate peroxidase APEX2 (Fig 2A and B). Notably, the functionality of the APEX2 fusion was examined by inducing biotinylation in N2a and SH-SY5Y cells (Figs 2C and S2A). For proximity proteomics cells were grown in the presence of biotin-phenol (BP) for 30 min followed by a 1-min H_2O_2-pulse to induce biotinylation. Subsequently, biotinylated proteins were subjected to streptavidin pull-downs. Conversely, interaction proteomics involved enrichment with anti-HA affinity resin and elution with HA peptide. In both cases, samples were digested with trypsin and analyzed by MS (Fig 2D). Expression of HA-FLAG- or APEX2-TBC1D7 or omission of BP was used as negative control conditions. Analysis of Cyclin-F interaction candidates identified in N2a and SH-SY5Y revealed several known interactors such as the $SCF^{Cyclin\text{-}F}$ ligase components SKP1, RBX1, and CUL1 as well as a number of their targets including CCP110, RRM2, CDK1, CDC6, and SFPQ (Fig 2E and Table S3). Besides, a large number of proteins were found enriched following Cyclin-F IP compared with the control TBC1D7 IP. Intriguingly, the interaction candidates with the greatest *t* test difference and a q-value < 0.05 featured a number of functional categories which were also found in the diGly proteomics experiments including chaperones (Dnajc7, Dnajb12, Stub1 in N2a; DNAJC7, DNAJC18, and FKBP8 in SH-SY5Y) and cytoskeleton associated proteins (Kif24, Atad3, Tubb4b, TUBB2B). The proximity partners detected in both cell lines covered a similar molecular landscape with multiple known Cyclin-F–binding partners (CUL1, SKP1, RBX1, CCP110, CDC6, RRM2, VCP, SFPQ, EIF2S1, EIF3L, and DHX9), chaperones (STIP1 HSP90AB1) and cytoskeleton-binding proteins (Myh10, Dsp, Vcl, and MAP1B) (Figs 2E and S2B and Table S4). The fact that we used different cell types and varying experimental conditions (HA-IP versus APEX2) might explain the observed discrepancies in the detection and scoring of established Cyclin-F–binding partners (Fig S2C). Comparison of both approaches revealed 103 proteins that were commonly found enriched by CCNF proximity and interaction proteomics (Fig 2F). Functional annotation clustering of these shared potential CCNF targets using DAVID yielded gene ontology (GO) terms in accordance to known functions of Cyclin-F in nuclear processes (e.g., chromosomal part) but also functions that were not primarily associated with Cyclin-F such as protein folding and heat shock protein binding (Fig 2G).

Validation of the HSP90 chaperone machinery as Cyclin-F–binding partner

Taking advantage of our parallel proteomics approaches, we searched the data sets for proteins that were enriched in CCNF's proximitome and interactome (Fig 2F) but carried decreased diGly sites when CCNF was deleted or mutated (Fig 1H). This analysis revealed two new potential Cyclin-F targets, TUBA1A and HSP90AB1 (Fig 3A). Given the role of altered proteostasis in ALS pathogenesis, we focused our subsequent efforts on HSP90AB1. First, we probed for the association of HSP90AB1 with Cyclin-F by IP and immunoblotting. In contrast to the control FBXO28, Cyclin-F showed clear binding to HSP90AB1 (Fig 3B). Intriguingly, two HSP90 co-chaperones DNAJC7 and STIP1 (also known as HOP) present in our proteomics data sets with similar but less prominent features as HSP90AB1 were likewise found to specifically associate with Cyclin-F compared to FBXO28, whereas the CUL1 adaptor SKP1 bound to both F-box proteins (Fig 3B and C). In addition, a number of other interaction candidates such as the Ub-binding protein TOLLIP and the SUMO E3 ligase TRIM28 were also confirmed as Cyclin-F–binding partners (Fig S3A and B). Second, we examined whether the ALS-linked mutations in Cyclin-F affect the binding to HSP90AB1. Thereto, we reconstituted CCNF KO SH-SY5Y cells with wild-type (WT) or mutant (V335M or D628V) HA-FLAG–tagged Cyclin-F and performed HA-IPs. However, Cyclin-F immunoprecipitates showed no overt changes in HSP90AB1 levels across the different Cyclin-F variants (Fig 3D). These findings indicate that HSP90AB1 is a new Cyclin-F interacting protein which binds to Cyclin-F independent of two different ALS-linked CCNF mutations. Notably, the HSP90AB1-Cyclin-F interaction could represent a ligase-substrate or chaperone-client relationship.

Cyclin-F–dependent ubiquitination of HSP90AB1 regulates its chaperone cycle

To test whether HSP90AB1 is indeed ubiquitinated, as suggested by our diGly proteomics, we performed denaturing IPs with HA-FLAG-HSP90AB1 and HA-FLAG-TBC1D7 as a negative control. Immunoblotting of HA immunoprecipitates with a K48 linkage specific polyUb antibody (Ub-K48) unveiled Ub conjugates on HSP90AB1 which were sensitive to treatment with the deubiquitinase USP2

(*t* test difference > 0.5, q-value < 0.05, FDR-corrected, *t* test). Top 10 significantly enriched proteins, known CCNF interactors (black circles) and selected candidates are highlighted. **(F)** Overlap between proximity partners (q-value < 0.05, *t* test difference > 2, *t* test) and interaction candidates (q-value < 0.05, *t* test difference > 1, *t* test). **(E, G)** Gene Ontology (GO) analysis of proteins found in the overlap of (E). Grey gradient represents *P*-values. The number of proteins (count) found associated with a given GO term is indicated by the size of the circles. BP, biological process; CC, cellular component; MF, molecular function.

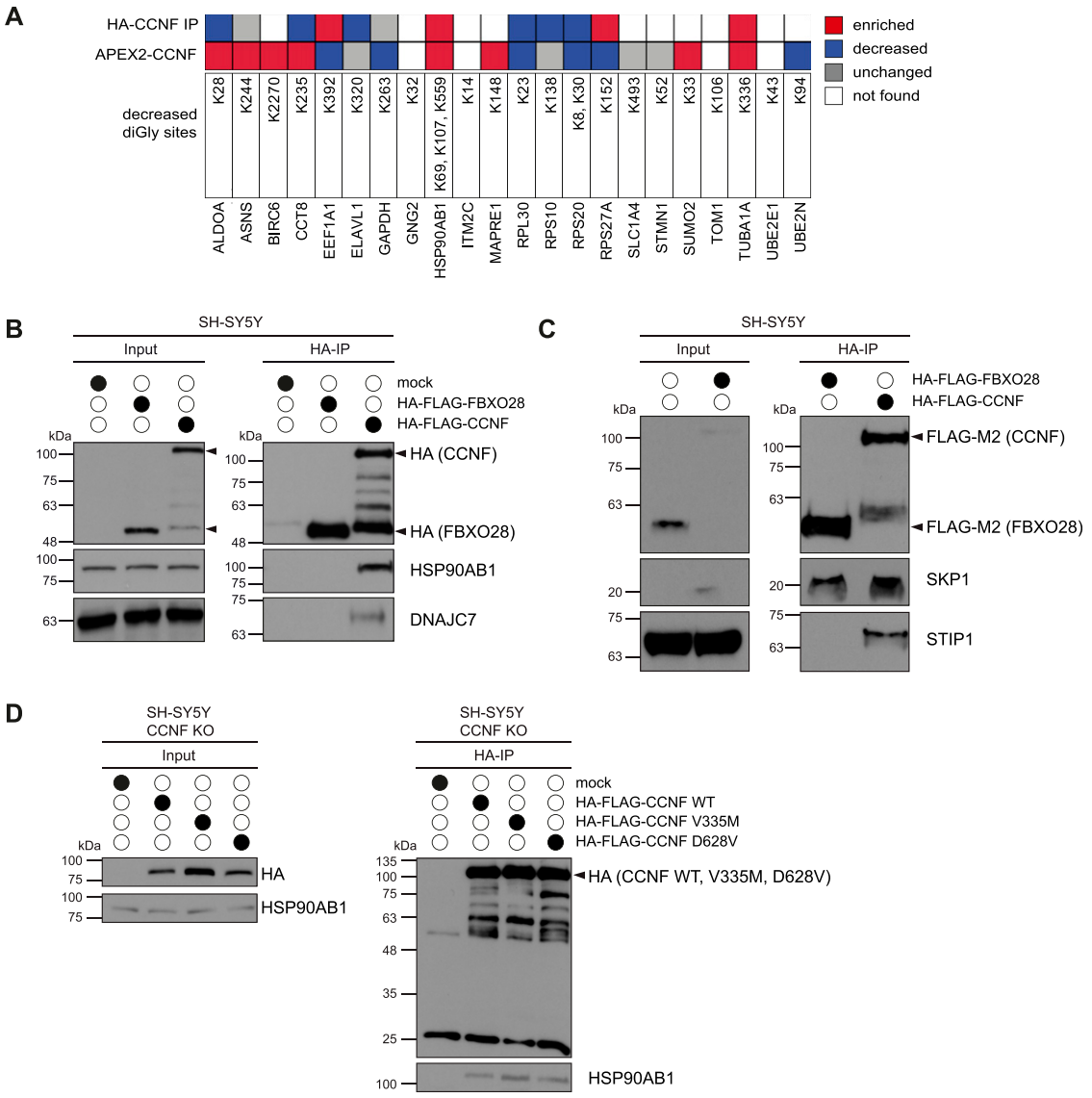

Figure 3. Identification of HSP90AB1 as potential Cyclin-F target.
(A) Overview of CCNF proximity partners and interaction candidates with decreased diGly sites in CCNF KO and mutant cells. Proteins found enriched or decreased by proximity proteomics (APEX2-CCNF) and/or immunoprecipitation mass spectrometry (HA-FLAG-CCNF IP) are marked red and blue, respectively. Unchanged proteins are marked in grey, whereas proteins that were not found are indicated with white boxes. **(B, C)** Lysates from parental (mock), HA-FLAG-FBXO28, or HA-FLAG-CCNF overexpressing SH-SY5Y cells were subjected to HA immunoprecipitation (IP), SDS–PAGE and immunoblotting. Arrows indicate specific protein bands. **(D)** CCNF KO SH-SY5Y cells re-expressing HA-FLAG-CCNF WT, V335M, or D628V or left untreated (mock) were lysed and incubated with HA-agarose followed by SDS–PAGE and immunoblotting. Arrows indicate specific protein bands.

(Fig 4A). To probe the role of cullin RING ligase (CRLs) such as $SCF^{Cyclin\text{-}F}$ in the ubiquitination of HSP90AB1, we performed denaturing IPs of HA-FLAG-HSP90AB1 from cells treated with the proteasome inhibitor Bortezomib or the NAE1 inhibitor MLN4924. Note that the latter blocks neddylation of cullins which is required for CLR activity. Intriguingly, Btz treatment led to a massive ubiquitination of HSP90AB1 which could be completely reversed by additional MLN4924 treatment (Fig 4B). Next, we asked whether HSP90AB1 ubiquitination was indeed dependent on Cyclin-F. Thereto, we used tandem ubiquitin binding entities (TUBE) with a preference for K48- and K63-linked Ub to examine the observed decrease in abundance for a number of diGly sites on HSP90AB1 in CCNF KO cells. Lysates from SH-SY5Y CCNF WT and KO cells were subjected to pull-downs with GST-TUBE. Immunoblot analysis with specific antibodies showed decreased protein levels of HSP90AB1 in cells lacking CCNF, whereas p62 (alias SQSTM1), a known but Cyclin-F unrelated ubiquitination target, was unaffected (Fig 4C). Notably, ubiquitination of p62 was detected in our diGly proteomics but did not show any changes in CCNF KO or mutant cells. Because ubiquitination can either be a signal for degradation or exert regulatory functions on the modified protein, we monitored the abundance of HSP90AB1 in SH-SY5Y CCNF WT and KO cells grown in

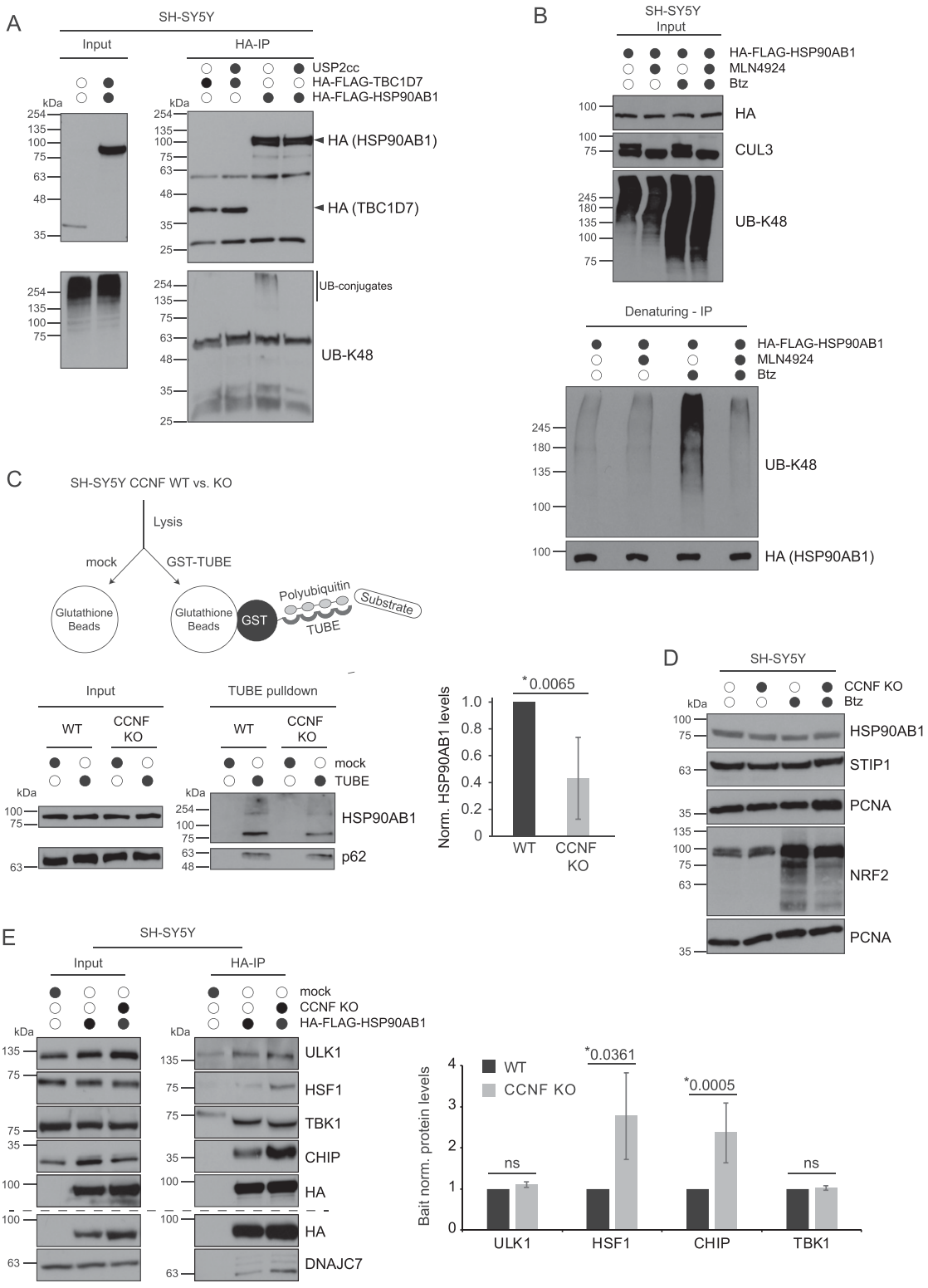

Figure 4. Ubiquitination of HSP90AB1 by Cul1$^{Cyclin\text{-}F}$ leads to altered client binding.
(A) SH-SY5Y cells expressing HA-FLAG-TBC1D7 or -HSP90AB1 were lysed under denaturing conditions, differentially treated with USP2cc and subjected to HA-IP. Arrows indicate specific protein bands. **(B)** SH-SY5Y cells expressing HA-FLAG-HSP90AB1 were grown in the absence or presence of MLN4924 and/or Bortezomib (Btz) followed by denaturing HA-IP. **(C)** Schematic representation of TUBE pull-downs (upper panel). Ubiquitin conjugates in lysates from SH-SY5Y CCNF WT and KO cells were enriched using TUBE pull-downs and detected by specific antibodies (lower left panel). Bar graph shows quantification of HSP90AB1 in TUBE pull-down (lower right panel). Statistical analysis (n = 3) of HSP90AB1 levels was performed using two-sided, unpaired *t* test. Data represent mean ± SD. **(D)** SH-SY5Y CCNF WT and KO cells were grown in the

the absence and presence of Btz. Whereas NRF2, a protein with fast-turnover by the proteasome, increased in abundance upon Btz treatment, the levels of HSP90AB1 and of one of its co-chaperones STIP1 were unaffected by either loss of CCNF, proteasome blockage or both (Fig 4D) Similar results were obtained in cycloheximide chase assays with endogenous and overexpressed HSP90AB1 (Fig S4A). This suggests a non-degradative function for the Cyclin-F–dependent ubiquitination of HSP90AB1. The cytosolic HSP90 complex is formed by homodimers of HSP90AA1 or HSP90AB1, assists in proper folding, stabilization and activation of client proteins and is highly regulated by co-chaperones and post-translational modifications (PTMs) such as phosphorylation. To gain first mechanistic insights into the relevance of HSP90 ubiquitination for its functionality, we monitored the binding of HSP90AB1 to some of its co-factors and client proteins. To this end, we expressed HA-FLAG-HSP90AB1 in SH-SY5Y CCNF WT and KO cells and performed HA-IPs following mild lysis. Remarkably, in CCNF KO cells, we detected significantly increased HSP90AB1 binding to the HSP90 client heat shock factor 1 (HSF1) which is a key component of the proteotoxic stress response. Moreover, the HSP90 co-factors and potential CCNF ubiquitination targets DNAJC7 and CHIP also showed enhanced binding to HSP90AB1 when its ubiquitination was reduced due to the lack of CCNF (Figs 4E and S4B). The fact that ULK1, TBK1, and STIP1 did not increase in abundance in HSP90 immunoprecipitates indicates that the effect of HSP90AB1 ubiquitination on its chaperone function might be client and co-factor specific (Fig 4E). Overall, these findings suggest that Cyclin-F controls HSP90 function in a ubiquitin dependent manner.

Discussion

In this study, we acquired ubiquitinome, proximity and interaction data to elucidate potential functions of $SCF^{Cyclin\text{-}F}$ in neuronal, respective patient-derived cells. Integration of these different data sets unveiled Cyclin-F association with cellular chaperone machinery components and HSP90AB1 ubiquitination by Cyclin-F. Remarkably, this ubiquitination is diminished in cells lacking CCNF or expressing mutated CCNF variants linked to ALS, implicating a potential loss-of-function mechanism for these mutants.

Missense mutations in CCNF contribute to the development of ALS (25, 27, 30). In this context, a number of studies proposed a gain of toxic function mechanism based on observations by semi-quantitative immunoblotting that levels of K48 linked polyUb increased upon expression of Cyclin-F S621G, K97R, or S195R (25, 26). In contrast, our mass spectrometry-based quantitative ubiquitinome profiling of ALS patient-derived LCLs carrying V335M and D628V mutant CCNF uncovered a prominent decrease in signature diGly peptides for K48- and K63-linked Ub chains. Consistent with this notion, diminished E3 ligase activity was reported for the CCNF mutation S509P (26). Moreover, several diGly sites that were found decreased in CCNF KO cells were regulated in the same direction in both ALS patient-derived LCLs. Based on these findings, we propose that the CCNF mutations V335M and D628V contribute to ALS pathogenesis via a loss of function mechanism. Although the molecular basis of Cyclin-F V335M– and D628V–driven dysfunction requires further analysis, reduced substrate ubiquitination is unlikely caused by changes in substrate-binding affinity or faulty $SCF^{Cyclin\text{-}F}$ complex assembly because we did not observe altered HSP90AB1 binding of CCNF V335M and D628V and $SCF^{Cyclin\text{-}F}$ complex formation was shown to be unaffected for several other CCNF mutants (30). Another scenario leading to a loss of function might be an altered presentation of substrate lysines towards RBX1 bound E2~Ub. Along this line, the V335M mutant might induce a conformational change in the substrate-binding cyclin domain which could result in diminished ubiquitination. Alternatively, V335M and D628V might alter the spatial arrangement of Cyclin-F in such ways that RBX1-mediated Ub transfer to designated targets is blocked or reduced by steric hindrances.

Intriguingly, we identified HSP90AB1 as a ubiquitinated substrate of the $SCF^{Cyclin\text{-}F}$ complex under basal, housekeeping conditions. HSP90AB1 is constitutively expressed and homodimerizes to yield a functional HSP90 complex. Nonetheless, HSP90AB1 can also built heterodimers with its structurally very similar but inducible isoform HSP90AA1 (35). The protomers of the HSP90 family share a common domain structure, consisting of an N-terminal domain (NTD) linked to the middle domain (MD) by an unstructured charged-linker region and a C-terminal domain (36, 37). The NTD forms a nucleotide-binding pocket, important for ATP binding as well as co-chaperone binding, whereas the MD is not only binding co-chaperones but is also important for HSP90 client binding. The carboxy-terminus of HSP90 protomers allows the constitutive dimerization of the complex and contains the MEEVD motif, crucial for the interaction with tetratricopeptide-containing repeat domain (TPR domain) containing proteins (38, 39). These TPR domains are present in several co-chaperones, including STIP1 (37, 40). The HSP90 cycle starts in an open position that transitions to a closed conformation by ATP hydrolysis with the help of co-chaperones. Thereby client maturation is enabled. This process is highly regulated at several levels by co-chaperones, PTMs and even by client binding itself (37). Phosphorylation, for example, generally decreases HSP90 ATPase activity, affects co-chaperone binding and client dynamics (41). Other PTMs such as acetylation (e.g., of K69) has reported effects on co-chaperone binding, ATP binding and cellular functions of the HSP90 complex (41, 42, 43). Interestingly, we discovered that K69 can also serve as ubiquitin acceptor sites, suggesting equal or opposing effects on HSP90AB1 function or localization. Other diGly sites in HSP90AB1 found in this study distribute throughout the protein (K107, K180, K275, K286, K435, K438, K531, K559, K568, K574, and K607) and unlikely serve as proteasomal eat-me signal because HSP90AB1 protein levels were neither changed by Btz treatment nor by the lack of Cyclin-F–mediated ubiquitination. Our findings seem to contradict previous data showing HSP90 ubiquitination by CHIP at several sites (e.g., K107, K204, K219, K275, K284, K347, and K399) and proteasomal degradation

absence or presence of Btz followed by lysis and immunoblotting. **(E)** SH-SY5Y WT and KO cells expressing HA-FLAG-HSP90AB1 or mock were subjected to HA-IP before SDS–PAGE and immunoblot analysis. Bar graph shows quantification of ULK1, HSF1, CHIP, and TBK1 in HSP90AB1 immunoprecipitates. Statistical analysis (n = 3) of HSP90AB1-binding proteins levels was performed using two-sided, unpaired *t* test. Data represent mean ± SD.

of HSP90AA1 in HEK cells (41, 44, 45). However, because HSP90AA1 is an inducible isoform, it might be regulated differently than the constitutively expressed HSP90AB1. It is noteworthy that we found some of the reported CHIP ubiquitination sites to also be potential targets of Cyclin-F (K107, K275, and K607), indicating possible redundancy between E3 ligases or different layers of Ub-dependent regulation. The increased binding of HSP90AB1 to its client HSF1 as well as to its co-factor CHIP in the absence of CCNF might provide possible explanations for likely regulatory functions of HSP90AB1 ubiquitination. Enhanced binding of clients could stem from chaperone complex stalling because of a decrease in ATPase activity or altered co-chaperone binding, leading to a change in complex dynamics and a potential blockage of the HSP90 cycle. These possibilities are in line with diGly sites found in the N-terminal part of HSPAB1 important for ATPase activity (K69 and K107) as well as with diGly sites located in domains responsible for co-chaperone binding (K69, K107, and K559).

HSP90 is involved in early embryonic development, germ cell maturation, cytoskeletal stabilization, cellular transformation, signal transduction, long-term cell adaptation and many other cellular processes through its diverse set of client proteins (35). Therefore, HSP90 dysfunction by altered regulatory PTMs might have detrimental effects on cells in the context of ALS. Our observation of a deregulated Cyclin-F-HSP90 axis could implicate effects on folding stress response (HSF1) and HSP90 function itself (CHIP) (46, 47, 48, 49, 50). These processes might converge on disturbed protein homeostasis, a typical phenomenon observed in ALS (23). Conversely, impairment of the proteasome as observed, for example, by C9orf72-derived dipeptide repeat proteins (51) might lead to a backlog within the UPS and affect the activities of E3 ligases such as $SCF^{Cyclin\text{-}F}$. While this hypothesis requires further testing, HSP90 functions might thus be generally compromised in ALS disease conditions even in the absence of mutations in CCNF.

Materials and Methods

CCNF ALS patient cells

The LCL line with p.D628V mutation was derived from a male patient with spinal onset of familial ALS at the age of 47 yr. Both his father and paternal grandfather were affected by the disease, in agreement with an autosomal-dominant mode of inheritance. The patient did not suffer from FTD comorbidity. Because of the loss of follow-up, the survival status of the patient is unknown. The LCL line with the p.V335M mutation was derived from a female ALS patient without a family history for the disease. She also had a spinal onset of disease at the age of 62 yr with distal extensor weakness in the lower extremities, followed by paresis in the upper extremities and subsequently bulbar symptoms. She had clinical signs of both upper and lower motor neuron degeneration. Sensory function and coordination were unremarkable. Both patients were subject to whole exome sequencing, and genetic variants in other known ALS disease genes were excluded. For the collection and use of blood cells from ALS patients as well as for whole exome sequencing of blood DNA, written informed consent was obtained from all individuals. The experiments have been approved by the local ethical committees of the Medical Faculties Ulm (Ulm University) and Mannheim (ethical committee II of the University of Heidelberg). Approval numbers are Nr. 19/12 and 2020-678N, respectively.

Transfections and treatments

Transfections were performed with 1 μg DNA per plasmid added to 200 μl OptiMEM (Invitrogen), Lipofectamine 2000 (Invitrogen) or X-tremeGENE HP (Roche) in a 1:3 ratio (μg DNA: μl of transfection reagent) and incubated for 20 min at RT prior to addition to cells. Cells were treated with 1 μM Bortezomib (Btz) for 8 h. Lysates were incubated with USP2 at 0.625 μM for 4 h at 4°C in an overhead shaker. CHX chase was performed using 100 μg/mL of CHX for 2–8 h at 37°C. Neddylation of CRLs was inhibited with 1 μM MLN4924 for 4 h at 37°C.

Table of reagents and resources.

Reagent or resource	Reference or source	Identifier or Cat. no.
Affinity beads/agarose		
ANTI-FLAG M2 Affinity Gel	Sigma-Aldrich	A2220-1ML
Glutathione Sepharose 4B	GE Healthcare	17-0756-01
HA peptide	Sigma-Aldrich	I2149-1MG
Anti-HA agarose	Sigma-Aldrich	A2095-5X1ML
Pierce Anti-HA agarose	Thermo Fisher Scientific	26182
PTMScan Ubiquitin Remnant Motif (K-ε-GG) Kit	Cell Signaling	5562
Streptavidin agarose	Sigma-Aldrich	S1638-5ML
UM101: TUBE 1	Lifesensors	UM-0101-1000
Primary Antibodies		

(Continued on following page)

Continued

Reagent or resource	Reference or source	Identifier or Cat. no.
α-tubulin	Abcam	ab7291
Anti-KAP1 antibody	Abcam	ab22553
APEX (IgG2A)	Regina Feederle	Custom made
Biotin	Pierce	31852
Biotin FITC	Abcam	ab6650
Cyclin-F	Santa Cruz	sc-952
DNAJC7	Proteintech	11090-1-AP
FlaG M2	Cell signaling	2368
HA.11	Covance/BioLegend	MMS-101P/901501
HSF1	Cell Signaling	4356
HSP90β	Cell Signaling	7411
Ub K48	Cell Signaling	8081
Nrf2	Abcam	ab62352
p62/SQSTM1	BD	610832
PCNA	Santa Cruz	sc-7907
PCNA (PC10)	Santa Cruz	sc-56
Skp1	Cell Signaling	2156
STIP1	Abcam	ab126724
STUB-1/CHIP	Bethyl Laboratories	A301-572A
TBK1/NAK	Abcam	ab40676
Tollip	Abcam	ab187198
Secondary ABs		
Anti-goat-HRP	Promega	V8051, RRID: AB_430838
Anti-mouse-HRP	Promega	W402B
Anti-rabbit-HRP	Promega	W401B
Anti-rat-HRP	Sigma-Aldrich	A-9037, RRID: AB_258429
Software/Tools		
Adobe Illustrator 2022	Adobe	
Fiji, ImageJ	N/A	Version 1.53j
gRNA design Tool	portals.broadinstitute.org/gpp/public/analysis-tools/sgrna-design	
gRNA design Tool - CRISPOR	crispor.tefor.net	
MaxQuant	N/A	Version 1.6.0.1
Perseus	N/A	Version 1.6.10.43
QuikChange Primer Design	https://www.agilent.com/store/primerDesignProgram.jsp	
R		Version 4.1.1
R-Studio		Version 1.4.1717
Plasmids/Vectors		
ORF CCNF	Dharmacon	MHS6278-202831979
ORF FBXO28	Dharmacon	OHS1770-202323126
ORF HSP90AB1	Horizon Discovery	MHS6278-202807158
pHAGE-N-myc-APEX2	Zellner et al (2021) (52)	
pMD2.G	Addgene	12259

(Continued on following page)

Continued

Reagent or resource	Reference or source	Identifier or Cat. no.
psPAX2	Addgene	12260
pSpCas9(BB)-2A-Puro (PX459) V2.0	Addgene	62988
gRNAs/Primers		
sgRNA1_mouse-Seq: CACCGAGACAACACGTATAAATACG	Thermo Fisher Scientific	Custom order
sgRNA2_mouse-Seq: CACCGGTAACTGACACTCCGCTCGG	Thermo Fisher Scientific	Custom order
sgRNA1_human CCNF- Seq: ACACCGCGTTTGGTTCTCCGCCCCGAG	Thermo Fisher Scientific	Custom order
sgRNA2_human_CCNF-Seq: ACACCGGTAGACCACGGTGACATCGG	Thermo Fisher Scientific	Custom order
Sequencing primer human CCNF gRNA1_fw TTTGTCCATGTGGTGTGTGT	Thermo Fisher Scientific	Custom order
Sequencing primer human CCNF gRNA1 rev TGAGATAGGAGAGGCGGGT	Thermo Fisher Scientific	Custom order
Sequencing primer human CCNF gRNA2 fw TTTCCCGGTTGCTTGCTT	Thermo Fisher Scientific	Custom order
Sequencing primer human CCNF gRNA2 rev CATGTCCTCCTCCTCACT	Thermo Fisher Scientific	Custom order
Sequencing primer mouse CCNF - gRNA2_fw GAGGAAGGTGGAGGATGT	Thermo Fisher Scientific	Custom order
Sequencing primer mouse CCNF - gRNA2_rev TCTCCTACAACTACTCCC	Thermo Fisher Scientific	Custom order
Sequencing primer mouse CCNF - gRNA1_fw GGGTTATGTAGGGGTCAG	Thermo Fisher Scientific	Custom order
Sequencing primer mouse CCNF - gRNA1_rev AGACAAGAGGGAGGAAAA	Thermo Fisher Scientific	Custom order
Cell lines		
LCL, ctrl 1, female	Jochen Weishaupt	This study
LCL, ctrl 2, female	Jochen Weishaupt	This study
LCL, CCNF V335M, female	Jochen Weishaupt	This study
LCL, ctrl 3, male	Jochen Weishaupt	This study
LCL, ctrl 4, male	Jochen Weishaupt	This study
LCL, CCNF D628V, male	Jochen Weishaupt	This study
N2a cells	ATCC	CCL-131
SH-SY5Y cells	ATCC	CRL-2266
Kits		
Amaxa SF Cell Line 4D-Nucleofector X Kit	Lonza	V4XC-2012
Pierce BCA Protein Assay Kit	Thermo Fisher Scientific	23225
PureLink Genomic DNA Kit	Invitrogen	K1820-02
QIAprep Spin Miniprep kit	QIAGEN	27106
Chemicals/enzymes		
Acrylamide solution	PanReac AppliChem	A0951
Ammonium bicarbonate	Sigma-Aldrich	9830
BbsI	NEB	R0539S
Benzonase	Merck Millipore	71205-3
Biotin-Phenol	Iris Biotech	LS-3500.5000
Bortezomib 99%	LC Labs	B-1408

(Continued on following page)

Continued

Reagent or resource	Reference or source	Identifier or Cat. no.
BSA	Sigma-Aldrich	A8022-100G
Complete	Roche	4693132001
Disodiumhydrogenphoshpate	Merck	1.06580.5000
Dithiothreitol	Sigma-Aldrich	43815-5G
Dulbecco's PBS	Thermo Fisher Scientific	14190169
Ethylenediaminetetraacetic acid	Merck	1.008418.1000
Glycerol	Roth	3783
GO-Taq polymerase	Promega	M784B
Hydrogenperoxide	Sigma-Aldrich	H1009
IGEPAL CA-630 (NP-40)	Sigma-Aldrich	I8896
KOD Hot Start DNA Polymerase	Sigma-Aldrich	71086
Lipofectamine 2000	Invitrogen	11668-019
N-Ethylmaleimide (NEM)	Sigma-Aldrich	E3876-5G
Opti-MEM	Invitrogen	31985-062
Paraformaldehyde solution 4%	Chemcruz	sc-281692
Phenylmethylsulfonyl fluoride	Sigma-Aldrich	P7626-1G
PhosSTOP	Roche	4906837001
ProLong Gold Antifade	Invitrogen	P36931
Puromycin dihydrochloride	Sigma-Aldrich	P8833-100mg
Pwo-polymerase	VWR	01-5010-88
Recombinant USP2	R&D Systems	E-504-050
Sodium L-ascorbate	Sigma-Aldrich	A7631
TCEP	ROTH	HN95.2
Trifluoroacetic acid	Honeywell Fluka	302031-100ML
Triton X-100	Merck	1.08603.1000
Trolox	Sigma-Aldrich	238813
Tropix I-Block	Appliedbiosystems	T2015
Trypsin, sequencing-grade	Promega	V5113
Western Lightning Plus-ECL	PerkinElmer	NEL104001EA
X-tremeGENE HP	Roche	06 366 236 001
Hardware/Consumables		
4D-NucleofectorTM X Unit	Lonza	
Amersham Protran 0.45 μm NC	GE Healthcare Life Science	10600002
EMPORE Octadecyl C18 47 mm	Supelco Analytical	66883-U
Lyophilisator, Alpha 1-2 LD Plus	CHRIST	N/A
Mini-PROTEAN Tetra cell	Bio-Rad	1658004EDU
Mini-Transblot cell	Bio-Rad	1703930
Sonifier	SONIFIER Branson	W-250D
Super RX-N	Fujifilm	47410 19289
Ultrafree-MC, HV 0.45 μm	Merck Millipore	UFC30HV00
Vacuum Centrifuge	Eppendorf	N/A
Zeiss LSM800 oil 60× objective	Zeiss	N/A
Easy-NLC1200	Thermo Fisher Scientific	N/A
QExactive^{HF} mass spectrometer	Thermo Fisher Scientific	N/A

Plasmid and cell line generation

PCR was performed to add attB sites to ORFs and cloned into pDONR223. Using recombinational cloning these ORFs were then moved to the following destination vectors: pHAGE-N-Flag-HA, pHAGE-C-FLAG-HA, and pHAGE-N-myc-APEX2 (52). Stable cell lines in SH-SY5Y and N2a cells were generated by lentiviral transduction. 1 μg pMD2.G, 1 μg pPAX2, and 1 μg destination vector was used for transfection. Puromycin (2 μg/ml) was added to the cells 24 h post transduction for selection.

Mutagenesis

Mutagenesis primers were designed using QuikChange Primer Design software (Agilent Technologies). KOD Hot Start or Pwo DNA Polymerase (Merck Millipore) were used according to the manufacturers' protocols. For Pwo DNA polymerase elongation periods were extend to 14 min per cycle. The PCR product was purified with the QIAquick PCR purification kit (QIAGEN) and amplified in *Escherichia coli*.

Knockout generation and validation

First single guide RNAs (sgRNAs) were designed using the sgRNA-design tool of the Broad Institute, CRISPick or CRISPOR (crispor.tefor.net) (53, 54 *Preprint*, 55). sgRNAs were provided with sticky end overhang sequences for ligation with BbsI-digested pSpCas9(BB)-2A-Puro V2.0 vector which was a gift from Feng Zhang (Addgene plasmid # 62988; http://n2t.net/addgene:62988; RRID:Addgene_62988) (56). After ligation cells were either transfected with two sgRNAs using XtremeGene HP DNA transfection reagent according to manufacturer's instructions (for N2a) or by electroporation with the 4D-Nucleofector X Unit using the Amaxa SF Cell Line 4D-Nucleofector X Kit according to manufacturer's instructions (for SH-SY5Y). 24 h post-transfection cells were grown in 4 μg/ml Puromycin for 48 h. Single cells were selected using serial dilution. Genomic DNA was purified (Invitrogen) and amplified by touchdown PCR using the GO-taq polymerase (Promega). Proper genome editing was verified by Sanger sequencing (by Eurofins Genomics EU) and immunoblotting.

Immunofluorescence

Cells were seeded on coverslips and washed three times with DPBS (GIBCO) followed by fixation with 4% PFA (Santa Cruz) for 10 min and permeabilization with 0.5% Triton X for 10 min. Subsequently, cells were blocked with 1% BSA in PBS for 1 h at RT. Fluorophore-coupled primary antibodies were incubated for 1 h at RT in the dark. Coverslips were mounted with mounting solution (Prolonged Gold with DAPI; Invitrogen) on microscope slides (Thermo Fisher Scientific) and imaged using a confocal microscope Zeiss LSM800 with a 63× magnification oil-immersion objective. Image analysis was performed with ImageJ 1.53j (Fiji).

Immunoblotting

Cells were washed with DPBS before harvesting by scraping on ice. Lysis was performed with RIPA buffer (50 mM Tris, pH 7.5, 150 mM NaCl, 0.1% SDS, 0.5% sodium desoxycholate, 1% Triton X, PhosStop [Roche], and protease inhibitor [Roche]) and protein concentrations were adjusted using BCA assays. Protein samples were separated by SDS–PAGE (100V) and transferred (2 h 15 min, 0.3 A) on a nitrocellulose membrane (0.45 μm pore size). Membranes were blocked with I-Block (Invitrogen) and incubated at 4°C overnight with the primary antibody. After washing three times with TBS-T-buffer, secondary antibody coupled to horseradish peroxidase was added to the membrane for 1 h at RT. Immunoblots were washed another three times with TBS-T before enhanced chemiluminescence analysis using ECL (PerkinElmer) and x-ray films (Fuji Medical).

Immunoprecipitation

Cells grown in 2–4 × 15 cm cell culture plates per sample were harvested by scraping on ice and stored at −80. Lysis was performed for 30 min at 4°C with MCLB buffer (50 mM Tris HCl, pH 7.5, 150 mM NaCl, 0.5% NP40, 1× PhosStop, and 1× protease inhibitor) or glycerol buffer (20 mM Tris, pH 7.5, 150 mM NaCl, 10% glycerol, 5 mM EDTA, 0.5% Triton X, 1× PhosStop, inhibitor, and 1× protease inhibitor). Samples were cleared from debris by centrifugation (20,000*g* for 10 min at 4°C) and Ultrafree-CL spin-filter tubes (Millipore CL 0.45). Protein concentrations of lysates were adjusted following determination by BCA and samples incubated overnight with pre-equilibrated anti-HA-agarose (Sigma/Pierce Anti-HA Agarose) or anti-Flag M2 affinity gel (Merck Millipore) using an overhead shaker at 4°C. Subsequently, agarose beads were washed five times with the respective buffer and eluted by boiling in SDS sample buffer (200 mM Tris-HCL, 6% SDS, 20% glycerol, 300 mM DTT, and bromophenol blue) (5 min at 95°C) or washed five more times with DPBS (GIBCO) before elution with HA peptide (Sigma-Aldrich). Eluted immune complexes were precipitated with TCA (final concentration 20%) and washed with ice cold acetone. Samples were resuspended in 50 mM ammonium bicarbonate buffer containing 10% acetonitrile and trypsinized for 4 h at 37°C.

APEX2-mediated biotinylation

Cells were grown in the presence of 500 μM biotin-phenol (Iris Biotech) for 30 min at 37°C and pulsed with 1 mM H_2O_2 at RT. Biotinylation was stopped by washing three times with quencher solution (10 mM sodium azide, 10 mM sodium ascorbate, 5 mM 6-Hydroxy-2,5,7,8-tetramethylchroman2-carboxylic acid [TROLOX], DPBS). The third quenching step was performed for 15 min before washing three times with DPBS. Cells were either lysed in RIPA buffer or frozen at −80°C after adjusting cell numbers.

Streptavidin pulldown

Biotinylated samples were thawed on ice and lysed in qRIPA buffer (50 mM Tris pH 7.5, 150 mM NaCl, 0.1% SDS, 0.5% sodium desoxycholate, 1% Triton X, 10 mM sodium azide, 10 mM sodium ascorbate, 5 mM TROLOX, PhosStop [Roche], and protease inhibitor [Roche]) for 40 min at 4°C. Samples were cleared from debris (20,000*g*, 10 min, 4°C) and incubated with pre-equilibrated streptavidin agarose beads (Sigma-Aldrich) overnight at 4°C in an overhead shaker. Pull-

downs were washed twice with RIPA buffer followed by four times washing with 3 M urea wash buffer (50 mM ABC buffer, 3 M urea). TCEP was added to a final concentration of 5 mM and incubated for 30 min at 55°C. Once cooled to RT samples were incubated with iodoacetamide (IAA) for 20 min at RT in the dark followed by addition of DTT (20 mM). Samples were then washed with 2 M urea wash buffer (50 mM ABC buffer, 2 M urea) before trypsinization overnight at 37°C.

Mass spectrometry

Digests were stopped by the addition of formic acid and samples were desalted on custom-made stage-tips (C18 material–Supelco Analytical) (57). Using an Easy-nLC1200 liquid chromatography (Thermo Fisher Scientific), peptides were loaded onto custom filled C18 reversed-phase columns and separated using a gradient of 5%–33% acetonitrile in 0.5% acetic acid over 90 min and detected on an Q Exactive HF mass spectrometer (Thermo Fisher Scientific). Dynamic exclusion was enabled for 30 s and singly charged species or species for which a charge could not be assigned were rejected. MS data were processed and analyzed using MaxQuant (1.6.0.1) (58, 59) and Perseus (1.6.10.43). Proximity proteomics was performed in triplicates and interaction proteomics experiments were performed in quadruplicates. Unique and razor peptides were used for quantification. Matches to common contaminants, reverse identifications and identifications based only on site-specific modifications were removed before further analysis. Log_2 H:L ratios were calculated. *t* tests were used to determine statistical significance between conditions. A q-value < 0.05 was considered statistically significant. Log_2 fold change (H:L) > 2 and >1 was used as cutoff for experiments involving HA-IPs and APEX2, respectively. Functional annotation enrichment analysis was performed using DAVID (60, 61) coupled to significance determination using Fisher's exact test and correction for multiple hypothesis testing by the Benjamini and Hochberg FDR.

diGly proteomics

Cells were cultured in lysine- and arginine-free DMEM supplemented with dialyzed FBS, 2 mM L-glutamine, 1 mM sodium pyruvate, penicillin/streptomycin, and light (K0) lysine (38 μg/mL) and arginine (66 μg/ml). Heavy medium was the same except the light lysine was replaced with K8-lysine (L-Lysine, 2HCl U-13C U-15N, Cambridge Isotope Laboratories Inc). Cells were processed as essentially as described in Fishkin et al (2016) (62). Briefly, cells were washed twice with ice-cold PBS and lysed in 5 ml denaturing lysis buffer (8M urea, 50 mM Tris [pH 8], 50 mM NaCl, 1× PIC [protease inhibitor cocktail, EDTA-free; Roche], 50 μM DUB inhibitor PR-619 [Millipore]). Samples were incubated on ice for 10 min and then sonicated with 3 × 20 s pulses. After removal of non-solubilized material (15,000*g*/10 min), differentially labeled lysates were mixed at equal ratios based on total protein determined by BCA (Pierce-Thermo; typically, 10 mg of total protein). After reduction with 5 mM DTT and alkylation with 10 mM chloroacetamide, lysates were digested with 5 ng/μl lys-C (Wako) for 1 h at RT. Subsequent digestion of peptides with trypsin (Promega) was performed as described (63). Lyophilized peptides were resuspended in 1.5 ml IAP buffer (50 mM MOPS [pH 7.4], 10 mM Na_2HPO_4, and 50 mM NaCl) and centrifuged to remove any insoluble material (2,500*g*/5 min). The supernatant was incubated with anti-diGly antibody (32 μg/IP) conjugated to protein A agarose beads (Cell Signaling) for 1 h at 4°C. Unbound peptides were removed through 3× washing with IAP buffer and once with PBS. Bound material was eluted 4× with 50 μl 0.15% TFA and peptides were desalted using C18 stage-tip method (57). Each sample was immunoprecipitated sequentially two times and each IP was analyzed separately by mass spectrometry. Peptides samples were separated on a nanoflow HPLC system (Thermo Fisher Scientific) using a 226 min gradient of 5–33% acetonitrile containing 0.5% acetic acid on custom filled C18 reversed-phase columns and analyzed on a Q Exactive HF mass spectrometer (Thermo Fisher Scientific) using data-dependent acquisition selecting the most intense peaks from each full MS scan acquired in the Orbitrap for subsequent MS/MS while excluding peptides with unassigned charge states or charge states below +3 from fragmentation (see RAW files for specific settings). Raw data files from quadruplicate samples were processed with MaxQuant (1.6.0.1) as described previously (58, 59) using a human (UP000005640) UNIPROT database and the following parameter settings: first search peptide mass tolerance 20 ppm, main search peptide mass tolerance 0.5 D, tryptic digestion allowing up to two missed cleavages, cysteine carbamidomethylation (57.021464) as fixed modification, methionine oxidation (15.994946), N-terminal protein acetylation (42.010565) and diGG (114.042927; excluded from the C terminus) as variable modifications, revert decoy mode and peptide, protein and site FDR ≤ 0.01. Perseus (1.6.10.43) was used for data sorting. Log_2 H:L ratios were calculated. *t* tests were used to determine statistical significance between conditions. A q-value < 0.05 was considered statistically significant. Log_2 fold change (H:L) > 0.5 and < −0.5 was used as cutoff. Heat maps were generated using MultiExperiment Viewer (64).

Denaturing immunoprecipitation

Cells in 2 × 15 cm cell culture dishes were harvested by scraping, washed with DPBS and frozen at −20°C. Lysis was carried out with a denaturing buffer containing 1% SDS (50 mM Tris pH 8.0, 150 mM NaCl, 0.5 mM DTT, 0.5 mM PMSF, 10 mM NEM, 0.5% NP40, 1% SDS, protease inhibitor [1×], benzonase) for 15 min at 4°C-Lysates were diluted to 0.1% SDS with NP40-buffer (50 mM Tris pH 8.0, 150 mM NaCl, 10 mM NEM, 0.5% NP40, 1× protease inhibitor) and sonicated (8 × 1 s pulse, 1 s rest) on ice. Debris was cleared by centrifugation (>20,000*g*, 10 min, 4°C) and protein concentrations adjusted across samples following BCA. Samples were incubated with pre-equilibrated anti-HA-agarose overnight at 4°C in an overhead shaker. Before elution, samples were washed either four times with USP2 wash buffer (50 mM Tris HCl, pH 8.0, 300 mM NaCl, 0.5% NP40, and protease inhibitor [1×]) and once with USP2 reaction buffer (50 mM Tris HCl, pH 8.0, 10 mM NaCl, 0.5 mM DTT, and 0.01% NP40) or five times with NP40 buffer followed by differential treatment with recombinant USP2.

TUBE pull-down

Cells in 2 × 15-cm cell culture dishes were harvested by scraping and washed with DPBS. Cell numbers were adjusted using a cell counter (Invitrogen Countess) and samples frozen at −20°C. Cell pellets

were lysed with TUBE buffer (50 mM Tris, pH 7.5, 150 mM NaCl, 1 mM EDTA, 1% NP40, 10% glycerol, 50 μM PR-619, 5 mM 1,10-phenantroline, 2 mM PMSF, 10 μM bortezomib, and 1× protease inhibitor cocktail) with or without 200 μg/μl GST-TUBE (Lifesensors). Samples were rotated on an overhead shaker for 10–15 min at 4°C before incubation with TBS-T (20 mM Tris, pH 7.5, 150 mM NaCl, and 0.1% Tween-20) pre-equilibrated glutathione sepharose (GE Healthcare) for 4 h on an overhead shaker at 4°C. Samples were washed four times with TBS-T and eluted with three times SDS sample buffer (200 mM Tris–HCL, 6% SDS, 20% glycerol, 300 mM DTT, and Bromophenol Blue).

Data Availability

The mass spectrometry proteomics data have been deposited to the ProteomeXchange Consortium via the PRIDE partner repository with the dataset identifier PXD030729.

Supplementary Information

Supplementary Information is available at https://doi.org/10.26508/lsa.202101359.

Acknowledgements

We thank Georg Werner for his extensive advice while creating the CCNF KO lines and we are very thankful to all members of the Behrends, Edbauer, and Haass lab for readily sharing reagents, advice, and critical discussions. This work was supported by the Deutsche Forschungsgemeinschaft (DFG, German Research Foundation) within the frameworks of the Munich Cluster for Systems Neurology (EXC 2145 SyNergy–ID 390857198) and the Collaborative Research Center 1177 (ID 259130777).

Author Contributions

A Siebert: conceptualization, data curation, formal analysis, validation, investigation, visualization, methodology, and writing—original draft, review, and editing.
V Gattringer: investigation and methodology.
JH Weishaupt: resources.
C Behrends: conceptualization, resources, formal analysis, supervision, funding acquisition, visualization, project administration, and writing—original draft, review, and editing.

Conflict of Interest Statement

The authors declare that they have no conflict of interest.

References

1. Komander D, Rape M (2012) The ubiquitin code. *Annu Rev Biochem* 81: 203–229. doi:10.1146/annurev-biochem-060310-170328
2. Hershko A, Ciechanover A, Varshavsky A (2000) Basic medical research award. The ubiquitin system. *Nat Med* 6: 1073–1081. doi:10.1038/80384
3. Ravid T, Hochstrasser M (2008) Diversity of degradation signals in the ubiquitin–proteasome system. *Nat Rev Mol Cell Biol* 9: 679–689. doi:10.1038/nrm2468
4. Petroski MD, Deshaies RJ (2005) Function and regulation of cullin–RING ubiquitin ligases. *Nat Rev Mol Cell Biol* 6: 9–20. doi:10.1038/nrm1547
5. Bai C, Sen P, Hofmann K, Ma L, Goebl M, Harper JW, Elledge SJ (1996) SKP1 connects cell cycle regulators to the ubiquitin proteolysis machinery through a novel motif, the F-box. *Cell* 86: 263–274. doi:10.1016/s0092-8674(00)80098-7
6. Schulman BA, Lindstrom DL, Harlow E (1998) Substrate recruitment to cyclin-dependent kinase 2 by a multipurpose docking site on cyclin A. *Proc Natl Acad Sci U S A* 95: 10453–10458. doi:10.1073/pnas.95.18.10453
7. D'Angiolella V, Esencay M, Pagano M (2013) A cyclin without cyclin-dependent kinases: cyclin F controls genome stability through ubiquitin-mediated proteolysis. *Trends Cell Biol* 23: 135–140. doi:10.1016/j.tcb.2012.10.011
8. Skowyra D, Craig KL, Tyers M, Elledge SJ, Harper JW (1997) F-box proteins are receptors that recruit phosphorylated substrates to the SCF ubiquitin-ligase complex. *Cell* 91: 209–219. doi:10.1016/s0092-8674(00)80403-1
9. Feldman RMR, Correll CC, Kaplan KB, Deshaies RJ (1997) A complex of Cdc4p, Skp1p, and cdc53p/cullin catalyzes ubiquitination of the phosphorylated CDK inhibitor Sic1p. *Cell* 91: 221–230. doi:10.1016/s0092-8674(00)80404-3
10. Cardozo T, Pagano M (2004) The SCF ubiquitin ligase: Insights into a molecular machine. *Nat Rev Mol Cell Biol* 5: 739–751. doi:10.1038/nrm1471
11. Yuan R, Liu Q, Segeren HA, Yuniati L, Guardavaccaro D, Lebbink RJ, Westendorp B, de Bruin A (2019) Cyclin F-dependent degradation of E2F7 is critical for DNA repair and G2-phase progression. *EMBO J* 38: e101430. doi:10.15252/embj.2018101430
12. Choudhury R, Bonacci T, Arceci A, Lahiri D, Mills CA, Kernan JL, Branigan TB, DeCaprio JA, Burke DJ, Emanuele MJ (2016) APC/C and SCF(cyclin F) constitute a reciprocal feedback circuit controlling S-phase entry. *Cell Rep* 16: 3359–3372. doi:10.1016/j.celrep.2016.08.058
13. D'Angiolella V, Donato V, Vijayakumar S, Saraf A, Florens L, Washburn MP, Dynlacht B, Pagano M (2010) SCF(Cyclin F) controls centrosome homeostasis and mitotic fidelity through CP110 degradation. *Nature* 466: 138–142. doi:10.1038/nature09140
14. D'Angiolella V, Donato V, Forrester FM, Jeong YT, Pellacani C, Kudo Y, Saraf A, Florens L, Washburn MP, Pagano M (2012) Cyclin F-mediated degradation of ribonucleotide reductase M2 controls genome integrity and DNA repair. *Cell* 149: 1023–1034. doi:10.1016/j.cell.2012.03.043
15. Elia AE, Boardman AP, Wang DC, Huttlin EL, Everley RA, Dephoure N, Zhou C, Koren I, Gygi SP, Elledge SJ (2015) Quantitative proteomic atlas of ubiquitination and acetylation in the DNA damage response. *Mol Cell* 59: 867–881. doi:10.1016/j.molcel.2015.05.006
16. Emanuele MJ, Elia AE, Xu Q, Thoma CR, Izhar L, Leng Y, Guo A, Chen YN, Rush J, Hsu PC, et al (2011) Global identification of modular cullin-RING ligase substrates. *Cell* 147: 459–474. doi:10.1016/j.cell.2011.09.019
17. Chang SC, Hung CS, Zhang BX, Hsieh TH, Hsu W, Ding JL (2021) A novel signature of CCNF-associated E3 ligases collaborate and counter each other in breast cancer. *Cancers (Basel)* 13: 2873. doi:10.3390/cancers13122873
18. Li J, Zhou L, Liu Y, Yang L, Jiang D, Li K, Xie S, Wang X, Wang S (2021) Comprehensive analysis of cyclin family gene expression in colon cancer. *Front Oncol* 11: 674394. doi:10.3389/fonc.2021.674394
19. Chia R, Chiò A, Traynor BJ (2018) Novel genes associated with amyotrophic lateral sclerosis: Diagnostic and clinical implications. *Lancet Neurol* 17: 94–102. doi:10.1016/s1474-4422(17)30401-5
20. Pan C, Jiao B, Xiao T, Hou L, Zhang W, Liu X, Xu J, Tang B, Shen L (2017) Mutations of CCNF gene is rare in patients with amyotrophic lateral sclerosis and frontotemporal dementia from Mainland China.

Amyotroph Lateral Scler Frontotemporal Degener 18: 265–268. doi:10.1080/21678421.2017.1293111

21. Tripolszki K, Gampawar P, Schmidt H, Nagy ZF, Nagy D, Klivenyi P, Engelhardt JI, Szell M (2019) Comprehensive genetic analysis of a Hungarian amyotrophic lateral sclerosis cohort. *Front Genet* 10: 732. doi:10.3389/fgene.2019.00732
22. Pasinelli P, Brown RH (2006) Molecular biology of amyotrophic lateral sclerosis: Insights from genetics. *Nat Rev Neurosci* 7: 710–723. doi:10.1038/nrn1971
23. Webster CP, Smith EF, Shaw PJ, De Vos KJ (2017) Protein homeostasis in amyotrophic lateral sclerosis: Therapeutic opportunities? *Front Mol Neurosci* 10: 123. doi:10.3389/fnmol.2017.00123
24. Williams KL, Topp S, Yang S, Smith B, Fifita JA, Warraich ST, Zhang KY, Farrawell N, Vance C, Hu X, et al (2016) CCNF mutations in amyotrophic lateral sclerosis and frontotemporal dementia. *Nat Commun* 7: 11253. doi:10.1038/ncomms11253
25. Lee A, Rayner SL, Gwee SSL, De Luca A, Shahheydari H, Sundaramoorthy V, Ragagnin A, Morsch M, Radford R, Galper J, et al (2018) Pathogenic mutation in the ALS/FTD gene, CCNF, causes elevated Lys48-linked ubiquitylation and defective autophagy. *Cell Mol Life Sci* 75: 335–354. doi:10.1007/s00018-017-2632-8
26. Cheng F, De Luca A, Hogan AL, Rayner SL, Davidson JM, Watchon M, Stevens CH, Munoz SS, Ooi L, Yerbury JJ, et al (2021) Unbiased label-free quantitative proteomics of cells expressing amyotrophic lateral sclerosis (ALS) mutations in CCNF reveals activation of the apoptosis pathway: A workflow to screen pathogenic gene mutations. *Front Mol Neurosci* 14: 627740. doi:10.3389/fnmol.2021.627740
27. Hogan AL, Don EK, Rayner SL, Lee A, Laird AS, Watchon M, Winnick C, Tarr IS, Morsch M, Fifita JA, et al (2017) Expression of ALS/FTD-linked mutant CCNF in zebrafish leads to increased cell death in the spinal cord and an aberrant motor phenotype. *Hum Mol Genet* 26: 2616–2626. doi:10.1093/hmg/ddx136
28. Tsai PC, Liao YC, Chen PL, Guo YC, Chen YH, Jih KY, Lin KP, Soong BW, Tsai CP, Lee YC (2018) Investigating CCNF mutations in a Taiwanese cohort with amyotrophic lateral sclerosis. *Neurobiol Aging* 62: 243.e1–243.e6. doi:10.1016/j.neurobiolaging.2017.09.031
29. Tian D, Li J, Tang L, Zhang N, Fan D (2018) Screening for CCNF mutations in a Chinese amyotrophic lateral sclerosis cohort. *Front Aging Neurosci* 10: 185. doi:10.3389/fnagi.2018.00185
30. Yu Y, Nakagawa T, Morohoshi A, Nakagawa M, Ishida N, Suzuki N, Aoki M, Nakayama K (2019) Pathogenic mutations in the ALS gene CCNF cause cytoplasmic mislocalization of Cyclin F and elevated VCP ATPase activity. *Hum Mol Genet* 28: 3486–3497. doi:10.1093/hmg/ddz119
31. Fung TK, Siu WY, Yam CH, Lau A, Poon RY (2002) Cyclin F is degraded during G2-M by mechanisms fundamentally different from other cyclins. *J Biol Chem* 277: 35140–35149. doi:10.1074/jbc.m205503200
32. Kong M, Barnes EA, Ollendorff V, Donoghue DJ (2000) Cyclin F regulates the nuclear localization of cyclin B1 through a cyclin–cyclin interaction. *EMBO J* 19: 1378–1388. doi:10.1093/emboj/19.6.1378
33. Dankert JF, Rona G, Clijsters L, Geter P, Skaar JR, Bermudez-Hernandez K, Sassani E, Fenyo D, Ueberheide B, Schneider R, et al (2016) Cyclin F-mediated degradation of SLBP limits H2A.X accumulation and apoptosis upon genotoxic stress in G2. *Mol Cell* 64: 507–519. doi:10.1016/j.molcel.2016.09.010
34. Lee A, Rayner SL, De Luca A, Gwee SSL, Morsch M, Sundaramoorthy V, Shahheydari H, Ragagnin A, Shi B, Yang S, et al (2017) Casein kinase II phosphorylation of cyclin F at serine 621 regulates the Lys48-ubiquitylation E3 ligase activity of the SCF((cyclin F)) complex. *Open Biol* 7: 170058. doi:10.1098/rsob.170058
35. Subbarao Sreedhar A, Kalmár É, Csermely P, Shen Y-F (2004) Hsp90 isoforms: Functions, expression and clinical importance. *FEBS Lett* 562: 11–15. doi:10.1016/s0014-5793(04)00229-7
36. Prodromou C, Panaretou B, Chohan S, Siligardi G, O'Brien R, Ladbury JE, Roe SM, Piper PW, Pearl LH (2000) The ATPase cycle of Hsp90 drives a molecular 'clamp' via transient dimerization of the N-terminal domains. *EMBO J* 19: 4383–4392. doi:10.1093/emboj/19.16.4383
37. Biebl MM, Buchner J (2019) Structure, function, and regulation of the Hsp90 machinery. *Cold Spring Harb Perspect Biol* 11: a034017. doi:10.1101/cshperspect.a034017
38. Ali MMU, Roe SM, Vaughan CK, Meyer P, Panaretou B, Piper PW, Prodromou C, Pearl LH (2006) Crystal structure of an Hsp90–nucleotide–p23/Sba1 closed chaperone complex. *Nature* 440: 1013–1017. doi:10.1038/nature04716
39. Pearl LH, Prodromou C (2006) Structure and mechanism of the Hsp90 molecular chaperone machinery. *Annu Rev Biochem* 75: 271–294. doi:10.1146/annurev.biochem.75.103004.142738
40. Young JC, Moarefi I, Hartl FU (2001) Hsp90: A specialized but essential protein-folding tool. *J Cell Biol* 154: 267–274. doi:10.1083/jcb.200104079
41. Backe SJ, Sager RA, Woodford MR, Makedon AM, Mollapour M (2020) Post-translational modifications of Hsp90 and translating the chaperone code. *J Biol Chem* 295: 11099–11117. doi:10.1074/jbc.rev120.011833
42. Hornbeck PV, Zhang B, Murray B, Kornhauser JM, Latham V, Skrzypek E (2015) PhosphoSitePlus, 2014: Mutations, PTMs and recalibrations. *Nucleic Acids Res* 43: D512–D520. doi:10.1093/nar/gku1267
43. Mertins P, Qiao JW, Patel J, Udeshi ND, Clauser KR, Mani DR, Burgess MW, Gillette MA, Jaffe JD, Carr SA (2013) Integrated proteomic analysis of post-translational modifications by serial enrichment. *Nat Methods* 10: 634–637. doi:10.1038/nmeth.2518
44. Kundrat L, Regan L (2010) Identification of residues on Hsp70 and Hsp90 ubiquitinated by the cochaperone CHIP. *J Mol Biol* 395: 587–594. doi:10.1016/j.jmb.2009.11.017
45. Qian S-B, McDonough H, Boellmann F, Cyr DM, Patterson C (2006) CHIP-mediated stress recovery by sequential ubiquitination of substrates and Hsp70. *Nature* 440: 551–555. doi:10.1038/nature04600
46. Moffatt NSC, Bruinsma E, Uhl C, Obermann WMJ, Toft D (2008) Role of the cochaperone Tpr2 in Hsp90 chaperoning. *Biochemistry* 47: 8203–8213. doi:10.1021/bi800770g
47. Brychzy A, Rein T, Winklhofer KF, Hartl FU, Young JC, Obermann WM (2003) Cofactor Tpr2 combines two TPR domains and a J domain to regulate the Hsp70/Hsp90 chaperone system. *EMBO J* 22: 3613–3623. doi:10.1093/emboj/cdg362
48. McDonough H, Patterson C (2003) CHIP: A link between the chaperone and proteasome systems. *Cell Stress Chaperones* 8: 303. doi:10.1379/1466-1268(2003)008<0303:calbtc>2.0.co;2
49. Zachari M, Ganley IG (2017) The mammalian ULK1 complex and autophagy initiation. *Essays Biochem* 61: 585–596. doi:10.1042/ebc20170021
50. Kmiecik SW, Mayer MP (2022) Molecular mechanisms of heat shock factor 1 regulation. *Trends Biochem Sci* 47: 218–234. doi:10.1016/j.tibs.2021.10.004
51. Guo Q, Lehmer C, Martínez-Sánchez A, Rudack T, Beck F, Hartmann H, Pérez-Berlanga M, Frottin F, Hipp MS, Hartl FU, et al (2018) In situ structure of neuronal C9orf72 Poly-GA aggregates reveals proteasome recruitment. *Cell* 172: 696–705.e12. doi:10.1016/j.cell.2017.12.030
52. Zellner S, Schifferer M, Behrends C (2021) Systematically defining selective autophagy receptor-specific cargo using autophagosome content profiling. *Mol Cell* 81: 1337–1354.e8. doi:10.1016/j.molcel.2021.01.009
53. Kim HK, Min S, Song M, Jung S, Choi JW, Kim Y, Lee S, Yoon S, Kim HH (2018) Deep learning improves prediction of CRISPR–Cpf1 guide RNA activity. *Nat Biotechnol* 36: 239–241. doi:10.1038/nbt.4061
54. Sanson KR, DeWeirdt PC, Sangree AK, Hanna RE, Hegde M, Teng T, Borys SM, Strand C, Joung JK, Kleinstiver BP, et al (2019) Optimization of AsCas12a for combinatorial genetic screens in human cells. *BioRxiv*. doi:10.1101/747170 (Preprint posted August 28, 2019)

55. Concordet J-P, Haeussler M (2018) CRISPOR: Intuitive guide selection for CRISPR/Cas9 genome editing experiments and screens. *Nucleic Acids Res* 46: W242–W245. doi:10.1093/nar/gky354

56. Ran FA, Hsu PD, Wright J, Agarwala V, Scott DA, Zhang F (2013) Genome engineering using the CRISPR-Cas9 system. *Nat Protoc* 8: 2281–2308. doi:10.1038/nprot.2013.143

57. Rappsilber J, Ishihama Y, Mann M (2003) Stop and go extraction tips for matrix-assisted laser desorption/ionization, nanoelectrospray, and LC/MS sample pretreatment in proteomics. *Anal Chem* 75: 663–670. doi:10.1021/ac026117i

58. Cox J, Mann M (2008) MaxQuant enables high peptide identification rates, individualized p.p.b.-range mass accuracies and proteome-wide protein quantification. *Nat Biotechnol* 26: 1367–1372. doi:10.1038/nbt.1511

59. Cox J, Neuhauser N, Michalski A, Scheltema RA, Olsen JV, Mann M (2011) Andromeda: A peptide search engine integrated into the MaxQuant environment. *J Proteome Res* 10: 1794–1805. doi:10.1021/pr101065j

60. Huang DW, Sherman BT, Lempicki RA (2009) Systematic and integrative analysis of large gene lists using DAVID bioinformatics resources. *Nat Protoc* 4: 44–57. doi:10.1038/nprot.2008.211

61. Huang DW, Sherman BT, Lempicki RA (2009) Bioinformatics enrichment tools: Paths toward the comprehensive functional analysis of large gene lists. *Nucleic Acids Res* 37: 1–13. doi:10.1093/nar/gkn923

62. Fiskin E, Bionda T, Dikic I, Behrends C (2016) Global analysis of host and bacterial ubiquitinome in response to Salmonella typhimurium infection. *Mol Cell* 62: 967–981. doi:10.1016/j.molcel.2016.04.015

63. Villen J, Gygi SP (2008) The SCX/IMAC enrichment approach for global phosphorylation analysis by mass spectrometry. *Nat Protoc* 3: 1630–1638. doi:10.1038/nprot.2008.150

64. Saeed AI, Sharov V, White J, Li J, Liang W, Bhagabati N, Braisted J, Klapa M, Currier T, Thiagarajan M, et al (2003) TM4: A free, open-source system for microarray data management and analysis. *Biotechniques* 34: 374–378. doi:10.2144/03342mt01

Table 1 - Ubiquitin remnant diGly profiling of CCNF WT vs. KO (N2a, SH-SY5Y) or mutant (patient-derived LCL) cells.

Table 2 – Protein expression profiling of CCNF WT vs. KO (N2a, SH-SY5Y) or mutant (patient-derived LCL) cells.

Table 3 – Interaction proteomics of HA-Flag-CCNF from N2a and SH-SY5Y cells.

Table 4 – Proximity proteomics of APEX2-CCNF from N2a and SH-SY5Y cells.

Figure S1: Reproducibility across diGly proteomics experiments.

(A) Venn diagrams of diGly peptides found in quadruplicate experiments in N2a and SH-SY5Y CCNF WT and KO cells as well as ctrl and CCNF mutant LCLs.

(B) Changes in protein abundance in CCNF WT vs. KO and ctrl vs. CCNF mutant in N2a, SH-SY5Y and LCLs, respectively. Bar graph shows percentage of quantified proteins with either no (grey), decreased (blue; $\log_2$ FC (H:L) < -0.5) or increased (red; $\log_2$ FC (H:L) > 0.5) total protein abundances changes in CCNF KO or mutant compared to the respective control (n = 4).

(C) Total abundance changes of proteins with commonly decreased diGly sites in CCNF KO and mutant cells (Figure 1G). White indicates undetected proteins, grey shows proteins with unchanged abundances, while blue and red labels proteins with decreased ($\log_2$ FC (H:L) < -0.5) and increased ($\log_2$ FC (H:L) > 0.5) abundance, respectively.

Figure S2: **Biotinylation in APEX2-CCNF expressing cells.**

(A) N2a and SH-SY5Y APEX2-CCNF expressing cells were differentially treated with biotin-phenol (BP) and H_2O_2 prior to PFA fixation and staining with Biotin-FITC and DAPI. Scale bar indicates 10 µm.

(B) Volcano plots showing proteins detected by proximity biotinylation with APEX2-CCNF or APEX2-TBC1D7 in biotin-phenol and H_2O_2 treated SH-SY5Y cells. Proteins enriched in proximity to APEX2-CCNF and APEX2-TBC1D7 are shown in orange (t-test difference > 0.75, FDR corrected, q-value < 0.05, Student's t-test) and blue (log_2 FC < -0.75, FDR corrected, q-value < 0.05, Student's t-test), respectively. Known interactors of CCNF are highlighted with black circle. Top hits for CCNF and TBC1D7 are highlighted.

(C) Heat map of known CCNF interactors found in IP-MS and proximity proteomics experiments in this study (Figure 2D). Abundance changes of CCNF interactors are highlighted in grey (unchanged), red (increased) and blue (decreased). Proteins marked in white were not detected in respective dataset.

Figure S3: TOLLIP and TRIM28 are potential CCNF binding partners.

(A, B) Lysates from parental (mock), HA-Flag-FBXO28 or HA-Flag-CCNF overexpressing SH-SY5Y cells were subjected to HA (A) or Flag (B) immunoprecipitation followed by SDS-PAGE and immunoblotting. Arrows indicate specific protein bands.

Figure S4: HSP90AB1 stability and CCNF-dependent HSP90 client and co-factor binding.

(A) Empty or HA-FLAG-HSP90AB1 expressing SH-SY5Y CCNF WT or KO cells were subjected to an 8 h pulse-chase with cycloheximide (CHX) and Btz.

(B) Lysates from HA-FLAG-HSP90AB1 overexpressing SH-SY5Y CCNF WT or KO cells were incubated with HA agarose prior to SDS-PAGE and immunoblotting. Arrows indicate specific protein bands.

Figure S1

A

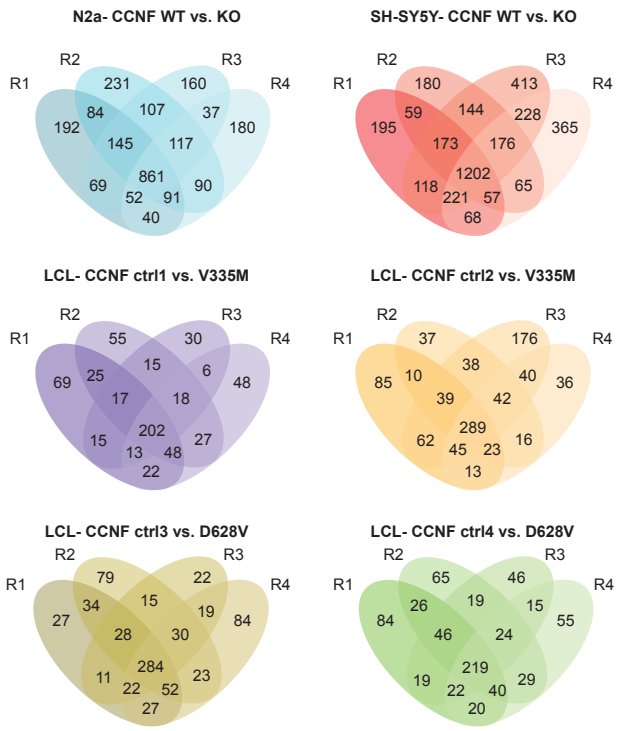

B

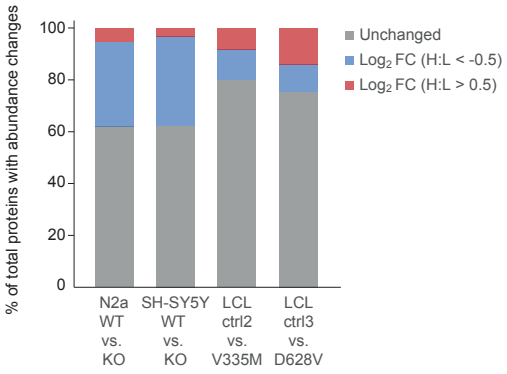

C

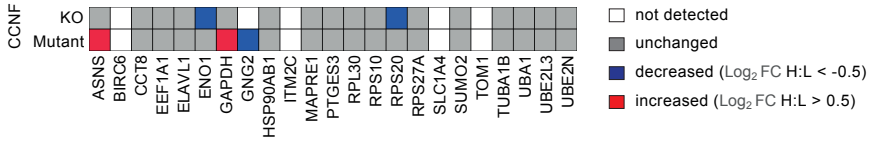

Figure S2

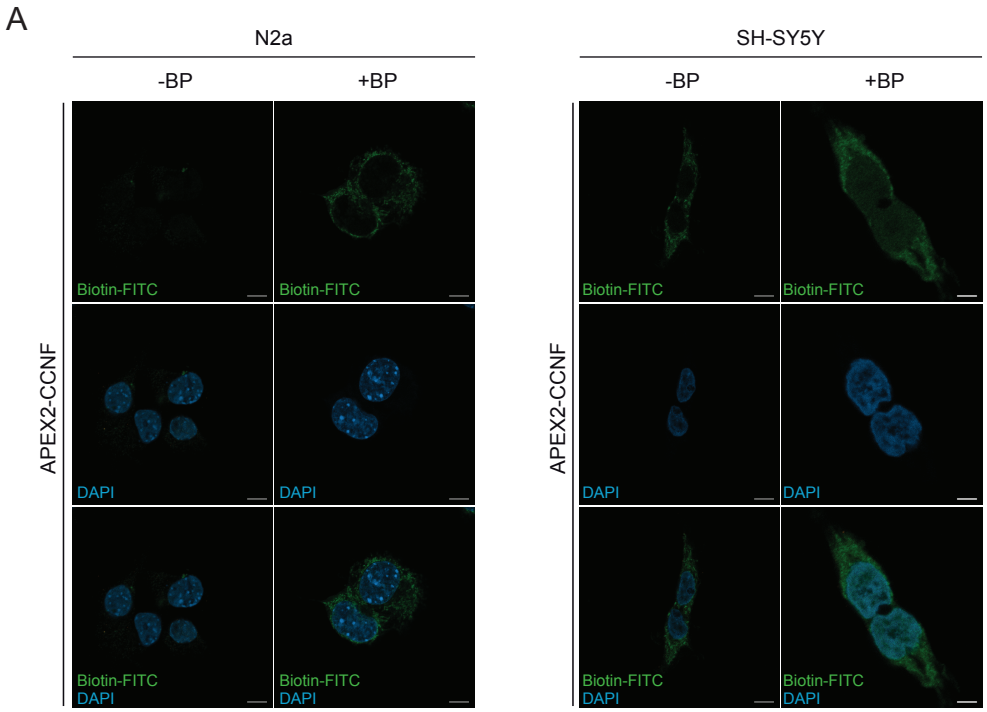
A
N2a
SH-SY5Y
-BP
+BP
APEX2-CCNF
Biotin-FITC
DAPI

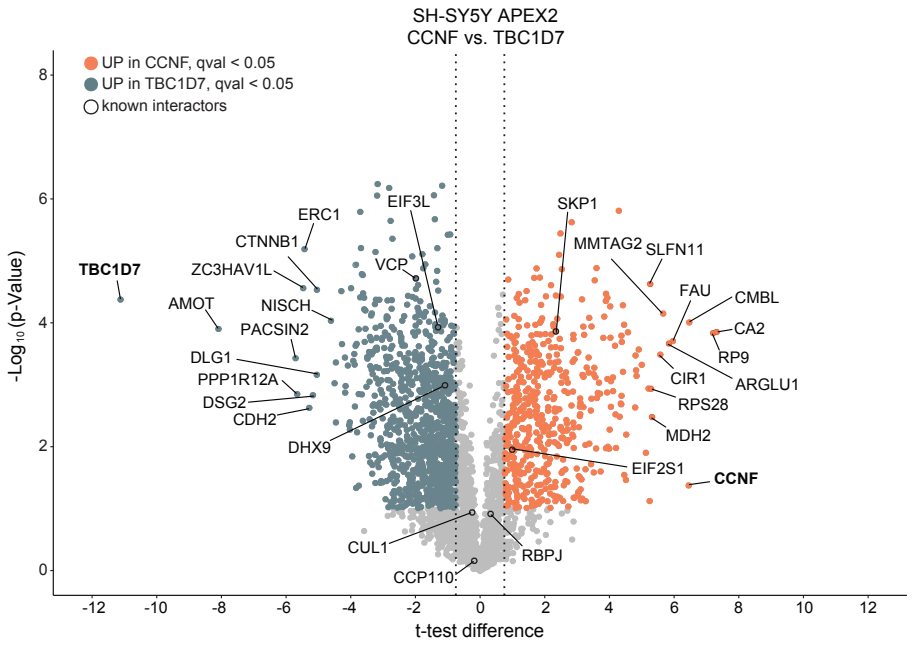
B
SH-SY5Y APEX2
CCNF vs. TBC1D7
UP in CCNF, qval < 0.05
UP in TBC1D7, qval < 0.05
known interactors
-Log10 (p-Value)
t-test difference
TBC1D7
ERC1
CTNNB1
ZC3HAV1L
AMOT
NISCH
PACSIN2
DLG1
PPP1R12A
DSG2
CDH2
DHX9
EIF3L
VCP
CUL1
CCP110
RBPJ
SKP1
MMTAG2
SLFN11
FAU
CMBL
CA2
RP9
CIR1
ARGLU1
RPS28
MDH2
EIF2S1
CCNF

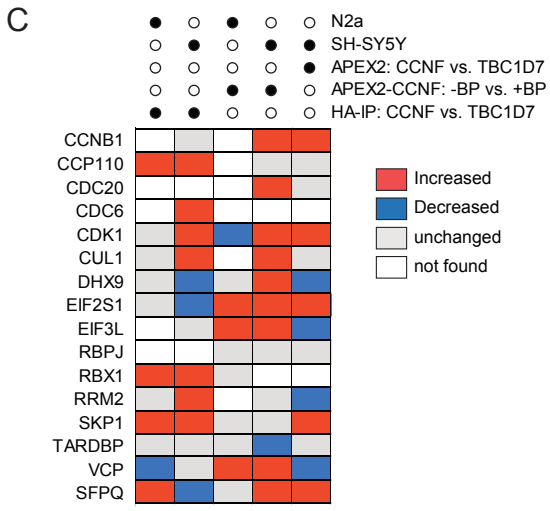
C
N2a
SH-SY5Y
APEX2: CCNF vs. TBC1D7
APEX2-CCNF: -BP vs. +BP
HA-IP: CCNF vs. TBC1D7
CCNB1
CCP110
CDC20
CDC6
CDK1
CUL1
DHX9
EIF2S1
EIF3L
RBPJ
RBX1
RRM2
SKP1
TARDBP
VCP
SFPQ
Increased
Decreased
unchanged
not found

Figure S3

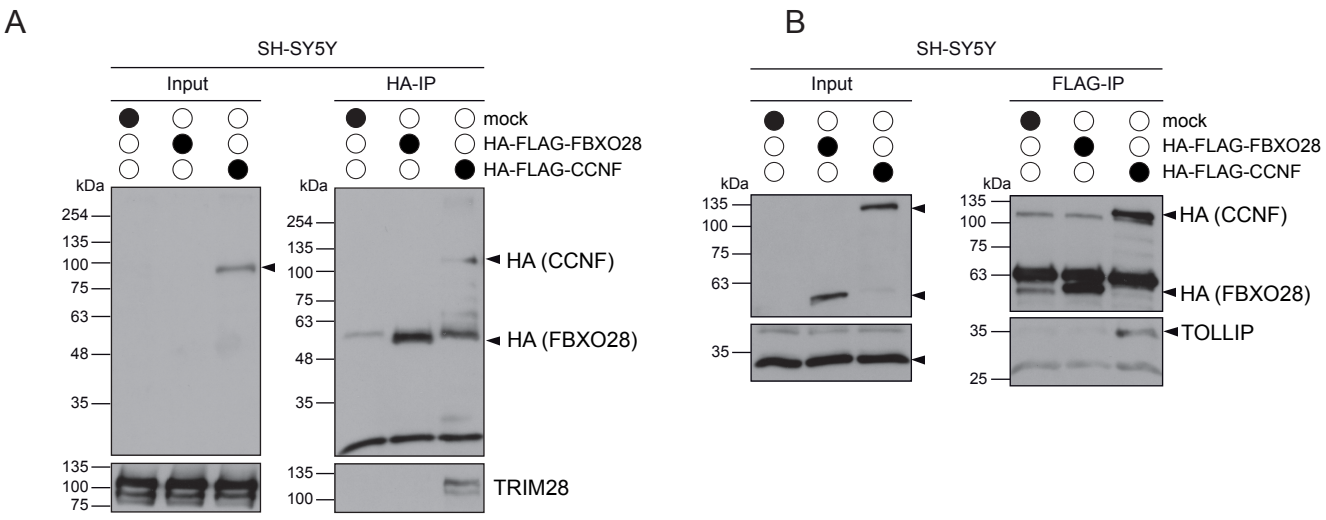
A
SH-SY5Y
Input
HA-IP
mock
HA-FLAG-FBXO28
HA-FLAG-CCNF
kDa
254
135
100
75
63
48
35
HA (CCNF)
HA (FBXO28)
TRIM28
B
SH-SY5Y
Input
FLAG-IP
mock
HA-FLAG-FBXO28
HA-FLAG-CCNF
HA (CCNF)
HA (FBXO28)
TOLLIP
25

Figure S4

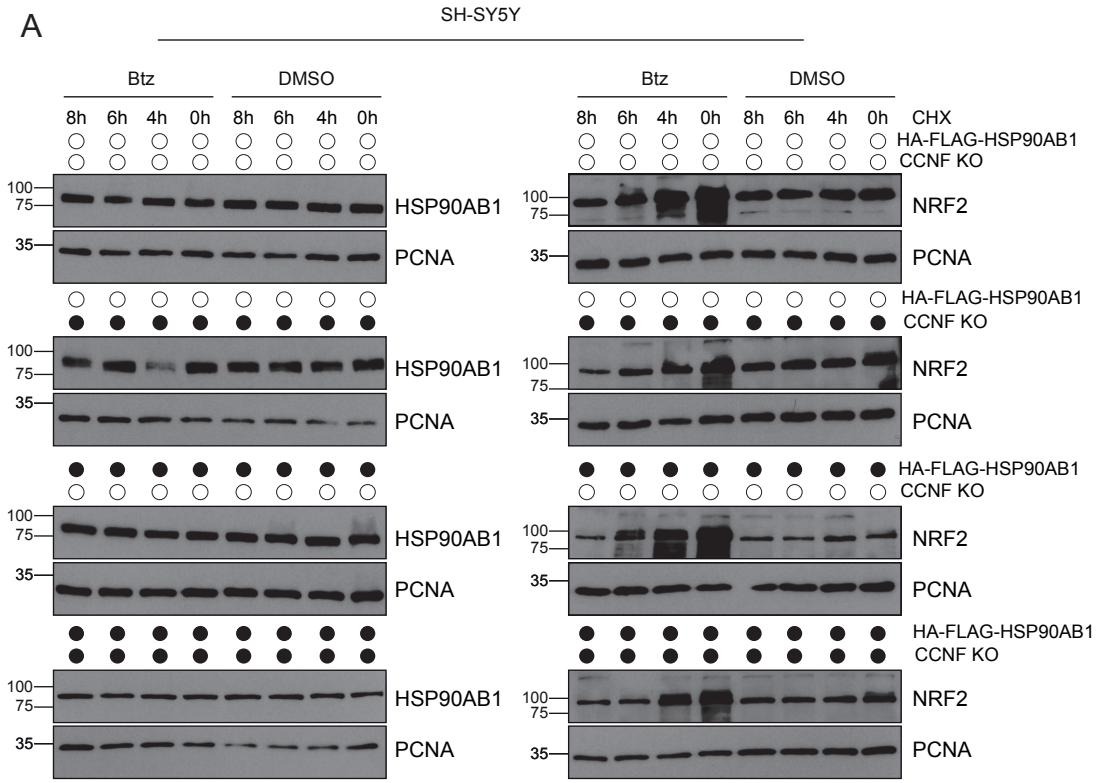
A
SH-SY5Y
Btz
DMSO
8h 6h 4h 0h 8h 6h 4h 0h
CHX
HA-FLAG-HSP90AB1
CCNF KO
100
75
35
HSP90AB1
PCNA
NRF2

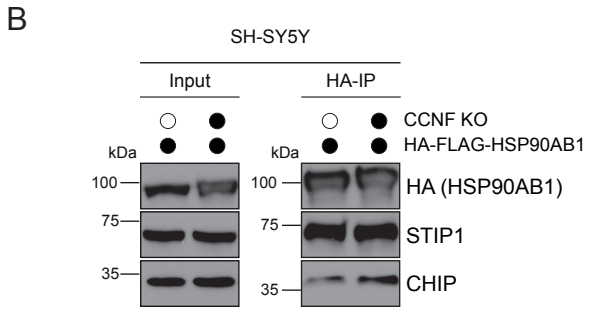
B
SH-SY5Y
Input
HA-IP
CCNF KO
HA-FLAG-HSP90AB1
kDa
100
75
35
HA (HSP90AB1)
STIP1
CHIP

2.2 Publication II

Ubiquitin profiling of lysophagy identifies actin stabilizer CNN2 as a target of VCP/p97 and uncovers a link to HSPB1

Published as:

Kravić B, Bionda T, Siebert A, Gahlot P, Levantovsky S, Behrends C, Meyer H. Ubiquitin profiling of lysophagy identifies actin stabilizer CNN2 as a target of VCP/p97 and uncovers a link to HSPB1. Mol Cell. 2022 Jul 21;82(14):2633-2649.e7. doi: 10.1016/j.molcel.2022.06.012. Epub 2022 Jul 5. PMID: 35793674.

Contribution:

In an exploratory approach to find novel interactors of CNN2, I performed state-of-the-art proximity proteomics using stable isotope labeling of amino acids in cell culture to investigate the proximity proteome of CNN2 in the context of lysosomal damage. This involved cloning CNN2 into the APEX2 vectors, establishing stable cell lines, as well as sample preparation and data analysis. Combined, my experiments led to the identification of HSPB1 as a novel interactor of CNN2 and p62 as a critical component in the lysophagic process.

3 References

1. Dobson, C.M., A. Šali, and M. Karplus, *Protein Folding: A Perspective from Theory and Experiment.* Angew Chem Int Ed Engl, 1998. **37**(7): p. 868-893.
2. Komander, D. and M. Rape, *The Ubiquitin Code.* Annual Review of Biochemistry, 2012. **81**(1): p. 203-229.
3. Balchin, D., M. Hayer-Hartl, and F.U. Hartl, *Recent advances in understanding catalysis of protein folding by molecular chaperones.* FEBS Letters, 2020. **594**(17): p. 2770-2781.
4. Ellis, R.J. and A.P. Minton, *Protein aggregation in crowded environments.* Biol Chem, 2006. **387**(5): p. 485-97.
5. Schieber, M. and Navdeep, *ROS Function in Redox Signaling and Oxidative Stress.* Current Biology, 2014. **24**(10): p. R453-R462.
6. Nandi, D., et al., *The ubiquitin-proteasome system.* Journal of Biosciences, 2006. **31**(1): p. 137-155.
7. Glick, D., S. Barth, and K.F. Macleod, *Autophagy: cellular and molecular mechanisms.* The Journal of Pathology, 2010. **221**(1): p. 3-12.
8. Zellner, S., M. Schifferer, and C. Behrends, *Systematically defining selective autophagy receptor-specific cargo using autophagosome content profiling.* Mol Cell, 2021. **81**(6): p. 1337-1354 e8.
9. Ghosh, R., et al., *Protein and Mitochondria Quality Control Mechanisms and Cardiac Aging.* Cells, 2020. **9**(4).
10. Anfinsen, C.B., *Principles that Govern the Folding of Protein Chains.* Science, 1973. **181**(4096): p. 223-230.
11. Hartl, F.U., *Molecular chaperones in cellular protein folding.* Nature, 1996. **381**(6583): p. 571-580.
12. Dunker, A.K., et al., *Function and structure of inherently disordered proteins.* Curr Opin Struct Biol, 2008. **18**(6): p. 756-64.
13. Lai, H.-Y., et al., *Multiple intermolecular interactions facilitate rapid evolution of essential genes.* Nature Ecology & Evolution, 2023. **7**(5): p. 745-755.
14. Balchin, D., M. Hayer-Hartl, and F.U. Hartl, *In vivo aspects of protein folding and quality control.* Science, 2016. **353**(6294): p. aac4354.
15. Garrido, C., et al., *Heat Shock Proteins: Endogenous Modulators of Apoptotic Cell Death.* Biochemical and Biophysical Research Communications, 2001. **286**(3): p. 433-442.
16. Hartl, F.U., A. Bracher, and M. Hayer-Hartl, *Molecular chaperones in protein folding and proteostasis.* Nature, 2011. **475**(7356): p. 324-332.
17. Szabo, A., et al., *The ATP hydrolysis-dependent reaction cycle of the Escherichia coli Hsp70 system DnaK, DnaJ, and GrpE.* Proceedings of the National Academy of Sciences, 1994. **91**(22): p. 10345-10349.
18. McCarty, J.S., et al., *The Role of ATP in the Functional Cycle of the DnaK Chaperone System.* Journal of Molecular Biology, 1995. **249**(1): p. 126-137.
19. Rudiger, S., *Substrate specificity of the DnaK chaperone determined by screening cellulose-bound peptide libraries.* The EMBO Journal, 1997. **16**(7): p. 1501-1507.
20. Hartl, F.U. and M. Hayer-Hartl, *Converging concepts of protein folding in vitro and in vivo.* Nature Structural & Molecular Biology, 2009. **16**(6): p. 574-581.
21. Morán Luengo, T., et al., *Hsp90 Breaks the Deadlock of the Hsp70 Chaperone System.* Molecular Cell, 2018. **70**(3): p. 545-552.e9.
22. Langer, T., et al., *Successive action of DnaK, DnaJ and GroEL along the pathway of chaperone-mediated protein folding.* Nature, 1992. **356**(6371): p. 683-689.

23. Subbarao Sreedhar, A., et al., *Hsp90 isoforms: functions, expression and clinical importance.* FEBS Letters, 2004. **562**(1-3): p. 11-15.
24. Biebl, M.M. and J. Buchner, *Structure, Function, and Regulation of the Hsp90 Machinery.* Cold Spring Harb Perspect Biol, 2019. **11**(9).
25. Dutta, R. and M. Inouye, *GHKL, an emergent ATPase/kinase superfamily.* Trends in Biochemical Sciences, 2000. **25**(1): p. 24-28.
26. Prodromou, C., et al., *The ATPase cycle of Hsp90 drives a molecular 'clamp' via transient dimerization of the N-terminal domains.* The EMBO Journal, 2000. **19**(16): p. 4383-4392.
27. Hessling, M., K. Richter, and J. Buchner, *Dissection of the ATP-induced conformational cycle of the molecular chaperone Hsp90.* Nature Structural & Molecular Biology, 2009. **16**(3): p. 287-293.
28. Hoter, A., M.E. El-Sabban, and H.Y. Naim, *The HSP90 Family: Structure, Regulation, Function, and Implications in Health and Disease.* Int J Mol Sci, 2018. **19**(9).
29. Tsutsumi, S., et al., *Hsp90 charged-linker truncation reverses the functional consequences of weakened hydrophobic contacts in the N domain.* Nature Structural & Molecular Biology, 2009. **16**(11): p. 1141-1147.
30. Shiau, A.K., et al., *Structural Analysis of E. coli hsp90 Reveals Dramatic Nucleotide-Dependent Conformational Rearrangements.* Cell, 2006. **127**(2): p. 329-340.
31. Louvion, J.-F., R. Warth, and D. Picard, *Two eukaryote-specific regions of Hsp82 are dispensable for its viability and signal transduction functions in yeast.* Proceedings of the National Academy of Sciences, 1996. **93**(24): p. 13937-13942.
32. Scheibel, T., et al., *The charged region of Hsp90 modulates the function of the N-terminal domain.* Proceedings of the National Academy of Sciences, 1999. **96**(4): p. 1297-1302.
33. Meyer, P., et al., *Structural and Functional Analysis of the Middle Segment of Hsp90: Implications for ATP Hydrolysis and Client Protein and Cochaperone Interactions.* Molecular Cell, 2003. **11**(3): p. 647-658.
34. Huai, Q., et al., *Structures of the N-Terminal and Middle Domains of E. coli Hsp90 and Conformation Changes upon ADP Binding.* Structure, 2005. **13**(4): p. 579-590.
35. Meng, X., et al., *Mutational analysis of Hsp90 alpha dimerization and subcellular localization: dimer disruption does not impede "in vivo' interaction with estrogen receptor.* Journal of Cell Science, 1996. **109**(7): p. 1677-1687.
36. Schopf, F.H., M.M. Biebl, and J. Buchner, *The HSP90 chaperone machinery.* Nat Rev Mol Cell Biol, 2017. **18**(6): p. 345-360.
37. Genest, O., S. Wickner, and S.M. Doyle, *Hsp90 and Hsp70 chaperones: Collaborators in protein remodeling.* Journal of Biological Chemistry, 2019. **294**(6): p. 2109-2120.
38. Scheibel, T., et al., *ATP-binding Properties of Human Hsp90.* Journal of Biological Chemistry, 1997. **272**(30): p. 18608-18613.
39. McLaughlin, S.H., H.W. Smith, and S.E. Jackson, *Stimulation of the weak ATPase activity of human hsp90 by a client protein.* J Mol Biol, 2002. **315**(4): p. 787-98.
40. Stebbins, C.E., et al., *Crystal Structure of an Hsp90–Geldanamycin Complex: Targeting of a Protein Chaperone by an Antitumor Agent.* Cell, 1997. **89**(2): p. 239-250.
41. Morishima, Y., et al., *Evidence for iterative ratcheting of receptor-bound hsp70 between its ATP and ADP conformations during assembly of glucocorticoid receptor.hsp90 heterocomplexes.* Biochemistry, 2001. **40**(4): p. 1109-16.
42. Johnson, B.D., et al., *Hop Modulates hsp70/hsp90 Interactions in Protein Folding.* Journal of Biological Chemistry, 1998. **273**(6): p. 3679-3686.
43. Wegele, H., et al., *Substrate transfer from the chaperone Hsp70 to Hsp90.* J Mol Biol, 2006. **356**(3): p. 802-11.
44. Richter, K., et al., *Sti1 Is a Non-competitive Inhibitor of the Hsp90 ATPase.* Journal of Biological Chemistry, 2003. **278**(12): p. 10328-10333.

45. Röhl, A., et al., *Hop/Sti1 phosphorylation inhibits its co-chaperone function.* EMBO reports, 2015. **16**(2): p. 240-249.
46. Panaretou, B., et al., *Activation of the ATPase Activity of Hsp90 by the Stress-Regulated Cochaperone Aha1.* Molecular Cell, 2002. **10**(6): p. 1307-1318.
47. Backe, S.J., et al., *Post-translational modifications of Hsp90 and translating the chaperone code.* Journal of Biological Chemistry, 2020. **295**(32): p. 11099-11117.
48. Soroka, J., et al., *Conformational Switching of the Molecular Chaperone Hsp90 via Regulated Phosphorylation.* Molecular Cell, 2012. **45**(4): p. 517-528.
49. Vaughan, C.K., et al., *Hsp90-Dependent Activation of Protein Kinases Is Regulated by Chaperone-Targeted Dephosphorylation of Cdc37.* Molecular Cell, 2008. **31**(6): p. 886-895.
50. Roe, S.M., et al., *The Mechanism of Hsp90 Regulation by the Protein Kinase-Specific Cochaperone p50cdc37.* Cell, 2004. **116**(1): p. 87-98.
51. Taipale, M., et al., *A quantitative chaperone interaction network reveals the architecture of cellular protein homeostasis pathways.* Cell, 2014. **158**(2): p. 434-448.
52. Qian, S.-B., et al., *CHIP-mediated stress recovery by sequential ubiquitination of substrates and Hsp70.* Nature, 2006. **440**(7083): p. 551-555.
53. McDonough, H. and C. Patterson, *CHIP: a link between the chaperone and proteasome systems.* Cell Stress & Chaperones, 2003. **8**(4): p. 303.
54. Kundrat, L. and L. Regan, *Identification of Residues on Hsp70 and Hsp90 Ubiquitinated by the Cochaperone CHIP.* Journal of Molecular Biology, 2010. **395**(3): p. 587-594.
55. Kampinga, H.H., et al., *Guidelines for the nomenclature of the human heat shock proteins.* Cell Stress and Chaperones, 2009. **14**(1): p. 105-111.
56. Stetler, R., et al., *HSP27: Mechanisms of Cellular Protection Against Neuronal Injury.* Current Molecular Medicine, 2009. **9**(7): p. 863-872.
57. de Jong, W.W., J.A.M. Leunissen, and C.E.M. Voorter, *Evolution of the alpha-crystallin/small heat-shock protein family.* Molecular Biology and Evolution, 1993.
58. Thériault, J.R., et al., *Essential Role of the NH2-terminal WD/EPF Motif in the Phosphorylation-activated Protective Function of Mammalian Hsp27.* Journal of Biological Chemistry, 2004. **279**(22): p. 23463-23471.
59. Lambert, H., et al., *HSP27 Multimerization Mediated by Phosphorylation-sensitive Intermolecular Interactions at the Amino Terminus.* Journal of Biological Chemistry, 1999. **274**(14): p. 9378-9385.
60. Muranova, L.K., et al., *Mutations in HspB1 and hereditary neuropathies.* Cell Stress and Chaperones, 2020. **25**(4): p. 655-665.
61. Ehrnsperger, M., M. Gaestel, and J. Buchner, *Analysis of chaperone properties of small Hsp's.* Methods Mol Biol, 2000. **99**: p. 421-9.
62. Ehrnsperger, M., et al., *The Dynamics of Hsp25 Quaternary Structure.* Journal of Biological Chemistry, 1999. **274**(21): p. 14867-14874.
63. Kostenko, S. and U. Moens, *Heat shock protein 27 phosphorylation: kinases, phosphatases, functions and pathology.* Cellular and Molecular Life Sciences, 2009. **66**(20): p. 3289-3307.
64. Arrigo, A.-P., *Mammalian HspB1 (Hsp27) is a molecular sensor linked to the physiology and environment of the cell.* Cell Stress and Chaperones, 2017. **22**(4): p. 517-529.
65. Jovcevski, B., et al., *Phosphomimics destabilize Hsp27 oligomeric assemblies and enhance chaperone activity.* Chem Biol, 2015. **22**(2): p. 186-95.
66. Rogalla, T., et al., *Regulation of Hsp27 Oligomerization, Chaperone Function, and Protective Activity against Oxidative Stress/Tumor Necrosis Factor α by Phosphorylation.* Journal of Biological Chemistry, 1999. **274**(27): p. 18947-18956.

67. Diaz-Latoud, C., et al., *Substitution of the unique cysteine residue of murine Hsp25 interferes with the protective activity of this stress protein through inhibition of dimer formation.* Antioxid Redox Signal, 2005. **7**(3-4): p. 436-45.
68. Gusev, N.B., N.V. Bogatcheva, and S.B. Marston, Biochemistry (Moscow), 2002. **67**(5): p. 511-519.
69. Lampros, M., et al., *The Role of Hsp27 in Chemotherapy Resistance.* Biomedicines, 2022. **10**(4): p. 897.
70. Jakob, U., et al., *Small heat shock proteins are molecular chaperones.* J Biol Chem, 1993. **268**(3): p. 1517-20.
71. Parcellier, A., et al., *HSP27 Is a Ubiquitin-Binding Protein Involved in I-κBα Proteasomal Degradation.* Molecular and Cellular Biology, 2003. **23**(16): p. 5790-5802.
72. Neininger, A. and M. Gaestel, *Evidence for ahsp25-Specific Mechanism Involved in Transcriptional Activation by Heat Shock.* Experimental Cell Research, 1998. **242**(1): p. 285-293.
73. Trinklein, N.D., et al., *Transcriptional regulation and binding of heat shock factor 1 and heat shock factor 2 to 32 human heat shock genes during thermal stress and differentiation.* Cell Stress & Chaperones, 2004. **9**(1): p. 21-28.
74. Nakagomi, S., et al., *Expression of the Activating Transcription Factor 3 Prevents c-Jun N-Terminal Kinase-Induced Neuronal Death by Promoting Heat Shock Protein 27 Expression and Akt Activation.* The Journal of Neuroscience, 2003. **23**(12): p. 5187-5196.
75. Wang, H., G. Lin, and Z. Zhang, *ATF5 promotes cell survival through transcriptional activation of Hsp27 in H9c2 cells.* Cell Biol Int, 2007. **31**(11): p. 1309-15.
76. Wilkerson, D.C., H.S. Skaggs, and K.D. Sarge, *HSF2 binds to the Hsp90, Hsp27, and c-Fos promoters constitutively and modulates their expression.* Cell Stress & Chaperones, 2007. **12**(3): p. 283.
77. D'Ydewalle, C., et al., *HDAC6 inhibitors reverse axonal loss in a mouse model of mutant HSPB1–induced Charcot-Marie-Tooth disease.* Nature Medicine, 2011. **17**(8): p. 968-974.
78. Pandey, P., et al., *Hsp27 functions as a negative regulator of cytochrome c-dependent activation of procaspase-3.* Oncogene, 2000. **19**(16): p. 1975-1981.
79. Qi, Z., et al., *Phosphorylation of heat shock protein 27 antagonizes TNF-α induced HeLa cell apoptosis via regulating TAK1 ubiquitination and activation of p38 and ERK signaling.* Cellular Signalling, 2014. **26**(7): p. 1616-1625.
80. Mounier, N. and A.-P. Arrigo, *Actin cytoskeleton and small heat shock proteins: how do they interact?* Cell Stress & Chaperones, 2002. **7**(2): p. 167.
81. Landry, J. and J. Huot, *Modulation of actin dynamics during stress and physiological stimulation by a signaling pathway involving p38 MAP kinase and heat-shock protein 27.* Biochem Cell Biol, 1995. **73**(9-10): p. 703-7.
82. Vahid, S., et al., *Molecular chaperone Hsp27 regulates the Hippo tumor suppressor pathway in cancer.* Scientific Reports, 2016. **6**(1): p. 31842.
83. Shiota, M., et al., *Hsp27 Regulates Epithelial Mesenchymal Transition, Metastasis, and Circulating Tumor Cells in Prostate Cancer.* Cancer Research, 2013. **73**(10): p. 3109-3119.
84. Gupta, A., A. Bansal, and K. Hashimoto-Torii, *HSP70 and HSP90 in neurodegenerative diseases.* Neuroscience Letters, 2020. **716**: p. 134678.
85. Hipp, M.S., P. Kasturi, and F.U. Hartl, *The proteostasis network and its decline in ageing.* Nat Rev Mol Cell Biol, 2019. **20**(7): p. 421-435.
86. Hyman, B.T., et al., *National Institute on Aging–Alzheimer's Association guidelines for the neuropathologic assessment of Alzheimer's disease.* Alzheimer's & Dementia, 2012. **8**(1): p. 1-13.

87. Haass, C., *The molecular significance of amyloid β-peptide for Alzheimer's disease.* European Archives of Psychiatry and Clinical Neuroscience, 1996. **246**(3): p. 118-123.
88. Trambauer, J., et al., *Chapter Six - Analyzing Amyloid-β Peptide Modulation Profiles and Binding Sites of γ-Secretase Modulators*, in *Methods in Enzymology*, M.H. Gelb, Editor. 2017, Academic Press. p. 157-183.
89. Saito, T., et al., *Potent amyloidogenicity and pathogenicity of Aβ43.* Nature Neuroscience, 2011. **14**(8): p. 1023-1032.
90. Wang, Y. and E. Mandelkow, *Tau in physiology and pathology.* Nature Reviews Neuroscience, 2016. **17**(1): p. 22-35.
91. Köpke, E., et al., *Microtubule-associated protein tau. Abnormal phosphorylation of a non-paired helical filament pool in Alzheimer disease.* J Biol Chem, 1993. **268**(32): p. 24374-84.
92. Gendron, T.F. and L. Petrucelli, *The role of tau in neurodegeneration.* Molecular Neurodegeneration, 2009. **4**(1): p. 13.
93. Maiti, P., et al., *Molecular Chaperone Dysfunction in Neurodegenerative Diseases and Effects of Curcumin.* BioMed Research International, 2014. **2014**: p. 1-14.
94. Evans, C.G., S. Wisén, and J.E. Gestwicki, *Heat Shock Proteins 70 and 90 Inhibit Early Stages of Amyloid β-(1–42) Aggregation in Vitro.* Journal of Biological Chemistry, 2006. **281**(44): p. 33182-33191.
95. Bohush, A., P. Bieganowski, and A. Filipek, *Hsp90 and Its Co-Chaperones in Neurodegenerative Diseases.* International Journal of Molecular Sciences, 2019. **20**(20): p. 4976.
96. Miyata, Y., H. Nakamoto, and L. Neckers, *The therapeutic target Hsp90 and cancer hallmarks.* Curr Pharm Des, 2013. **19**(3): p. 347-65.
97. Basso, A.D., et al., *Akt Forms an Intracellular Complex with Heat Shock Protein 90 (Hsp90) and Cdc37 and Is Destabilized by Inhibitors of Hsp90 Function.* Journal of Biological Chemistry, 2002. **277**(42): p. 39858-39866.
98. Hu, S., et al., *Molecular chaperones and Parkinson's disease.* Neurobiol Dis, 2021. **160**: p. 105527.
99. Hernandez, D.G., X. Reed, and A.B. Singleton, *Genetics in Parkinson disease: Mendelian versus non-Mendelian inheritance.* Journal of Neurochemistry, 2016. **139**: p. 59-74.
100. Outeiro, T.F., et al., *Formation of Toxic Oligomeric α-Synuclein Species in Living Cells.* PLoS ONE, 2008. **3**(4): p. e1867.
101. Tao, J., et al., *Hsp70 chaperone blocks α-synuclein oligomer formation via a novel engagement mechanism.* Journal of Biological Chemistry, 2021. **296**: p. 100613.
102. Uryu, K., et al., *Convergence of Heat Shock Protein 90 with Ubiquitin in Filamentous α-Synuclein Inclusions of α-Synucleinopathies.* The American Journal of Pathology, 2006. **168**(3): p. 947-961.
103. Putcha, P., et al., *Brain-Permeable Small-Molecule Inhibitors of Hsp90 Prevent α-Synuclein Oligomer Formation and Rescue α-Synuclein-Induced Toxicity.* Journal of Pharmacology and Experimental Therapeutics, 2010. **332**(3): p. 849-857.
104. Cyran, A.M. and A. Zhitkovich, *Heat Shock Proteins and HSF1 in Cancer.* Front Oncol, 2022. **12**: p. 860320.
105. Hershko, A., A. Ciechanover, and A. Varshavsky, *Basic Medical Research Award. The ubiquitin system.* Nat Med, 2000. **6**(10): p. 1073-81.
106. Ravid, T. and M. Hochstrasser, *Diversity of degradation signals in the ubiquitin–proteasome system.* Nature Reviews Molecular Cell Biology, 2008. **9**(9): p. 679-689.
107. Woelk, T., et al., *The ubiquitination code: a signalling problem.* Cell Div, 2007. **2**: p. 11.
108. Clague, M.J., S. Urbe, and D. Komander, *Breaking the chains: deubiquitylating enzyme specificity begets function.* Nat Rev Mol Cell Biol, 2019. **20**(6): p. 338-352.

109. Liu, C.-W., et al., *ATP Binding and ATP Hydrolysis Play Distinct Roles in the Function of 26S Proteasome.* Molecular Cell, 2006. **24**(1): p. 39-50.
110. Dong, Y., et al., *Cryo-EM structures and dynamics of substrate-engaged human 26S proteasome.* Nature, 2019. **565**(7737): p. 49-55.
111. Račková, L. and E. Csekes, *Proteasome Biology: Chemistry and Bioengineering Insights.* Polymers, 2020. **12**(12): p. 2909.
112. Chen, L. and K. Madura, *Evidence for distinct functions for human DNA repair factors hHR23A and hHR23B.* FEBS Letters, 2006. **580**(14): p. 3401-3408.
113. Finley, D., *Recognition and Processing of Ubiquitin-Protein Conjugates by the Proteasome.* Annual Review of Biochemistry, 2009. **78**(1): p. 477-513.
114. Vijay-Kumar, S., C.E. Bugg, and W.J. Cook, *Structure of ubiquitin refined at 1.8Åresolution.* Journal of Molecular Biology, 1987. **194**(3): p. 531-544.
115. Lange, O.F., et al., *Recognition Dynamics Up to Microseconds Revealed from an RDC-Derived Ubiquitin Ensemble in Solution.* Science, 2008. **320**(5882): p. 1471-1475.
116. Dikic, I., S. Wakatsuki, and K.J. Walters, *Ubiquitin-binding domains — from structures to functions.* Nature Reviews Molecular Cell Biology, 2009. **10**(10): p. 659-671.
117. Shih, S.C., K.E. Sloper-Mould, and L. Hicke, *Monoubiquitin carries a novel internalization signal that is appended to activated receptors.* The EMBO Journal, 2000. **19**(2): p. 187-198.
118. Sloper-Mould, K.E., et al., *Distinct Functional Surface Regions on Ubiquitin.* Journal of Biological Chemistry, 2001. **276**(32): p. 30483-30489.
119. Swatek, K.N. and D. Komander, *Ubiquitin modifications.* Cell Res, 2016. **26**(4): p. 399-422.
120. Hu, M., et al., *Crystal Structure of a UBP-Family Deubiquitinating Enzyme in Isolation and in Complex with Ubiquitin Aldehyde.* Cell, 2002. **111**(7): p. 1041-1054.
121. Rahighi, S., et al., *Specific Recognition of Linear Ubiquitin Chains by NEMO Is Important for NF-κB Activation.* Cell, 2009. **136**(6): p. 1098-1109.
122. Ye, Y., et al., *Polyubiquitin binding and cross-reactivity in the USP domain deubiquitinase USP21.* EMBO reports, 2011. **12**(4): p. 350-357.
123. Kamadurai, H.B., et al., *Insights into ubiquitin transfer cascades from a structure of a UbcH5B approximately ubiquitin-HECT(NEDD4L) complex.* Mol Cell, 2009. **36**(6): p. 1095-102.
124. Reyes-Turcu, F.E., et al., *The Ubiquitin Binding Domain ZnF UBP Recognizes the C-Terminal Diglycine Motif of Unanchored Ubiquitin.* Cell, 2006. **124**(6): p. 1197-1208.
125. Jin, L., et al., *Mechanism of Ubiquitin-Chain Formation by the Human Anaphase-Promoting Complex.* Cell, 2008. **133**(4): p. 653-665.
126. Haglund, K., P.P. Di Fiore, and I. Dikic, *Distinct monoubiquitin signals in receptor endocytosis.* Trends in Biochemical Sciences, 2003. **28**(11): p. 598-604.
127. Hoeller, D., et al., *Regulation of ubiquitin-binding proteins by monoubiquitination.* Nature Cell Biology, 2006. **8**(2): p. 163-169.
128. Ronai, Z.E.A., *Monoubiquitination in proteasomal degradation.* Proceedings of the National Academy of Sciences, 2016. **113**(32): p. 8894-8896.
129. Dittmar, G. and K.F. Winklhofer, *Linear Ubiquitin Chains: Cellular Functions and Strategies for Detection and Quantification.* Frontiers in Chemistry, 2020. **7**.
130. Ikeda, F. and I. Dikic, *Atypical ubiquitin chains: new molecular signals. 'Protein Modifications: Beyond the Usual Suspects' review series.* EMBO Rep, 2008. **9**(6): p. 536-42.
131. Matsumoto, M.L., et al., *K11-Linked Polyubiquitination in Cell Cycle Control Revealed by a K11 Linkage-Specific Antibody.* Molecular Cell, 2010. **39**(3): p. 477-484.

132. Yuan, W.-C., et al., *K33-Linked Polyubiquitination of Coronin 7 by Cul3-KLHL20 Ubiquitin E3 Ligase Regulates Protein Trafficking.* Molecular Cell, 2014. **54**(4): p. 586-600.
133. Kulathu, Y. and D. Komander, *Atypical ubiquitylation — the unexplored world of polyubiquitin beyond Lys48 and Lys63 linkages.* Nature Reviews Molecular Cell Biology, 2012. **13**(8): p. 508-523.
134. Boname, J.M., et al., *Efficient Internalization of MHC I Requires Lysine-11 and Lysine-63 Mixed Linkage Polyubiquitin Chains.* Traffic, 2010. **11**(2): p. 210-220.
135. Andrew, et al., *Quantitative Proteomic Atlas of Ubiquitination and Acetylation in the DNA Damage Response.* Molecular Cell, 2015. **59**(5): p. 867-881.
136. Elia, A.E., et al., *Quantitative Proteomic Atlas of Ubiquitination and Acetylation in the DNA Damage Response.* Mol Cell, 2015. **59**(5): p. 867-81.
137. Lee, I. and H. Schindelin, *Structural Insights into E1-Catalyzed Ubiquitin Activation and Transfer to Conjugating Enzymes.* Cell, 2008. **134**(2): p. 268-278.
138. Leidecker, O., et al., *The ubiquitin E1 enzyme Ube1 mediates NEDD8 activation under diverse stress conditions.* Cell Cycle, 2012. **11**(6): p. 1142-1150.
139. Bialas, J., M. Groettrup, and A. Aichem, *Conjugation of the Ubiquitin Activating Enzyme UBE1 with the Ubiquitin-Like Modifier FAT10 Targets It for Proteasomal Degradation.* PLOS ONE, 2015. **10**(3): p. e0120329.
140. Groettrup, M., et al., *Activating the ubiquitin family: UBA6 challenges the field.* Trends in Biochemical Sciences, 2008. **33**(5): p. 230-237.
141. Groen, E.J.N. and T.H. Gillingwater, *UBA1: At the Crossroads of Ubiquitin Homeostasis and Neurodegeneration.* Trends Mol Med, 2015. **21**(10): p. 622-632.
142. Kulkarni, M. and H.E. Smith, *E1 Ubiquitin-Activating Enzyme UBA-1 Plays Multiple Roles throughout C. elegans Development.* PLoS Genetics, 2008. **4**(7): p. e1000131.
143. McGrath, J.P., S. Jentsch, and A. Varshavsky, *UBA 1: an essential yeast gene encoding ubiquitin-activating enzyme.* The EMBO Journal, 1991. **10**(1): p. 227-236.
144. Williams, K.M., et al., *Structural insights into E1 recognition and the ubiquitin-conjugating activity of the E2 enzyme Cdc34.* Nature Communications, 2019. **10**(1).
145. Tokgöz, Z., et al., *E1-E2 Interactions in Ubiquitin and Nedd8 Ligation Pathways.* Journal of Biological Chemistry, 2012. **287**(1): p. 311-321.
146. Schulman, B.A. and J. Wade Harper, *Ubiquitin-like protein activation by E1 enzymes: the apex for downstream signalling pathways.* Nature Reviews Molecular Cell Biology, 2009. **10**(5): p. 319-331.
147. Hershko, A., et al., *Components of ubiquitin-protein ligase system. Resolution, affinity purification, and role in protein breakdown.* J Biol Chem, 1983. **258**(13): p. 8206-14.
148. Ye, Y. and M. Rape, *Building ubiquitin chains: E2 enzymes at work.* Nature Reviews Molecular Cell Biology, 2009. **10**(11): p. 755-764.
149. Wenzel, D.M., et al., *UBCH7 reactivity profile reveals parkin and HHARI to be RING/HECT hybrids.* Nature, 2011. **474**(7349): p. 105-108.
150. Dawn, Kate, and Rachel, *E2s: structurally economical and functionally replete.* Biochemical Journal, 2011. **433**(1): p. 31-42.
151. Stewart, M.D., et al., *E2 enzymes: more than just middle men.* Cell Res, 2016. **26**(4): p. 423-40.
152. Kim, H.C. and J.M. Huibregtse, *Polyubiquitination by HECT E3s and the Determinants of Chain Type Specificity.* Molecular and Cellular Biology, 2009. **29**(12): p. 3307-3318.
153. Walden, H. and K. Rittinger, *RBR ligase-mediated ubiquitin transfer: a tale with many twists and turns.* Nat Struct Mol Biol, 2018. **25**(6): p. 440-445.
154. Berndsen, C.E. and C. Wolberger, *New insights into ubiquitin E3 ligase mechanism.* Nature Structural & Molecular Biology, 2014. **21**(4): p. 301-307.

155. Dou, H., et al., *BIRC7–E2 ubiquitin conjugate structure reveals the mechanism of ubiquitin transfer by a RING dimer.* Nature Structural & Molecular Biology, 2012. **19**(9): p. 876-883.
156. Mattiroli, F., et al., *RNF168 Ubiquitinates K13-15 on H2A/H2AX to Drive DNA Damage Signaling.* Cell, 2012. **150**(6): p. 1182-1195.
157. Deol, K.K., S. Lorenz, and E.R. Strieter, *Enzymatic Logic of Ubiquitin Chain Assembly.* Frontiers in Physiology, 2019. **10**.
158. Martinez-Chacin, R.C., et al., *Ubiquitin chain-elongating enzyme UBE2S activates the RING E3 ligase APC/C for substrate priming.* Nature Structural & Molecular Biology, 2020. **27**(6): p. 550-560.
159. Wijk, S.J.L. and H.T.M. Timmers, *The family of ubiquitin-conjugating enzymes (E2s): deciding between life and death of proteins.* The FASEB Journal, 2010. **24**(4): p. 981-993.
160. Pruneda, J.N., et al., *Ubiquitin in Motion: Structural Studies of the Ubiquitin-Conjugating Enzyme∼Ubiquitin Conjugate.* Biochemistry, 2011. **50**(10): p. 1624-1633.
161. Yuan, L., et al., *Structural insights into the mechanism and E2 specificity of the RBR E3 ubiquitin ligase HHARI.* Nature Communications, 2017. **8**(1).
162. Pruneda, J.N., et al., *E2~Ub conjugates regulate the kinase activity ofShigellaeffector OspG during pathogenesis.* The EMBO Journal, 2014: p. n/a-n/a.
163. Branigan, E., et al., *Structural basis for the RING-catalyzed synthesis of K63-linked ubiquitin chains.* Nature Structural & Molecular Biology, 2015. **22**(8): p. 597-602.
164. Plechanovová, A., et al., *Structure of a RING E3 ligase and ubiquitin-loaded E2 primed for catalysis.* Nature, 2012. **489**(7414): p. 115-120.
165. Deshaies, R.J. and C.A.P. Joazeiro, *RING Domain E3 Ubiquitin Ligases.* Annual Review of Biochemistry, 2009. **78**(1): p. 399-434.
166. Bui, Q.T., et al., *Ubiquitin-Conjugating Enzymes in Cancer.* Cells, 2021. **10**(6): p. 1383.
167. Yang, Q., et al., *E3 ubiquitin ligases: styles, structures and functions.* Molecular Biomedicine, 2021. **2**(1).
168. Huibregtse, J.M., et al., *A family of proteins structurally and functionally related to the E6-AP ubiquitin-protein ligase.* Proceedings of the National Academy of Sciences, 1995. **92**(7): p. 2563-2567.
169. Kumar, S., A.L. Talis, and P.M. Howley, *Identification of HHR23A as a Substrate for E6-associated Protein-mediated Ubiquitination.* Journal of Biological Chemistry, 1999. **274**(26): p. 18785-18792.
170. Huibregtse, J.M., J.C. Yang, and S.L. Beaudenon, *The large subunit of RNA polymerase II is a substrate of the Rsp5 ubiquitin-protein ligase.* Proceedings of the National Academy of Sciences, 1997. **94**(8): p. 3656-3661.
171. Schwarz, S.E., J.L. Rosa, and M. Scheffner, *Characterization of Human hect Domain Family Members and Their Interaction with UbcH5 and UbcH7.* Journal of Biological Chemistry, 1998. **273**(20): p. 12148-12154.
172. Pickart, C.M., *Mechanisms underlying ubiquitination.* Annu. Rev. Biochem., 2001. **70**: p. 503–533.
173. You, J. and C.M. Pickart, *A HECT Domain E3 Enzyme Assembles Novel Polyubiquitin Chains.* Journal of Biological Chemistry, 2001. **276**(23): p. 19871-19878.
174. Huang, H., et al., *K33-Linked Polyubiquitination of T Cell Receptor-ζ Regulates Proteolysis-Independent T Cell Signaling.* Immunity, 2010. **33**(1): p. 60-70.
175. Chastagner, P., A. Israël, and C. Brou, *Itch/AIP4 mediates Deltex degradation through the formation of K29-linked polyubiquitin chains.* EMBO reports, 2006. **7**(11): p. 1147-1153.

176. Peng, D.J., et al., *Noncanonical K27-linked polyubiquitination of TIEG1 regulates Foxp3 expression and tumor growth.* J Immunol, 2011. **186**(10): p. 5638-47.
177. Spratt, Donald E., H. Walden, and Gary S. Shaw, *RBR E3 ubiquitin ligases: new structures, new insights, new questions.* Biochemical Journal, 2014. **458**(3): p. 421-437.
178. Dove, K.K., et al., *Structural Studies of HHARI/UbcH7∼Ub Reveal Unique E2∼Ub Conformational Restriction by RBR RING1.* Structure, 2017. **25**(6): p. 890-900.e5.
179. Kirisako, T., et al., *A ubiquitin ligase complex assembles linear polyubiquitin chains.* The EMBO Journal, 2006. **25**(20): p. 4877-4887.
180. Chaugule, V.K., et al., *Autoregulation of Parkin activity through its ubiquitin-like domain.* The EMBO Journal, 2011. **30**(14): p. 2853-2867.
181. Deol, K.K., S.J. Eyles, and E.R. Strieter, *Quantitative Middle-Down MS Analysis of Parkin-Mediated Ubiquitin Chain Assembly.* Journal of the American Society for Mass Spectrometry, 2020. **31**(5): p. 1132-1139.
182. Freemont, P.S., I.M. Hanson, and J. Trowsdale, *A novel cysteine-rich sequence motif.* Cell, 1991. **64**(3): p. 483-4.
183. Zheng, N., et al., *Structure of the Cul1–Rbx1–Skp1–F boxSkp2 SCF ubiquitin ligase complex.* Nature, 2002. **416**(6882): p. 703-709.
184. Borden, K.L., et al., *The solution structure of the RING finger domain from the acute promyelocytic leukaemia proto-oncoprotein PML.* The EMBO Journal, 1995. **14**(7): p. 1532-1541.
185. Tao, H., et al., *Structure of the MID1 Tandem B-Boxes Reveals an Interaction Reminiscent of Intermolecular Ring Heterodimers.* Biochemistry, 2008. **47**(8): p. 2450-2457.
186. Vander Kooi, C.W., et al., *The Prp19 U-box Crystal Structure Suggests a Common Dimeric Architecture for a Class of Oligomeric E3 Ubiquitin Ligases.* Biochemistry, 2006. **45**(1): p. 121-130.
187. Aravind, L. and E.V. Koonin, *The U box is a modified RING finger — a common domain in ubiquitination.* Current Biology, 2000. **10**(4): p. R132-R134.
188. Lee, S.-O., et al., *The RING domain of mitochondrial E3 ubiquitin ligase 1 and its complex with Ube2D2: crystallization and X-ray diffraction.* Acta Crystallographica Section F Structural Biology Communications, 2020. **76**(1): p. 1-7.
189. Petroski, M.D. and R.J. Deshaies, *Function and regulation of cullin–RING ubiquitin ligases.* Nature Reviews Molecular Cell Biology, 2005. **6**(1): p. 9-20.
190. Seol, J.H., et al., *Cdc53/cullin and the essential Hrt1 RING-H2 subunit of SCF define a ubiquitin ligase module that activates the E2 enzyme Cdc34.* Genes Dev, 1999. **13**(12): p. 1614-26.
191. Branigan, E., J. Carlos Penedo, and R.T. Hay, *Ubiquitin transfer by a RING E3 ligase occurs from a closed E2~ubiquitin conformation.* Nature Communications, 2020. **11**(1).
192. Saha, A. and R.J. Deshaies, *Multimodal Activation of the Ubiquitin Ligase SCF by Nedd8 Conjugation.* Molecular Cell, 2008. **32**(1): p. 21-31.
193. Petroski, M.D. and R.J. Deshaies, *Mechanism of Lysine 48-Linked Ubiquitin-Chain Synthesis by the Cullin-RING Ubiquitin-Ligase Complex SCF-Cdc34.* Cell, 2005. **123**(6): p. 1107-1120.
194. Williamson, A., et al., *Regulation of Ubiquitin Chain Initiation to Control the Timing of Substrate Degradation.* Molecular Cell, 2011. **42**(6): p. 744-757.
195. Yu, H., et al., *Identification of a novel ubiquitin-conjugating enzyme involved in mitotic cyclin degradation.* Current Biology, 1996. **6**(4): p. 455-466.
196. Harper, J.W. and B.A. Schulman, *Cullin-RING Ubiquitin Ligase Regulatory Circuits: a Quarter Century Beyond the F-box Hypothesis.* Annu Rev Biochem, 2021.
197. Jin, J., et al., *Systematic analysis and nomenclature of mammalian F-box proteins.* Genes & Development, 2004. **18**(21): p. 2573-2580.

198. Chang Bai, P.S., Kay Hofmann, Lei Ma, Mark Goebl, J. Wade Harper, Stephen J. Elledge, *SKP1 Connects Cell Cycle Regulators to the Ubiquitin Proteolysis Machinery through a Novel Motif, the F-Box.* Cell, 1996. **86**: p. 263–274.
199. Angers, S., et al., *Molecular architecture and assembly of the DDB1–CUL4A ubiquitin ligase machinery.* Nature, 2006. **443**(7111): p. 590-593.
200. Jin, J., et al., *A Family of Diverse Cul4-Ddb1-Interacting Proteins Includes Cdt2, which Is Required for S Phase Destruction of the Replication Factor Cdt1.* Molecular Cell, 2006. **23**(5): p. 709-721.
201. He, Y.J., et al., *DDB1 functions as a linker to recruit receptor WD40 proteins to CUL4–ROC1 ubiquitin ligases.* Genes & Development, 2006. **20**(21): p. 2949-2954.
202. Kamura, T., et al., *MUF1, A Novel Elongin BC-interacting Leucine-rich Repeat Protein That Can Assemble with Cul5 and Rbx1 to Reconstitute a Ubiquitin Ligase.* Journal of Biological Chemistry, 2001. **276**(32): p. 29748-29753.
203. Kamura, T., et al., *Activation of HIF1α ubiquitination by a reconstituted von Hippel-Lindau (VHL) tumor suppressor complex.* Proceedings of the National Academy of Sciences, 2000. **97**(19): p. 10430-10435.
204. Kamura, T., et al., *VHL-box and SOCS-box domains determine binding specificity for Cul2-Rbx1 and Cul5-Rbx2 modules of ubiquitin ligases.* Genes Dev, 2004. **18**(24): p. 3055-65.
205. Furukawa, M., et al., *Targeting of protein ubiquitination by BTB–Cullin 3–Roc1 ubiquitin ligases.* Nature Cell Biology, 2003. **5**(11): p. 1001-1007.
206. Pintard, L., et al., *The BTB protein MEL-26 is a substrate-specific adaptor of the CUL-3 ubiquitin-ligase.* Nature, 2003. **425**(6955): p. 311-316.
207. Geyer, R., et al., *BTB/POZ Domain Proteins Are Putative Substrate Adaptors for Cullin 3 Ubiquitin Ligases.* Molecular Cell, 2003. **12**(3): p. 783-790.
208. Xu, L., et al., *BTB proteins are substrate-specific adaptors in an SCF-like modular ubiquitin ligase containing CUL-3.* Nature, 2003. **425**(6955): p. 316-321.
209. Zhuang, M., et al., *Structures of SPOP-Substrate Complexes: Insights into Molecular Architectures of BTB-Cul3 Ubiquitin Ligases.* Molecular Cell, 2009. **36**(1): p. 39-50.
210. Harper, J.W. and M.K. Tan, *Understanding cullin-RING E3 biology through proteomics-based substrate identification.* Mol Cell Proteomics, 2012. **11**(12): p. 1541-50.
211. Wang, X. and D.S. Martin, *The COP9 signalosome and cullin-RING ligases in the heart.* Am J Cardiovasc Dis, 2015. **5**(1): p. 1-18.
212. Rabut, G. and M. Peter, *Function and regulation of protein neddylation.* EMBO reports, 2008. **9**(10): p. 969-976.
213. Liakopoulos, D., *A novel protein modification pathway related to the ubiquitin system.* The EMBO Journal, 1998. **17**(8): p. 2208-2214.
214. Osaka, F., et al., *A new NEDD8-ligating system for cullin-4A.* Genes & Development, 1998. **12**(15): p. 2263-2268.
215. Gong, L. and E.T.H. Yeh, *Identification of the Activating and Conjugating Enzymes of the NEDD8 Conjugation Pathway.* Journal of Biological Chemistry, 1999. **274**(17): p. 12036-12042.
216. Huang, D.T., et al., *E2-RING expansion of the NEDD8 cascade confers specificity to cullin modification.* Mol Cell, 2009. **33**(4): p. 483-95.
217. Cavadini, S., et al., *Cullin–RING ubiquitin E3 ligase regulation by the COP9 signalosome.* Nature, 2016. **531**(7596): p. 598-603.
218. Zheng, J., et al., *CAND1 Binds to Unneddylated CUL1 and Regulates the Formation of SCF Ubiquitin E3 Ligase Complex.* Molecular Cell, 2002. **10**(6): p. 1519-1526.
219. Chamovitz, D.A., et al., *The COP9 complex, a novel multisubunit nuclear regulator involved in light control of a plant developmental switch.* Cell, 1996. **86**(1): p. 115-121.

220. Lyapina, S., et al., *Promotion of NEDD-CUL1 conjugate cleavage by COP9 signalosome.* Science, 2001. **292**(5520): p. 1382-5.
221. Bornstein, G., D. Ganoth, and A. Hershko, *Regulation of neddylation and deneddylation of cullin1 in SCF(Skp2) ubiquitin ligase by F-box protein and substrate.* Proceedings of the National Academy of Sciences, 2006. **103**(31): p. 11515-11520.
222. Chew, E.-H. and T. Hagen, *Substrate-mediated Regulation of Cullin Neddylation.* Journal of Biological Chemistry, 2007. **282**(23): p. 17032-17040.
223. Enchev, R.I., et al., *Structural basis for a reciprocal regulation between SCF and CSN.* Cell Rep, 2012. **2**(3): p. 616-27.
224. Mosadeghi, R., et al., *Structural and kinetic analysis of the COP9-Signalosome activation and the cullin-RING ubiquitin ligase deneddylation cycle.* eLife, 2016. **5**.
225. Faull, S.V., et al., *Structural basis of Cullin 2 RING E3 ligase regulation by the COP9 signalosome.* Nature Communications, 2019. **10**(1).
226. Baek, K., et al., *NEDD8 nucleates a multivalent cullin–RING–UBE2D ubiquitin ligation assembly.* Nature, 2020. **578**(7795): p. 461-466.
227. Baek, K., D.C. Scott, and B.A. Schulman, *NEDD8 and ubiquitin ligation by cullin-RING E3 ligases.* Curr Opin Struct Biol, 2021. **67**: p. 101-109.
228. Schulman, B.A., et al., *Insights into SCF ubiquitin ligases from the structure of the Skp1–Skp2 complex.* Nature, 2000. **408**(6810): p. 381-386.
229. Winston, J.T., et al., *A family of mammalian F-box proteins.* Current Biology, 1999. **9**(20): p. 1180-S3.
230. Edward T Kipreos, M.P., *The F-box protein family.* Genome Biology, 2000.
231. Cardozo, T. and M. Pagano, *The SCF ubiquitin ligase: insights into a molecular machine.* Nat Rev Mol Cell Biol, 2004. **5**(9): p. 739-51.
232. Skowyra, D., et al., *F-Box Proteins Are Receptors that Recruit Phosphorylated Substrates to the SCF Ubiquitin-Ligase Complex.* Cell, 1997. **91**(2): p. 209-219.
233. Skaar, J.R., J.K. Pagan, and M. Pagano, *Mechanisms and function of substrate recruitment by F-box proteins.* Nat Rev Mol Cell Biol, 2013. **14**(6): p. 369-81.
234. Wasserman, D., et al., *Cell cycle oscillators underlying orderly proteolysis of E2F8.* 2019.
235. Dankert, J.F., et al., *Cyclin F-Mediated Degradation of SLBP Limits H2A.X Accumulation and Apoptosis upon Genotoxic Stress in G2.* Mol Cell, 2016. **64**(3): p. 507-519.
236. Koepp, D.M., et al., *Phosphorylation-dependent ubiquitination of cyclin E by the SCFFbw7 ubiquitin ligase.* Science, 2001. **294**(5540): p. 173-7.
237. Ryan, M. Welcker, and Bruce, *Tumor Suppression by the Fbw7 Ubiquitin Ligase: Mechanisms and Opportunities.* Cancer Cell, 2014. **26**(4): p. 455-464.
238. Nguyen, K.T., et al., *Control of protein degradation by N-terminal acetylation and the N-end rule pathway.* Experimental & Molecular Medicine, 2018. **50**(7): p. 1-8.
239. Kim, S.Y., et al., *Skp2 Regulates Myc Protein Stability and Activity.* Molecular Cell, 2003. **11**(5): p. 1177-1188.
240. Nakayama, K., et al., *Targeted disruption of Skp2 results in accumulation of cyclin E and p27Kip1, polyploidy and centrosome overduplication.* The EMBO Journal, 2000. **19**(9): p. 2069-2081.
241. Wang, F., et al., *Deacetylation of FOXO3 by SIRT1 or SIRT2 leads to Skp2-mediated FOXO3 ubiquitination and degradation.* Oncogene, 2012. **31**(12): p. 1546-1557.
242. Asmamaw, M.D., et al., *Skp2 in the ubiquitin-proteasome system: A comprehensive review.* Medicinal Research Reviews, 2020. **40**(5): p. 1920-1949.
243. Liu, Y., et al., *Systematic analysis of the expression and prognosis relevance of FBXO family reveals the significance of FBXO1 in human breast cancer.* Cancer Cell International, 2021. **21**(1).

244. Clijsters, L., et al., *Cyclin F Controls Cell-Cycle Transcriptional Outputs by Directing the Degradation of the Three Activator E2Fs.* Mol Cell, 2019. **74**(6): p. 1264-1277 e7.
245. Kraus, F., *A Novel Cyclin Gene (CCNF) in the Region of the Polycystic Kidney Disease Gene (PKD1).* GENOMICS, 1994. **24**: p. 27-33.
246. Chang Bai, R.R.a.S.J.E., *Human cyclin F.* The EMBO Journal, 1994. **13**(24): p. 6087-6098.
247. D'Angiolella, V., et al., *SCF(Cyclin F) controls centrosome homeostasis and mitotic fidelity through CP110 degradation.* Nature, 2010. **466**(7302): p. 138-42.
248. Monica Kong, E.A.B., Vincent Ollendorff and Daniel J.Donoghue, *Cyclin F regulates the nuclear localization of cyclin B1 through a cyclin–cyclin interaction.* The EMBO Journal, 2000. **19**(6): p. The EMBO Journal.
249. D'Angiolella, V., M. Esencay, and M. Pagano, *A cyclin without cyclin-dependent kinases: cyclin F controls genome stability through ubiquitin-mediated proteolysis.* Trends Cell Biol, 2013. **23**(3): p. 135-40.
250. Feldman, R.M.R., et al., *A Complex of Cdc4p, Skp1p, and Cdc53p/Cullin Catalyzes Ubiquitination of the Phosphorylated CDK Inhibitor Sic1p.* Cell, 1997. **91**(2): p. 221-230.
251. Kim, J., et al., *Low-dielectric-constant polyimide aerogel composite films with low water uptake.* Polymer Journal, 2016. **48**(7): p. 829-834.
252. D'Angiolella, V., et al., *Cyclin F-mediated degradation of ribonucleotide reductase M2 controls genome integrity and DNA repair.* Cell, 2012. **149**(5): p. 1023-34.
253. Tetzlaff, M.T., et al., *Cyclin F disruption compromises placental development and affects normal cell cycle execution.* Mol Cell Biol, 2004. **24**(6): p. 2487-98.
254. Klein, D.K., et al., *Cyclin F suppresses B-Myb activity to promote cell cycle checkpoint control.* Nat Commun, 2015. **6**: p. 5800.
255. Burdova, K., et al., *E2F1 proteolysis via SCF-cyclin F underlies synthetic lethality between cyclin F loss and Chk1 inhibition.* EMBO J, 2019. **38**(20): p. e101443.
256. Yuan, R., et al., *Cyclin F-dependent degradation of E2F7 is critical for DNA repair and G2-phase progression.* EMBO J, 2019. **38**(20): p. e101430.
257. Rosner, H.I. and C.S. Sorensen, *E2F transcription regulation: an orphan cyclin enters the stage.* EMBO J, 2019. **38**(20): p. e103421.
258. Emanuele, M.J., et al., *Global identification of modular cullin-RING ligase substrates.* Cell, 2011. **147**(2): p. 459-74.
259. Deshmukh, R.S., S. Sharma, and S. Das, *Cyclin F-Dependent Degradation of RBPJ Inhibits IDH1(R132H)-Mediated Tumorigenesis.* Cancer Res, 2018. **78**(22): p. 6386-6398.
260. Mills, C.A., et al., *Sirtuin 5 is Regulated by the SCF-Cyclin F Ubiquitin Ligase and is Involved in Cell Cycle Control.* Mol Cell Biol, 2020.
261. Walter, D., et al., *SCF(Cyclin F)-dependent degradation of CDC6 suppresses DNA re-replication.* Nat Commun, 2016. **7**: p. 10530.
262. Choudhury, R., et al., *APC/C and SCF(cyclin F) Constitute a Reciprocal Feedback Circuit Controlling S-Phase Entry.* Cell Rep, 2016. **16**(12): p. 3359-3372.
263. Mavrommati, I., et al., *beta-TrCP- and Casein Kinase II-Mediated Degradation of Cyclin F Controls Timely Mitotic Progression.* Cell Rep, 2018. **24**(13): p. 3404-3412.
264. Chang, S.C., et al., *A Novel Signature of CCNF-Associated E3 Ligases Collaborate and Counter Each Other in Breast Cancer.* Cancers (Basel), 2021. **13**(12).
265. Li, J., et al., *Comprehensive Analysis of Cyclin Family Gene Expression in Colon Cancer.* Front Oncol, 2021. **11**: p. 674394.
266. Chia, R., A. Chiò, and B.J. Traynor, *Novel genes associated with amyotrophic lateral sclerosis: diagnostic and clinical implications.* The Lancet Neurology, 2018. **17**(1): p. 94-102.

267. Pan, C., et al., *Mutations of CCNF gene is rare in patients with amyotrophic lateral sclerosis and frontotemporal dementia from Mainland China.* Amyotroph Lateral Scler Frontotemporal Degener, 2017. **18**(3-4): p. 265-268.
268. Tripolszki, K., et al., *Comprehensive Genetic Analysis of a Hungarian Amyotrophic Lateral Sclerosis Cohort.* Front Genet, 2019. **10**: p. 732.
269. Hurley, J.H. and L.N. Young, *Mechanisms of Autophagy Initiation.* Annual Review of Biochemistry, 2017. **86**(1): p. 225-244.
270. Itakura, E., et al., *Beclin 1 Forms Two Distinct Phosphatidylinositol 3-Kinase Complexes with Mammalian Atg14 and UVRAG.* Molecular Biology of the Cell, 2008. **19**(12): p. 5360-5372.
271. Kihara, A., et al., *Two Distinct Vps34 Phosphatidylinositol 3–Kinase Complexes Function in Autophagy and Carboxypeptidase Y Sorting inSaccharomyces cerevisiae.* Journal of Cell Biology, 2001. **152**(3): p. 519-530.
272. Matscheko, N., et al., *Atg11 tethers Atg9 vesicles to initiate selective autophagy.* PLOS Biology, 2019. **17**(7): p. e3000377.
273. Volinia, S., et al., *A human phosphatidylinositol 3-kinase complex related to the yeast Vps34p-Vps15p protein sorting system.* The EMBO Journal, 1995. **14**(14): p. 3339-3348.
274. He, C., et al., *Self-Interaction Is Critical for Atg9 Transport and Function at the Phagophore Assembly Site during Autophagy.* Molecular Biology of the Cell, 2008. **19**(12): p. 5506-5516.
275. Ganley, I.G., et al., *ULK1·ATG13·FIP200 Complex Mediates mTOR Signaling and Is Essential for Autophagy.* Journal of Biological Chemistry, 2009. **284**(18): p. 12297-12305.
276. Lin, M.G. and J.H. Hurley, *Structure and function of the ULK1 complex in autophagy.* Current Opinion in Cell Biology, 2016. **39**: p. 61-68.
277. Jung, C.H., et al., *ULK-Atg13-FIP200 Complexes Mediate mTOR Signaling to the Autophagy Machinery.* Molecular Biology of the Cell, 2009. **20**(7): p. 1992-2003.
278. Ma, M., et al., *Cryo-EM structure and biochemical analysis reveal the basis of the functional difference between human PI3KC3-C1 and -C2.* Cell Research, 2017. **27**(8): p. 989-1001.
279. Axe, E.L., et al., *Autophagosome formation from membrane compartments enriched in phosphatidylinositol 3-phosphate and dynamically connected to the endoplasmic reticulum.* Journal of Cell Biology, 2008. **182**(4): p. 685-701.
280. Proikas-Cezanne, T., et al., *WIPI-1α (WIPI49), a member of the novel 7-bladed WIPI protein family, is aberrantly expressed in human cancer and is linked to starvation-induced autophagy.* Oncogene, 2004. **23**(58): p. 9314-9325.
281. Lamb, C.A., T. Yoshimori, and S.A. Tooze, *The autophagosome: origins unknown, biogenesis complex.* Nature Reviews Molecular Cell Biology, 2013. **14**(12): p. 759-774.
282. Hannah, et al., *WIPI2 Links LC3 Conjugation with PI3P, Autophagosome Formation, and Pathogen Clearance by Recruiting Atg12–5-16L1.* Molecular Cell, 2014. **55**(2): p. 238-252.
283. Birgisdottir, Å.B., T. Lamark, and T. Johansen, *The LIR motif – crucial for selective autophagy.* Journal of Cell Science, 2013. **126**(15): p. 3237-3247.
284. Xie, Z., U. Nair, and D.J. Klionsky, *Atg8 Controls Phagophore Expansion during Autophagosome Formation.* Molecular Biology of the Cell, 2008. **19**(8): p. 3290-3298.
285. Jiang, W., et al., *Key Regulators of Autophagosome Closure.* Cells, 2021. **10**(11): p. 2814.
286. Kriegenburg, F., C. Ungermann, and F. Reggiori, *Coordination of Autophagosome–Lysosome Fusion by Atg8 Family Members.* Current Biology, 2018. **28**(8): p. R512-R518.
287. Hansen, M., D.C. Rubinsztein, and D.W. Walker, *Autophagy as a promoter of longevity: insights from model organisms.* Nat Rev Mol Cell Biol, 2018. **19**(9): p. 579-593.

288. Ballabio, A. and J.S. Bonifacino, *Lysosomes as dynamic regulators of cell and organismal homeostasis.* Nature Reviews Molecular Cell Biology, 2020. **21**(2): p. 101-118.
289. Boya, P. and G. Kroemer, *Lysosomal membrane permeabilization in cell death.* Oncogene, 2008. **27**(50): p. 6434-6451.
290. Emmerson, B.T., et al., *Reaction of MDCK cells to crystals of monosodium urate monohydrate and uric acid.* Kidney International, 1990. **37**(1): p. 36-43.
291. Van Der Wel, N., et al., *M. tuberculosis and M. leprae Translocate from the Phagolysosome to the Cytosol in Myeloid Cells.* Cell, 2007. **129**(7): p. 1287-1298.
292. Papadopoulos, C., B. Kravic, and H. Meyer, *Repair or Lysophagy: Dealing with Damaged Lysosomes.* Journal of Molecular Biology, 2020. **432**(1): p. 231-239.
293. Repnik, U., et al., *LLOMe does not release cysteine cathepsins to the cytosol but inactivates them in transiently permeabilized lysosomes.* Journal of Cell Science, 2017. **130**(18): p. 3124-3140.
294. Skowyra, M.L., et al., *Triggered recruitment of ESCRT machinery promotes endolysosomal repair.* Science, 2018. **360**(6384): p. eaar5078.
295. Radulovic, M., et al., *ESCRT-mediated lysosome repair precedes lysophagy and promotes cell survival.* The EMBO Journal, 2018. **37**(21): p. e99753.
296. Palmieri, M., et al., *Characterization of the CLEAR network reveals an integrated control of cellular clearance pathways.* Human Molecular Genetics, 2011. **20**(19): p. 3852-3866.
297. Jia, J., et al., *Galectins Control mTOR in Response to Endomembrane Damage.* Molecular Cell, 2018. **70**(1): p. 120-135.e8.
298. Koerver, L., et al., *The ubiquitin-conjugating enzyme UBE2QL1 coordinates lysophagy in response to endolysosomal damage.* EMBO reports, 2019. **20**(10).
299. Thurston, T.L.M., et al., *Galectin 8 targets damaged vesicles for autophagy to defend cells against bacterial invasion.* Nature, 2012. **482**(7385): p. 414-418.
300. Papadopoulos, C. and H. Meyer, *Detection and Clearance of Damaged Lysosomes by the Endo-Lysosomal Damage Response and Lysophagy.* Current Biology, 2017. **27**(24): p. R1330-R1341.
301. Chauhan, S., et al., *TRIMs and Galectins Globally Cooperate and TRIM16 and Galectin-3 Co-direct Autophagy in Endomembrane Damage Homeostasis.* Developmental Cell, 2016. **39**(1): p. 13-27.
302. Nazio, F., et al., *mTOR inhibits autophagy by controlling ULK1 ubiquitylation, self-association and function through AMBRA1 and TRAF6.* Nature Cell Biology, 2013. **15**(4): p. 406-416.
303. Bussi, C., et al., *Alpha-synuclein fibrils recruit TBK1 and OPTN to lysosomal damage sites and induce autophagy in microglial cells.* Journal of Cell Science, 2018. **131**(23): p. jcs226241.
304. Yoshida, Y., et al., *Ubiquitination of exposed glycoproteins by SCF (FBXO27) directs damaged lysosomes for autophagy.* Proceedings of the National Academy of Sciences, 2017. **114**(32): p. 8574-8579.
305. Stolz, A., et al., *Cdc48: a power machine in protein degradation.* Trends in Biochemical Sciences, 2011. **36**(10): p. 515-523.
306. Umoh, M.E., et al., *A proteomic network approach across the ALS-FTD disease spectrum resolves clinical phenotypes and genetic vulnerability in human brain.* EMBO Molecular Medicine, 2018. **10**(1): p. 48-62.
307. Abati, E., et al., *Silence superoxide dismutase 1 (SOD1): a promising therapeutic target for amyotrophic lateral sclerosis (ALS).* Expert Opinion on Therapeutic Targets, 2020. **24**(4): p. 295-310.
308. Groups, T.L.a.M., *Clinical and neuropathological criteria for frontotemporal dementia.* Journal of Neurology, Neurosurgery & Psychiatry, 1994. **57**(4): p. 416-418.

309. Knopman, D.S., et al., *The incidence of frontotemporal lobar degeneration in Rochester, Minnesota, 1990 through 1994.* Neurology, 2004. **62**(3): p. 506-508.
310. Ratnavalli, E., et al., *The prevalence of frontotemporal dementia.* Neurology, 2002. **58**(11): p. 1615-1621.
311. Hodges, J.R., et al., *Clinicopathological correlates in frontotemporal dementia.* Annals of Neurology, 2004. **56**(3): p. 399-406.
312. Berrios, G.E. and D.M. Girling, *Introduction: Pick's disease and the 'frontal lobe' dementias.* History of Psychiatry, 1994. **5**(20): p. 539-541.
313. Ferrari, R., et al., *FTD and ALS: A Tale of Two Diseases.* Current Alzheimer Research, 2011. **8**(3): p. 273-294.
314. Alzheimer, A., *Über eigenartige Krankheitsfälle des späteren Alters.* History of Psychiatry, 1991. **2**(5): p. 74-101.
315. Josephs, K.A., *Frontotemporal dementia and related disorders: Deciphering the enigma.* Annals of Neurology, 2008. **64**(1): p. 4-14.
316. Gorno-Tempini, M.L., et al., *The logopenic/phonological variant of primary progressive aphasia.* Neurology, 2008. **71**(16): p. 1227-1234.
317. Rosen, H.J., et al., *Patterns of cerebral atrophy in primary progressive aphasia.* Am J Geriatr Psychiatry, 2002. **10**(1): p. 89-97.
318. Bang, J., S. Spina, and B.L. Miller, *Frontotemporal dementia.* The Lancet, 2015. **386**(10004): p. 1672-1682.
319. Kumar, D.R., et al., *Jean-Martin Charcot: The Father of Neurology.* Clinical Medicine & Research, 2011. **9**(1): p. 46-49.
320. Pasinelli, P. and R.H. Brown, *Molecular biology of amyotrophic lateral sclerosis: insights from genetics.* Nature Reviews Neuroscience, 2006. **7**(9): p. 710-723.
321. Chiò, A., et al., *Global Epidemiology of Amyotrophic Lateral Sclerosis: A Systematic Review of the Published Literature.* Neuroepidemiology, 2013. **41**(2): p. 118-130.
322. Arthur, K.C., et al., *Projected increase in amyotrophic lateral sclerosis from 2015 to 2040.* Nature Communications, 2016. **7**(1): p. 12408.
323. Abrahams, S., et al., *Word retrieval in amyotrophic lateral sclerosis: a functional magnetic resonance imaging study.* Brain, 2004. **127**(7): p. 1507-1517.
324. Mackenzie, I.R.A. and H. H. Feldman, *Ubiquitin Immunohistochemistry Suggests Classic Motor Neuron Disease, Motor Neuron Disease With Dementia, and Frontotemporal Dementia of the Motor Neuron Disease Type Represent a Clinicopathologic Spectrum.* Journal of Neuropathology and Experimental Neurology, 2005. **64**(8): p. 730-739.
325. Peters, O.M., M. Ghasemi, and R.H. Brown, *Emerging mechanisms of molecular pathology in ALS.* Journal of Clinical Investigation, 2015. **125**(5): p. 1767-1779.
326. Ghasemi, M. and R.H. Brown, *Genetics of Amyotrophic Lateral Sclerosis.* Cold Spring Harbor Perspectives in Medicine, 2018. **8**(5): p. a024125.
327. Andersen, P.M. and A. Al-Chalabi, *Clinical genetics of amyotrophic lateral sclerosis: what do we really know?* Nature Reviews Neurology, 2011. **7**(11): p. 603-615.
328. Brown, R.H. and A. Al-Chalabi, *Amyotrophic Lateral Sclerosis.* New England Journal of Medicine, 2017. **377**(2): p. 162-172.
329. Fang, T., et al., *Gene Therapy in Amyotrophic Lateral Sclerosis.* Cells, 2022. **11**(13): p. 2066.
330. Ling, S.-C., M. Polymenidou, and Don, *Converging Mechanisms in ALS and FTD: Disrupted RNA and Protein Homeostasis.* Neuron, 2013. **79**(3): p. 416-438.
331. Hutton, M., et al., *Association of missense and 5'-splice-site mutations in tau with the inherited dementia FTDP-17.* Nature, 1998. **393**(6686): p. 702-705.
332. Baker, M., et al., *Mutations in progranulin cause tau-negative frontotemporal dementia linked to chromosome 17.* Nature, 2006. **442**(7105): p. 916-919.

333. Cruts, M., et al., *Null mutations in progranulin cause ubiquitin-positive frontotemporal dementia linked to chromosome 17q21.* Nature, 2006. **442**(7105): p. 920-924.
334. Watts, G., et al., *Novel VCP mutations in inclusion body myopathy associated with Paget disease of bone and frontotemporal dementia.* Clinical Genetics, 2007. **72**(5): p. 420-426.
335. Johnson, J.O., et al., *Exome Sequencing Reveals VCP Mutations as a Cause of Familial ALS.* Neuron, 2010. **68**(5): p. 857-864.
336. Chen, S., et al., *Genetics of amyotrophic lateral sclerosis: an update.* Molecular Neurodegeneration, 2013. **8**(1): p. 28.
337. Bowling, A.C., et al., *Superoxide Dismutase Activity, Oxidative Damage, and Mitochondrial Energy Metabolism in Familial and Sporadic Amyotrophic Lateral Sclerosis.* Journal of Neurochemistry, 1993. **61**(6): p. 2322-2325.
338. Bunton-Stasyshyn, R.K.A., et al., *SOD1 Function and Its Implications for Amyotrophic Lateral Sclerosis Pathology.* The Neuroscientist, 2015. **21**(5): p. 519-529.
339. Deng, H., K. Gao, and J. Jankovic, *The role of FUS gene variants in neurodegenerative diseases.* Nature Reviews Neurology, 2014. **10**(6): p. 337-348.
340. Buratti, E. and F.E. Baralle, *The multiple roles of TDP-43 in pre-mRNA processing and gene expression regulation.* RNA Biology, 2010. **7**(4): p. 420-429.
341. Ratti, A. and E. Buratti, *Physiological functions and pathobiology of TDP-43 and FUS/TLS proteins.* Journal of Neurochemistry, 2016. **138**: p. 95-111.
342. Wang, W.-Y., et al., *Interaction of FUS and HDAC1 regulates DNA damage response and repair in neurons.* Nature Neuroscience, 2013. **16**(10): p. 1383-1391.
343. Ayala, Y.M., et al., *Structural determinants of the cellular localization and shuttling of TDP-43.* Journal of Cell Science, 2008. **121**(22): p. 3778-3785.
344. Zinszner, H., et al., *TLS (FUS) binds RNA in vivo and engages in nucleo-cytoplasmic shuttling.* Journal of Cell Science, 1997. **110**(15): p. 1741-1750.
345. Vance, C., et al., *ALS mutant FUS disrupts nuclear localization and sequesters wild-type FUS within cytoplasmic stress granules.* Human Molecular Genetics, 2013. **22**(13): p. 2676-2688.
346. Giordana, M.T., et al., *TDP-43 Redistribution is an Early Event in Sporadic Amyotrophic Lateral Sclerosis.* Brain Pathology, 2010. **20**(2): p. 351-360.
347. Suk, T.R. and M.W.C. Rousseaux, *The role of TDP-43 mislocalization in amyotrophic lateral sclerosis.* Molecular Neurodegeneration, 2020. **15**(1).
348. Takeuchi, R., et al., *Heterogeneity of cerebral TDP-43 pathology in sporadic amyotrophic lateral sclerosis: Evidence for clinico-pathologic subtypes.* Acta Neuropathologica Communications, 2016. **4**(1).
349. Neumann, M., et al., *TDP-43 Proteinopathy in Frontotemporal Lobar Degeneration and Amyotrophic Lateral Sclerosis.* Archives of Neurology, 2007. **64**(10): p. 1388.
350. Buratti, E., *TDP-43 post-translational modifications in health and disease.* Expert Opinion on Therapeutic Targets, 2018. **22**(3): p. 279-293.
351. Sreedharan, J., et al., *TDP-43 Mutations in Familial and Sporadic Amyotrophic Lateral Sclerosis.* Science, 2008. **319**(5870): p. 1668-1672.
352. Kang, J., et al., *A unified mechanism for LLPS of ALS/FTLD-causing FUS as well as its modulation by ATP and oligonucleic acids.* PLOS Biology, 2019. **17**(6): p. e3000327.
353. Weingarten, M.D., et al., *A protein factor essential for microtubule assembly.* Proceedings of the National Academy of Sciences, 1975. **72**(5): p. 1858-1862.
354. Naseri, N.N., et al., *The complexity of tau in Alzheimer's disease.* Neuroscience Letters, 2019. **705**: p. 183-194.
355. Arendt, T., J.T. Stieler, and M. Holzer, *Tau and tauopathies.* Brain Research Bulletin, 2016. **126**: p. 238-292.

356. Ogura, T. and A.J. Wilkinson, *AAA+ superfamily ATPases: common structure-diverse function.* Genes to Cells, 2001. **6**(7): p. 575-597.
357. Arhzaouy, K., et al., *VCP maintains lysosomal homeostasis and TFEB activity in differentiated skeletal muscle.* Autophagy, 2019. **15**(6): p. 1082-1099.
358. Van Rheenen, W., et al., *Genome-wide association analyses identify new risk variants and the genetic architecture of amyotrophic lateral sclerosis.* Nature Genetics, 2016. **48**(9): p. 1043-1048.
359. Lamb, R., et al., *A novel TBK1 mutation in a family with diverse frontotemporal dementia spectrum disorders.* Molecular Case Studies, 2019. **5**(3): p. a003913.
360. Fecto, F., *SQSTM1 Mutations in Familial and Sporadic Amyotrophic Lateral Sclerosis.* Archives of Neurology, 2011. **68**(11): p. 1440.
361. Abramzon, Y.A., et al., *The Overlapping Genetics of Amyotrophic Lateral Sclerosis and Frontotemporal Dementia.* Front Neurosci, 2020. **14**: p. 42.
362. Gijselinck, I., et al., *A C9orf72 promoter repeat expansion in a Flanders-Belgian cohort with disorders of the frontotemporal lobar degeneration-amyotrophic lateral sclerosis spectrum: a gene identification study.* The Lancet Neurology, 2012. **11**(1): p. 54-65.
363. Dejesus-Hernandez, M., et al., *Expanded GGGGCC Hexanucleotide Repeat in Noncoding Region of C9ORF72 Causes Chromosome 9p-Linked FTD and ALS.* Neuron, 2011. **72**(2): p. 245-256.
364. Alan, et al., *A Hexanucleotide Repeat Expansion in C9ORF72 Is the Cause of Chromosome 9p21-Linked ALS-FTD.* Neuron, 2011. **72**(2): p. 257-268.
365. Haeusler, A.R., C.J. Donnelly, and J.D. Rothstein, *The expanding biology of the C9orf72 nucleotide repeat expansion in neurodegenerative disease.* Nature Reviews Neuroscience, 2016. **17**(6): p. 383-395.
366. Iacoangeli, A., et al., *C9orf72 intermediate expansions of 24–30 repeats are associated with ALS.* Acta Neuropathologica Communications, 2019. **7**(1).
367. Beck, J., et al., *Large C9orf72 Hexanucleotide Repeat Expansions Are Seen in Multiple Neurodegenerative Syndromes and Are More Frequent Than Expected in the UK Population.* The American Journal of Human Genetics, 2013. **92**(3): p. 345-353.
368. Gijselinck, I., et al., *The C9orf72 repeat size correlates with onset age of disease, DNA methylation and transcriptional downregulation of the promoter.* Molecular Psychiatry, 2016. **21**(8): p. 1112-1124.
369. Ghasemi, M., K. Keyhanian, and C. Douthwright, *Glial Cell Dysfunction in C9orf72-Related Amyotrophic Lateral Sclerosis and Frontotemporal Dementia.* Cells, 2021. **10**(2): p. 249.
370. Webster, C.P., et al., *Protein Homeostasis in Amyotrophic Lateral Sclerosis: Therapeutic Opportunities?* Frontiers in Molecular Neuroscience, 2017. **10**(123).
371. Hergesheimer, R.C., et al., *The debated toxic role of aggregated TDP-43 in amyotrophic lateral sclerosis: a resolution in sight?* Brain, 2019. **142**(5): p. 1176-1194.
372. Bergemalm, D., et al., *Superoxide dismutase-1 and other proteins in inclusions from transgenic amyotrophic lateral sclerosis model mice.* Journal of Neurochemistry, 2010. **114**(2): p. 408-418.
373. Watanabe, M., et al., *Histological Evidence of Protein Aggregation in Mutant SOD1 Transgenic Mice and in Amyotrophic Lateral Sclerosis Neural Tissues.* Neurobiology of Disease, 2001. **8**(6): p. 933-941.
374. Tummala, H., et al., *Inhibition of Chaperone Activity Is a Shared Property of Several Cu,Zn-Superoxide Dismutase Mutants That Cause Amyotrophic Lateral Sclerosis.* Journal of Biological Chemistry, 2005. **280**(18): p. 17725-17731.
375. Ganesan, S., et al., *Mutant SOD1 detoxification mechanisms in intact single cells.* Cell Death & Differentiation, 2008. **15**(2): p. 312-321.

376. Marino, M., et al., *Differences in protein quality control correlate with phenotype variability in 2 mouse models of familial amyotrophic lateral sclerosis.* Neurobiology of Aging, 2015. **36**(1): p. 492-504.
377. Chen, H.-J., et al., *The heat shock response plays an important role in TDP-43 clearance: evidence for dysfunction in amyotrophic lateral sclerosis.* Brain, 2016. **139**(5): p. 1417-1432.
378. Zhang, Y.-J., et al., *Phosphorylation regulates proteasomal-mediated degradation and solubility of TAR DNA binding protein-43 C-terminal fragments.* Molecular Neurodegeneration, 2010. **5**(1): p. 33.
379. Lackie, R.E., et al., *The Hsp70/Hsp90 Chaperone Machinery in Neurodegenerative Diseases.* Frontiers in neuroscience, 2017. **11**: p. 254-254.
380. Miguel, L., et al., *Accumulation of insoluble forms of FUS protein correlates with toxicity in Drosophila.* Neurobiology of Aging, 2012. **33**(5): p. 1008.e1-1008.e15.
381. Anagnostou, G., et al., *Vesicle associated membrane protein B (VAPB) is decreased in ALS spinal cord.* Neurobiology of Aging, 2010. **31**(6): p. 969-985.
382. Farhan, S.M.K., et al., *Exome sequencing in amyotrophic lateral sclerosis implicates a novel gene, DNAJC7, encoding a heat-shock protein.* Nature Neuroscience, 2019. **22**(12): p. 1966-1974.
383. Lee, A., et al., *Pathogenic mutation in the ALS/FTD gene, CCNF, causes elevated Lys48-linked ubiquitylation and defective autophagy.* Cell Mol Life Sci, 2018. **75**(2): p. 335-354.
384. Cheng, F., et al., *Unbiased Label-Free Quantitative Proteomics of Cells Expressing Amyotrophic Lateral Sclerosis (ALS) Mutations in CCNF Reveals Activation of the Apoptosis Pathway: A Workflow to Screen Pathogenic Gene Mutations.* Front Mol Neurosci, 2021. **14**: p. 627740.
385. Hogan, A.L., et al., *Expression of ALS/FTD-linked mutant CCNF in zebrafish leads to increased cell death in the spinal cord and an aberrant motor phenotype.* Hum Mol Genet, 2017. **26**(14): p. 2616-2626.
386. Williams, K.L., et al., *CCNF mutations in amyotrophic lateral sclerosis and frontotemporal dementia.* Nature Communications, 2016. **7**(1): p. 11253.
387. Tsai, P.C., et al., *Investigating CCNF mutations in a Taiwanese cohort with amyotrophic lateral sclerosis.* Neurobiol Aging, 2018. **62**: p. 243 e1-243 e6.
388. Tian, D., et al., *Screening for CCNF Mutations in a Chinese Amyotrophic Lateral Sclerosis Cohort.* Front Aging Neurosci, 2018. **10**: p. 185.
389. Yu, Y., et al., *Pathogenic mutations in the ALS gene CCNF cause cytoplasmic mislocalization of Cyclin F and elevated VCP ATPase activity.* Hum Mol Genet, 2019. **28**(20): p. 3486-3497.
390. Peng, J., et al., *A proteomics approach to understanding protein ubiquitination.* Nature Biotechnology, 2003. **21**(8): p. 921-926.
391. Ordureau, A., C. Münch, and J, *Quantifying Ubiquitin Signaling.* Molecular Cell, 2015. **58**(4): p. 660-676.
392. Xu, G., J.S. Paige, and S.R. Jaffrey, *Global analysis of lysine ubiquitination by ubiquitin remnant immunoaffinity profiling.* Nature Biotechnology, 2010. **28**(8): p. 868-873.
393. Kim, W., et al., *Systematic and Quantitative Assessment of the Ubiquitin-Modified Proteome.* Molecular Cell, 2011. **44**(2): p. 325-340.
394. Ong, S.-E., et al., *Stable Isotope Labeling by Amino Acids in Cell Culture, SILAC, as a Simple and Accurate Approach to Expression Proteomics.* Molecular & Cellular Proteomics, 2002. **1**(5): p. 376-386.
395. Cox, J. and M. Mann, *Quantitative, High-Resolution Proteomics for Data-Driven Systems Biology.* Annual Review of Biochemistry, 2011. **80**(1): p. 273-299.

396. Wagner, S.A., et al., *A Proteome-wide, Quantitative Survey of In Vivo Ubiquitylation Sites Reveals Widespread Regulatory Roles.* Molecular & Cellular Proteomics, 2011. **10**(10): p. M111.013284.
397. Fulzele, A. and E.J. Bennett, *Ubiquitin diGLY Proteomics as an Approach to Identify and Quantify the Ubiquitin-Modified Proteome.* Methods Mol Biol, 2018. **1844**: p. 363-384.
398. Roux, K.J., et al., *A promiscuous biotin ligase fusion protein identifies proximal and interacting proteins in mammalian cells.* Journal of Cell Biology, 2012. **196**(6): p. 801-810.
399. Kim, D.I., et al., *Probing nuclear pore complex architecture with proximity-dependent biotinylation.* Proceedings of the National Academy of Sciences, 2014. **111**(24): p. E2453-E2461.
400. Lam, S.S., et al., *Directed evolution of APEX2 for electron microscopy and proximity labeling.* Nature Methods, 2015. **12**(1): p. 51-54.
401. Rhee, H.-W., et al., *Proteomic Mapping of Mitochondria in Living Cells via Spatially Restricted Enzymatic Tagging.* Science, 2013. **339**(6125): p. 1328-1331.

4 Acknowledgments

Fast 7 Jahre nachdem ich meine Doktorarbeit begonnen habe, sitze ich hier und habe das Vergnügen, mich bei den Menschen zu bedanken, die mich auf diesem Weg begleitet und unterstützt haben. In den letzten Monaten habe ich immer wieder darüber nachgedacht, was diese Zeit für mich bedeutet hat und obwohl es nicht immer einfach war, habe ich viele tolle Menschen kennen und lieben gelernt. Außerdem bin ich als Wissenschaftler und Mensch gewachsen, habe meine Grenzen kennen gelernt und bin die nächsten Schritte in meiner Karriere gegangen.

Zuerst möchte ich mich bei **Christian** für die Möglichkeit bedanken, meine Arbeit in deiner neu gebildeten Münchner Gruppe zu schreiben, für die vielen wissenschaftlichen Diskussionen, die spannenden Projekte, ja auch für SOGA3 und unseren erfolgreichen Abschluss des CCNF-Projektes. Ich bin dir auch sehr dankbar dafür, dass wir die Möglichkeit hatten, Einfluss darauf zu nehmen, wer unsere Gruppe bereichert, was eine sehr familiäre Atmosphäre ermöglicht hat. Danke auch für die Flexibilität, die du uns im Labor gegeben hast und auch für die Zeit, die wir außerhalb des Labors miteinander verbracht haben.

Ein herzliches Dankeschön an die **Prüfungskommission** für die Übernahme der Begutachtung meiner Doktorarbeit.

Der nächste Dank geht ohne Zweifel an die gesamte **AG Behrends**. Ohne euch hätte ich es nicht geschafft. Als ich damals mit **Franzi** angefangen habe und wir nach München gekommen sind, habe ich zwar schon einige Zeit in Laboren verbracht, aber eine Doktorarbeit ist doch etwas anderes. Also danke Franzi, für die Einarbeitung, das Einrichten des Labors und die Zeit, die wir zusammen verbracht haben, durch deinen Einsatz haben wir beide nur wenige Monate nicht arbeiten können.

Nach und nach wurde unser Labor immer größer. Im Sommer waren wir plötzlich richtig viele und es fühlte sich an wie unsere kleine verrückte Lab-Familie. Ich möchte jedem und jeder Einzelnen von euch danken.

Zuerst möchte ich mich beim alten Lab-Team bedanken. **Vanessa**, **Julia**, **Susa**, **Karsten**, **Lukas B.** und **Laura**, danke für eure Freundschaft, euren Humor, die lustigen und absurden Momente, die wir zusammen erlebt haben. Danke für das Splitten von Zellen, das nach Hause schicken, wenn man mal wieder nicht vernünftig genug war auf sich aufzupassen und für euer offenes Ohr in allen Lebenslagen. Ich konnte mich auf jeden von euch verlassen und wenn nichts funktioniert hat, wart

ihr einer der wenigen Gründe, wieso ich nicht einfach aufgegeben habe. Es war echt verrückt nach 6 Jahren einen neuen Schritt zu gehen in dem Wissen, dass jeder von uns früher oder später einen neuen Abschnitt beginnen wird, weshalb ich noch ein paar persönliche Dankeschön loswerden will. An **Susa** für die tollen Gespräche und unsere fantastischen Kletter-Sessions. Der Satz „Kraft in meine Arme.“, ist seitdem in mein Gehirn gebrannt. An **JJ** für das Austauschen von Musik, die witzigen Gespräche und die gegenseitige Unterstützung, um endlich Ubiquitinierung nachzuweisen. An **Karsten** für die Trips in die Berge, das gemeinsame Langlaufen mit mehr oder weniger Erfolg meinerseits, und deine Contenance im Labor. An **Lukas B.**, auch wenn du den Weg im Labor nicht bis zum Ende mit uns gegangen bist, so bist du doch einer meiner besten Freunde in München geworden. Danke dir für die Wanderungen, die Gespräche bei einem Bier, das gemeinsame Klettern, und deine entspannte Art. Natürlich geht mein Dank auch an **Laura**, unserer Frohnatur im Labor. Danke dir für die vielen Gespräche, unsere gemeinsamen Konzertbesuche, deine Tipps im Umgang mit Rückschlägen, fürs Mitfiebern im Labor und deinen Support bei der Jobsuche.

Nun möchte ich mich auch bei den neuen Teammitgliedern bedanken, die ich kennenlernen durfte. Danke **Sophie, Debjani**, **Alina L.** und **Alina R.** für eine großartige gemeinsame Zeit und dafür, dass ihr das Labor mit eurem neuen Eifer und positiver Einstellung bereichert habt. **Sophie** danke für die vielen leckeren Kuchen und deine Begeisterung für die Wissenschaft und unsere Bench-Gespräche. **Debjani** danke dir für die vielen Gespräche über Wissenschaft und alles, was darüber hinausgeht und die witzigen Momente im Labor. **Alina L.** ich glaube wir haben uns außerhalb des Labors fast öfter unterhalten als im Labor. Danke dir für die witzige gemeinsame Zeit. **Alina R** danke auch dir für deine positive Energie und ich freue mich auf viele weitere Treffen.

Ich weiß, dass ich unserer gemeinsamen Zeit mit diesem kurzen Paragrafen nie gerecht werden kann, weshalb ich es auch gar nicht weiter versuchen werde. Vielmehr bleibt mir zu sagen, ich freue mich auf unsere nächsten Treffen.

In meiner Zeit als Doktorand hatte ich das Glück nicht nur eine tolle Arbeitsgruppe vorzufinden, sondern auch ein gut vernetztes und hilfsbereites Forschungsumfeld. Ich möchte mich bei den Eddies, der AG Steiner, der AG Schmid, den Capells, sowie der AG Haas für das Teilen von Wissen, Equipment, Chemikalien und einer positiven Atmosphäre bedanken. AGs bestehen aber nun mal aus Menschen und einigen möchte ich gerne noch einmal gesondert danken.

Los geht es mit den Eddies. Danke **Mareike** für dein offenes Ohr, die witzigen Diskussionen, das gemeinsame Feiern und deine besonnene Art. **Hanne**, es war mir eine Ehre mit dir die btS im ISD zu vertreten, mit dir zu feiern und zu scherzen. Danke **Katie** für deine offene Art, die gemeinsamen

Feiern und Stunden, die wir singend verbracht haben. **Ali** danke dir fürs Philosophieren, Zocken, UFC schauen und dafür, dass du einfach ein verdammt guter Freund geworden bist. Natürlich darf ich auch die Steiners nicht vergessen. Danke **Jojo** für die gemeinsame Zeit, das Klettern & Wandern, die Grillabende, das Philosophieren und Diskutieren beim x-ten Bier zu später Stunde und für die vielen witzigen Momente. Danke **Lukas F.** für die gemeinsamen Abende im Luigi, die tiefgründigen Gespräche, für dein Vertrauen und dein offenes Ohr. **Nadine**, als 3rd floor representatives, haben wir ja schon echt einiges auf die Beine gestellt. Danke dir für die lustigen Momente, die Oktoberfest lectures, die Spieleabende, die BOTMs und einfach für die gemeinsame Zeit. Danke **Edgar**, ich hoffe es geht dir gut in der Schweiz und danke dir für die gemeinsame Zeit, sei es beim Klettern, beim Bier trinken auf dem Berg oder außerhalb. Ich möchte mich auch bei **Georg** danken. Danke, dass du dir die Zeit genommen hast, mir CRISPR-Cas9 zu zeigen, ich glaube nicht, dass mein zweites Projekt so gut und einfach verlaufen wäre, wenn du mir nicht geholfen hättest. Danke für die vielen Spaziergänge, Gespräche und lustigen Momente, die wir zusammen verbracht haben.

Den aufmerksamen Leser wird aufgefallen sein, dass ich bisher nur Menschen im 3rd Floor gedankt habe, aber der Rest des Gebäudes hatte natürlich auch großartige Menschen zu bieten. Zwei Personen möchte ich noch hervorheben. Danke **Julien** & **Angelika** für die witzigen Trash-Movie Abende, die Tage in den Bergen und für eure Freundschaft.

Meine Arbeit wäre außerdem nicht möglich gewesen ohne **Sabine** und **Willi**, die dafür gesorgt haben, dass wir Doktoranden alles hatten, was wir für unsere Arbeit brauchten. Danke auch an **Annette** und **Selma** für die organisatorische Unterstützung. Außerdem möchte ich mich bei **Tobias** bedanken, der mir die Teilnahme am Podcast der Exzellenzcluster ermöglicht hat und mir auch Tipps zur universitären Wissenschaftskommunikation gegeben hat.

Das alles wäre nicht möglich gewesen ohne meine **Eltern**, die mir mein Leben lang alles ermöglicht haben, mir den Rücken freigehalten haben und immer an mich geglaubt haben. Danke für alles. Auch meiner Schwester **Veronika** möchte ich für ihr stets offenes Ohr danken.

Eine besondere Person möchte ich natürlich nicht unerwähnt lassen, ein ehemaliges Eddie-Lab-Mitglied, meine wundervolle Partnerin, **Meike**. Vielleicht war es Schicksal, dass mich nach München verschlagen hat, habe ich mich das eine oder andere Mal gefragt, auch wenn ich nicht an Schicksal glaube. Aber wie erkläre ich mir sonst, dass ich mich in Frankfurt beworben habe, nach München gezogen bin und dich gefunden habe? Jetzt sind es bald 7 Jahre, die wir zusammen sind und wir haben in dieser Zeit eine Doktorarbeit, eine Pandemie und einen Bachelor durchgestanden, ohne uns aus den Augen zu verlieren. Ich möchte dir für jeden einzelnen Tag danken, für deine Unterstützung,

deine Aufmunterungen und deinen unerschütterlichen Glauben daran, dass das alles funktionieren wird.

Ich habe so viel gelernt und in alter Ohrwurm-Manier ist mir natürlich ein Liedzitat eingefallen, das ich gerne noch teilen möchte:

'Life is about love, last minutes and lost evenings,

About fire in our bellies and furtive little feelings,

And the aching amplitudes that set our needles all a-flickering,

And help us with remembering that the only thing that's left to do is live."

Frank Turner –

I Knew Prufrock Before He Got Famous

5 Affidavit

Eidesstattliche Versicherung

Hiermit erkläre ich, Alexander Siebert, an Eides statt, dass ich die vorliegende Dissertation mit dem Titel:

MASS SPECTROMETRY-BASED EXPLORATION OF NOVEL INTERACTORS IN UBIQUITIN-MEDIATED PROCESSES

selbständig verfasst, mich außer der angegebenen keiner weiteren Hilfsmittel bedient und alle Erkenntnisse, die aus dem Schrifttum ganz oder annähernd übernommen sind, als solche kenntlich gemacht und nach ihrer Herkunft unter Bezeichnung der Fundstelle einzeln nachgewiesen habe.

Ich erkläre des Weiteren, dass die hier vorgelegte Dissertation nicht in gleicher oder in ähnlicher Form bei einer anderen Stelle zur Erlangung eines akademischen Grades eingereicht wurde.

Teile dieser Arbeit sind bereits in internationalen Fachzeitschriften veröffentlicht worden.

München, 16.3.2024	Alexander Siebert
Ort, Datum	Unterschrift Doktorandin bzw. Doktorand